Novel Enhancements and Analytical Applications of Amperometric Nitric Oxide (NO) Sensors

by

Zheng Zheng

A dissertation submitted in partial fulfillment
of the requirements for the degree of
Doctor of Philosophy
(Chemistry)
at the University of Michigan
2016

Doctoral Committee:

Professor Marc B. Hershenson
Associate Professor Stephen Maldonado
Professor Mark E. Meyerhoff, Chair
Professor Michael D. Morris

2016

DEDICATION

This Work is Dedicated To:

My parents,
for their unconditional love and support

ACKNOWLEDGEMENTS

Throughout my time at the University of Michigan, I've had the support and guidance of many great individuals. First and foremost, I'd like to acknowledge the critical role that my PhD advisor Dr. Mark Meyerhoff, has played in my development as both a scientist and a person. Thank you, Mark, for going above and beyond what is expected of PhD mentors and conveying onto me much of the wisdom you have accrued over your many years as an effective scientist, educator, and mentor. Without your guidance, I'm not sure I would have gained the maturity and perspective that I did during my PhD studies.

Next, I'd like to thank my committee members; thank you, Dr. Stephen Maldonado, Dr. Michael Morris, and Dr. Marc Hershenson for serving on my dissertation committee. I appreciate your insight and wisdom as these have been invaluable to the way I think about my research and to the completion of this dissertation. Thank you, Dr. Robert Kennedy for being on my candidacy committee, for mentoring me during my first rotation, and for your role in helping me secure my first job.

A PhD is a long and often arduous endeavor, but I found myself lifted by the many fantastic people I've grown to know and love in the Meyerhoff Research Group. I'd like to thank the fellow graduate students in the Meyerhoff lab for their mutual support, encouragement, friendship, and occasional co-misery; thank you Natalie Crist, Andrea Bell, Elizabeth Brisbois, Wenyi Cai, Bo Peng, Si Yang, Alex Wolf, Hang Ren, Alex Ketchum, Yaqi Wo, Kyoung Ha Cha, Stephen Ferguson, and Joshua Doverspike for sharing this PhD experience with me. I'd also like

to thank the undergraduates and visiting students that I've come to know during my PhD; thank you Anant Balijepalli, Ian VonWald, Alessandro Colletta, and Joanna Zajda.

I'd like to thank the post-doctoral fellows and visiting scholars that have made their way through our group for their expertise, wisdom, and friendship; thank you, Dr. Gary Jensen, Dr. Dipankar Koley, Dr. Kun Liu, Dr. Yu Qin, Dr. Gergely Lautner, Dr. Woong Hee Lee, and Dr. Xuewei Wang. I'd like to extend special thanks to Dr. Gary Jensen who was my lab mentor when I first joined the group and also a co-author on my first publication. Thank you for being ready to answer all of my questions, and sharing with me your knowledge and experience.

There are also a number of friends I'd like to acknowledge in and outside the Meyerhoff lab for their companionship and support. Thank you, Adam Schneider, for being a great roommate throughout our time in Ann Arbor, and for sharing our mutual passion for sports, music, and animated comedies. Thank you, Eli Fahrenkrug, for being a wise friend, an inspiring scientist with a great DIY attitude, and for introducing me to my love of commuting by bicycle and drinking artisanal coffee. Thank you, Jonathon Bennion, Matthew Gunsch, and Kevin Ileka, for being fantastic roommates during my third year of graduate school and all the great times/shenanigans at our house on Woodlawn. Thank you, Alex Wolf and Alex Ketchum for sharing with me the graduate school experience as well as our love of video games, comics, and movies.

Finally, I'd like to thank my loving parents, Dr. Renjian Zheng and Dr. Xianchun Huang, for whom this dissertation is dedicated. Thank you for your unconditional love and showing me the value of work ethic, humility, courage, and generosity. Your support has helped me through trying times and allowed me to view things in a more positive light. I love you both dearly.

TABLE OF CONTENTS

LIST OF TABLES

LIST OF FIGURES

ABSTRACT

Novel Enhancements and Analytical Applications of Amperometric Nitric Oxide (NO) Sensors

by

Zheng Zheng

Chair: Mark E. Meyerhoff

Improvements to the selectivity of the Shibuki-design and solid-polymer electrolyte (SPE) based amperometric NO sensors are described in this dissertation. Novel applications of SPE-based NO sensors are also demonstrated with results compared with those obtained using chemiluminescence as a reference method.

The selectivity with respect to aqueous-phase interfering species of Shibuki-type sensors is substantial; however, certain gas-phase species such as CO are major interferences. By increasing the pH of the internal electrolyte solution, the selectivity of Shibuki-design sensors vs. CO can be improved by up to 100-fold (Chapter 2). This improvement is the result of more extensive Pt-oxides formed on the electrode surface that inhibits CO adsorption.

Gas-phase detection of NO requires a high surface area electrode, which can be deposited into the surface of a solid-polymer electrolyte (SPE) such as Nafion (Chapter 3). Pt-Nafion sensors exhibited excellent performance with a limit of detection (LOD) of 4.3 ± 1.1 ppb and response time under 5 s. Detection of NO released from NO-donor doped biomedical polymer films and electrochemically reduced nitrite solutions was performed using Pt-Nafion sensors and

repeated using chemiluminescence. Strong agreement was found for both the NO-releasing films and the electrochemically reduced nitrite solution. In Chapter 4, several strategies were explored to enhance the selectivity of the Pt-Nafion sensors. Filtration of the sample gas was shown to be promising for the removal of CO (using an activated carbon fiber filter) and NH_3 (using various acid traps) although further optimization of conditions is needed. Sampled current/sensitivity voltammetry of NO, CO and NH_3 did not reveal a potential range with substantially improved selectivity and applying the principles developed in Chapter 2 (elevated internal electrolyte) also proved ineffective because Nafion cannot transport anions such as OH^- or NO_2^-.

Despite the current selectivity limitations, Pt-Nafion sensors have other useful applications (Chapter 5). The determination of nitrite and GSNO was examined with LOD of 26±5 nM and 17±10 nM, respectively. NO delivered by a cost-effective inhaled nitric oxide therapy (INO) system was monitored with no adverse effects from altering O_2 concentration. NO_2 sensing and scrubbing were also developed as potential safety measures.

CHAPTER 1

INTRODUCTION

1.1 Significance of Nitric Oxide (NO)

Until the late 1980's, NO was largely regarded as an intermediate in chemical production and as an insidious environmental pollutant resulting from industrial and automotive combustion. However, in 1987, NO was identified as the endothelial-derived relaxing factor (EDRF)[1,2] and significant research efforts have since been made to elucidate and understand its many roles as they pertain to physiological and biochemical processes. In order to probe these systems, for both research and clinical purposes, analytical tools are required to isolate, identify, and quantify NO with sufficient spatial/temporal resolution, sensitivity, and selectivity. In this dissertation, novel modifications, materials, and sensor configurations are explored in an effort to improve the performance and applicability of amperometric nitric oxide sensors in potential research and clinical settings.

1.1.1 Physiological Origins and Basic Chemistry of NO

Since its discovery as the EDRF, NO has been implicated in a number of critical physiological functions in addition to vasodilation, including neurotransmission,[3,4] inhibition of platelet adhesion /activation,[5,6] and as a potent antimicrobial agent.[7] NO is generated

endogenously as the result of the catalyzed conversion of L-arginine to L-citrulline via heme-based enzymes known as NO synthases.[8] There are three isoforms of NO synthase (NOS): endothelial-NOS (eNOS),[9] neuronal-NOS (nNOS),[3,10] and inducible-NOS (iNOS).[5,11]

Endothelial-NOS and nNOS are calcium (Ca^{2+}) dependent enzymes and their production of NO is regulated by calcium concentrations while iNOS activity is calcium independent, and is upregulated in response to inflammation. The mechanism of NOS-catalyzed NO production[12–15] (Figure 1.1) proceeds via a two-electron oxidation of L-arginine in the presence of oxygen and one equivalent of NADPH to form an N-hydroxy-L-arginine intermediate (NOHLA). NOHLA then undergoes a three-electron oxidation in the presence of oxygen and 0.5 equivalents of NADPH to form L-citrulline and NO. In its role as a vasodilator, NO produced in the endothelial cell wall, which lines all blood vessels, diffuses toward the underlying smooth muscle cells and activates soluble guanylate cyclase, resulting in a cascade of enzymatic reactions that ultimately results in smooth muscle relaxation and vasodilation. NO also serves to inhibit platelet adhesion and activation along the endothelial wall to prevent blood clots and ensure unobstructed blood flow. More in-depth treatments of the biochemistry of NOS and physiology of NO are presented in a number of reviews[16–20] and texts.[21]

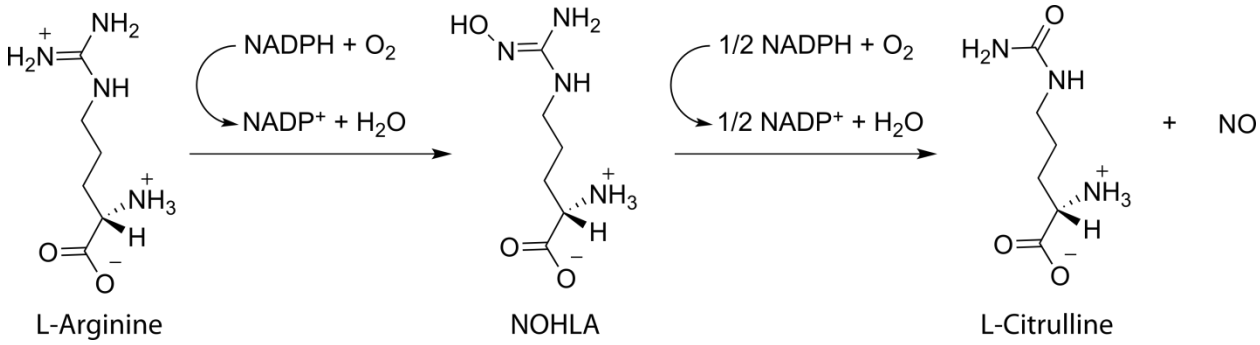

Figure 1.1. NOS-mediated synthesis of NO from L-arginine.

NO is a diatomic radical that exists as a colorless gas under standard conditions and is a highly transient molecule in oxygenated environments due to third-order reactivity with oxygen[22] to produce NO_2 (1.1), N_2O_3 (1.2), and ultimately nitrite (NO_2^-) in the presence of water (1.3). NO is also rapidly scavenged by oxyhemoglobin, which is present physiologically in blood at concentrations up to 10 mM, to form methemoglobin and nitrate (NO_3^-) (1.4) at a rate of $3x10^7$ M^{-1} s^{-1}.[23] Reactive oxygen species such as superoxide also react with NO to generate compounds of even greater oxidative stress such as peroxynitrite (1.5).[24]

$$2NO + O_2 \rightarrow 2NO_2 \quad (1.1)$$

$$NO + NO_2 \leftrightarrow N_2O_3 \quad (1.2)$$

$$N_2O_3 + H_2O \rightarrow 2NO_2^- + 2H^+ \quad (1.3)$$

$$\text{Hb-Fe(II)-}O_2 + NO \rightarrow \text{Hb-Fe(III)} + NO_3^- \quad (1.4)$$

$$NO + O_2^- \rightarrow OONO^- \quad (1.5)$$

Due to the reactive promiscuity of NO towards physiologically relevant compounds, NO has a lifetime on the order of milliseconds within the blood stream and seconds extravascularly;[25,26] therefore, free NO does not exist to a significant extent in most biological environments. This presents a unique challenge to investigators seeking to understand its properties and interactions with already complex physiological systems.

1.1.2 NO-Releasing Compounds: S-Nitrosothiols (RSNO) and Nitrite

While free NO is relatively transient under physiological conditions and is produced in response to changes in [Ca^{2+}] and inflammation, there are other sources or "reservoirs" of NO that liberate NO under given conditions. These compounds represent alternative sources of NO when NOS-mediated NO production is dysfunctional, and have the potential for applications in therapeutic strategies where additional NO is required.

S-Nitrosothiols (RSNO) are small thiol-based molecules (e.g., cysteine, N-acetyl-penicillamine, etc.) as well as proteins and peptides with cysteine residues where the thiol groups are nitrosated (Figure 1.2). The roles of endogenous RSNO's are analogous to those of NO and include (but are not limited to) vasodilation and neurotransmission. Endogenous levels of RSNOs may also serve as diagnostic indicators of a number of critical physiological conditions and ailments such as endothelial cell dysfunction, sepsis,[27] and cystic fibrosis.[28]

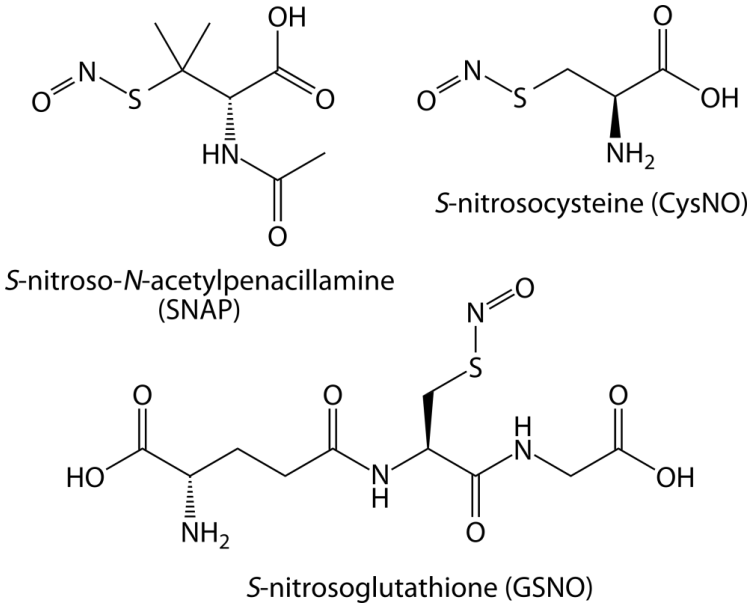

Figure 1.2. Structures of common S-nitrosothiols.

RSNO formation occurs endogenously when a portion of NO from NOS-mediated production is oxidized to nitrous acid (HNO_2) and eventually N_2O_3 (1.2-1.3, 1.6-1.7), which spontaneously decomposes to nitrosonium ions (NO^+) and nitrite (1.8); NO^+ can then react with the free thiol on a cysteine residue to produce an RSNO.[29] Low molecular weight (LMW) RSNO's are more thermodynamically stable and the transfer of NO from a high molecular weight (HMW) RSNO to an LMW RSNO occurs spontaneously; this is known as trans-nitrosation.[30] Common LMW RSNO's found endogenously include *S*-nitrosocysteine (CysNO) and *S*-nitrosoglutathione (GSNO), while HMW RSNO's include *S*-nitrosoalbumin (AlbSNO) and *S*-nitrosohemoglobin (HbSNO). NO is released from RSNO's when the S-NO bond is cleaved by thermal excitation, visible light irradiation,[31] or metal ion catalysis,[32] generating 0.5 equivalents of the corresponding disulfide (1.9).

$$H^+ + NO_2^- \leftrightarrow HNO_2 \quad (1.6)$$

$$2HNO_2 \leftrightarrow H_2O + N_2O_3 \quad (1.7)$$

$$N_2O_3 \rightarrow NO_2^- + NO^+ \quad (1.8)$$

$$2RS\text{-}NO \rightarrow RS\text{-}SR + 2NO \quad (1.9)$$

RSNO's can also be prepared synthetically for the purpose of studying their chemistries *in vitro* and as NO-donor molecules for incorporation into biomedical polymers to enhance biocompatibility and to impart anti-microbial properties.[33,34] Simple nitrosation of physiologically relevant RSH's can be achieved by generating NO^+ in the presence of a cysteine-containing molecule like glutathione by forming nitrous acid (1.5-1.8) using nitrite and a strong acid such as sulfuric acid. A similar procedure is employed in the synthesis of solid crystalline

S-nitroso-*N*-acetyl-penicillamine (SNAP),[33,35] a model RSNO used extensively as a source of NO in biomaterials because of its relatively high stability, low toxicity, and favorable behavior within biomedical polymer phases.

Nitrite was once thought to be primarily an end-product of NO oxidation (along with nitrate), but is, in fact, the largest vascular reservoir of NO[17,36] and is perhaps the simplest and most stable source of NO. Reduction of endogenous nitrite anions can occur via several routes including enzymatic reduction via xanthine oxidoreductase, non-enzymatic reduction via acidification in the stomach, and reaction with ascorbate, polyphenols, and deoxyhemoglobin.[17,36,37] These findings suggest that nitrite is recycled *in vivo* as an alternative source of NO, especially under hypoxic conditions.

From a laboratory perspective, nitrite is an inexpensive and stable source for NO production. A common preparation of saturated NO stock solution involves acidifying a large quantity of nitrite (pKa = 3.4) with an excess of protons (often from sulfuric acid) to produce HNO_2, which spontaneously decomposes to NO and NO_2 gas. The gas mixture is then filtered through sodium hydroxide (NaOH) to remove NO_2 leaving pure NO gas. This is often the preferred method for obtaining pure NO; disproportionation of NO under high pressure to N_2O and NO_2 makes storage of pure NO gas in pressurized cylinders uneconomical and impractical. Low concentrations of NO in an inert balance gas such as N_2 are much more stable.

Nitrite can also be electrochemically reduced to NO at varying rates depending on the magnitude of the applied potential or current, although side products are often formed (N_2O, N_2, NH_2OH, NH_3).[38] Preferential NO generation and lowering of the required applied potential or current for this electrochemical reduction can be achieved through catalysis via inorganic copper ion (Cu(II)) complexes that mimic the metalized active sites of nitrite reductase enzymes.[39]

There is immense potential in this technique because of the advantages associated with nitrite as an NO source (low cost, stable, solid/dissolved phase rather than compressed gas) and the unprecedented degree of control that can be imposed over the NO-release functionality.

There are other synthetic NO-donor compounds such as diazeniumdiolates (NONOates); however, their NO-release properties have proven difficult to control (proton driven release, which may require release of another compound to supply protons) and the NO released can oxidize to an intermediate that can back-react with amine sites that had initially possessed the diazeniumdiolate functional group to form toxic nitrosamines. Therefore, for the purposes of this dissertation, only RSNO's and nitrite will be explored and exploited as target analytes and controlled sources of NO.

1.2 Electrochemical Detection of NO

The transient nature of NO creates a unique problem for investigators seeking to understand its role and influence on physiological phenomena. A number of techniques have emerged for the quantitative characterization of NO within a number of different sample matrices and phases; however, most rely on, non-portable, and often indirect routes such as the Griess assay, which measures nitrite spectroscopically[40,41] after NO oxidation in oxygenated solutions, or by measuring methemoglobin after NO reaction with oxyhemoglobin.[42] Electron paramagnetic resonance (EPR)[43] and fluorescence[44,45] are more direct and sensitive methods, but they still require the formation of NO complexes with exogenous spin traps and fluorescent tags, respectively. A more comprehensive review of existing analytical techniques for NO characterization is available.[46]

The most direct methods for NO measurement are currently chemiluminescence and electrochemical techniques. Chemiluminescence is considered the gold standard for NO detection in research and clinical settings. There are two common reactants used to generate chemiluminescence from NO: luminol/H_2O_2 and ozone (O_3). The luminol-based system[47] is employed for high sensitivity and selectivity measurements of NO in aqueous phase (LOD of 0.1 pM[48] or 0.3 ppb[49] if gaseous sample is bubbled into luminol solution) while the ozone-based system[48] (Figure 1.3) is better suited for gas phase NO measurements (LOD of 0.5 ppb) because it relies on a homogeneous gas-phase reaction. The ozone-based method can also be used for aqueous samples and is available through commercial instrumentation (General Electric's Nitric Oxide Analyzer or NOA) and is easier to maintain. The reaction between O_3 and NO generates NO_2 in an excited state which, upon relaxation to the ground state, emits a photon at wavelengths (600-1200 nm and above; most interfering ozone reactions generate photons of wavelengths <600 nm and are filtered out)[50] specific to the reaction.

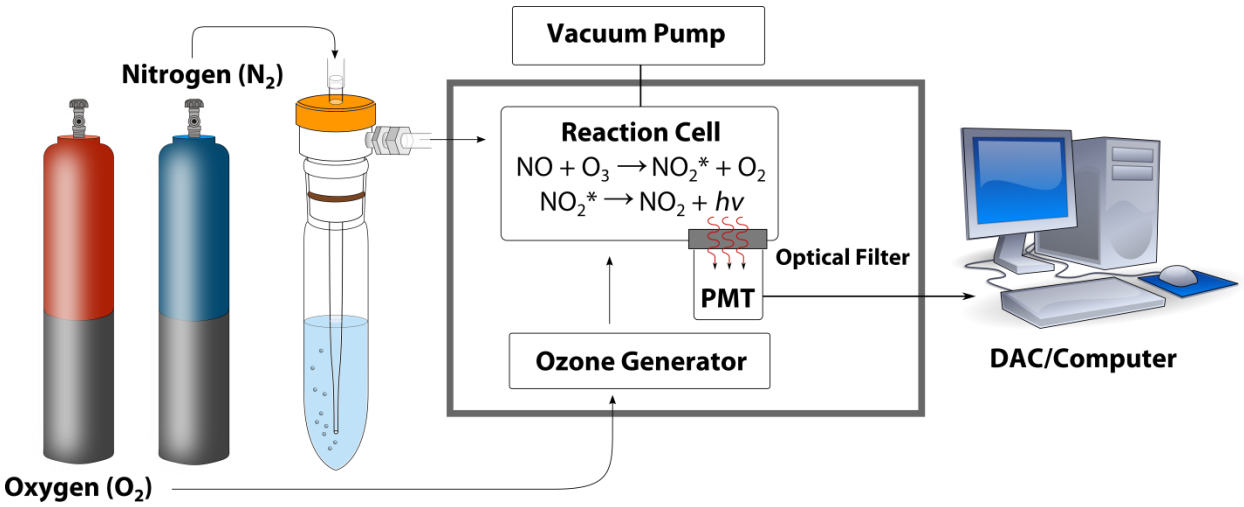

Figure 1.3. Schematic of ozone-based chemiluminescence NO analyzer.

Despite the high sensitivity and high selectivity of chemiluminescence techniques, they suffer poor spatial resolution, lack of portability and high cost to acquire (e.g., $25-35,000), maintain and operate. Chemiluminescence is thus a tolerable but impractical method for use in clinical point-of-care settings. Electrochemical methods can offer smaller form-factor, better spatial resolution, and competitive analytical performance at a lower cost, making them attractive and viable alternatives to more costly and arduous methods for both clinical and research applications.

1.2.1 Clark-type Amperometric Sensors

One of the earliest electrochemical NO sensors developed was an adaptation of the Clark-type oxygen sensor. This compact amperometric NO sensor was pioneered by neuroscientist Katsuei Shibuki in 1991 to monitor changing NO concentrations at the surface of rat cerebellums in response to electrical white matter stimulation and addition of a NOS inhibitor (*N*-methylarginine).[51–53] Like the Clark-type oxygen sensors, Shibuki's NO sensor consisted of an electrochemical cell (Pt working electrode, Ag/AgCl reference electrode, 0.3 mM HCl in 30 mM NaCl internal electrolyte) enclosed in an insulating housing, which had an opening near the working electrode that was sealed with a gas-permeable membrane (GPM) made from chloroprene rubber (Figure 1.4).[46] NO is a gas-phase molecule under ambient conditions and can readily diffuse across the GPM into the internal electrolyte and be electrochemically oxidized to nitrite and nitrate at the working electrode under constant potential, generating a current proportional to the NO concentration. The GPM prevents the diffusion of aqueous interfering electroactive species such as nitrite, ascorbate, urate, and acetaminophen, into the sensor and thus provides impressive selectivity against such species.

Another advantage of this design is the isolation of the reference electrode from the sample environment, allowing the investigator to control and maintain a relatively constant reference potential with minimal risk of reference electrode fouling.

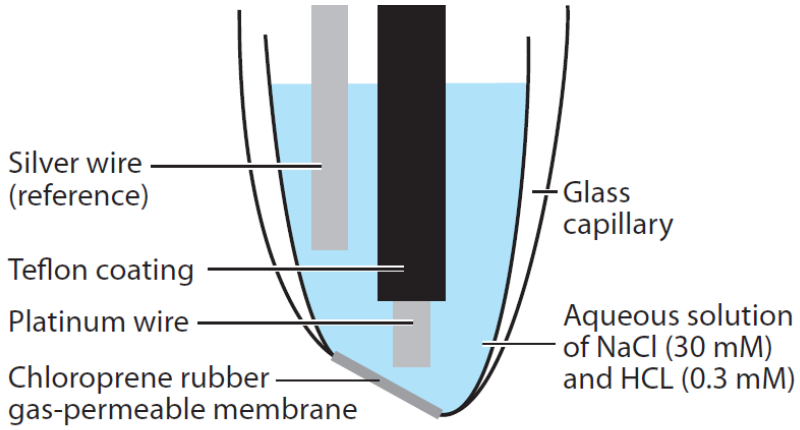

Figure 1.4. Schematic of the Shibuki-design amperometric NO sensor.[46]

Since the inception of the Shibuki-design NO sensor, a number of important developments have been made to improve its analytical performance and viability in research applications. For example, porous polytetrafluoroethylene (PTFE or Teflon®) gas permeable membranes have since been adopted in several sensor designs.[54–56] In 2004, Youngmi Lee *et al.* platinized the working electrode (electrodeposited clusters of Pt, also known as Pt-black, on the working surface), which improved sensitivity and limits of detection by about an order of magnitude (1 nM).[54,55] The sensor was then used to monitor changes in NO production at the surface of porcine kidney slices in response to the addition of various NO precursors such as arginine, protamine, and various polyarginine sources.[54] The improvement in analytical performance was attributed to the increased surface area and catalytic activity of Pt black.

In 2011, Cha and Meyerhoff[56] demonstrated improved selectivity over ammonia and nitrite by infusing the pores of the PTFE GPM with Teflon AF, a copolymer of tetrafluoroethylene and 2,2-bis(trifluoroethylene)-4,5-difluoro-1,3-dioxole. It was postulated that Teflon AF rejects certain gas molecules because of preferential NO partitioning into the fluoropolymer vs. that of NH_3.[56] The coating did not adversely affect the sensor's sensitivity towards NO although an increase in response time was observed and is expected due to the hindrance of mass transport by a less porous GPM.

Selectivity vs. carbon monoxide (CO) has received greater attention in recent years after a long period of NO sensor development that largely overlooked this issue. CO is a small gas molecule with physiological concentrations up to an order of magnitude greater than NO.[57,58] CO has important physiological functions of its own, many of which are incredibly similar to those of NO.[59] Endogenous CO concentrations have also been shown to have varying degrees of interdependence with NO concentrations in certain systems,[59,60] further complicating analysis. Strategies for combatting CO interference will be investigated and considered at great length in this dissertation.

The Shibuki-design is also the basis for amperometric RSNO sensors, which indirectly measure RSNO's via detection of local NO release upon RSNO decomposition near the sensing surface. The earliest reports of electrochemical RSNO detection utilized homogeneous catalysis of RSNO's in bulk solution prior to NO detection,[61] which served as a valuable initial proof-of-concept, but had practical limitations.

The base sensor for a modern Shibuki-design RSNO sensor is identical to that of an amperometric Shibuki-design NO sensor; however, an additional membrane layer is applied atop the GPM which contains a catalyst that locally decomposes RSNO to NO. The NO produced

then diffuses across the GPM and is detected at the working electrode (Figure 1.5).[62] The earliest amperometric Shibuki-design RSNO sensors were developed using copper-based catalysts loaded into polyurethane-based polymer films and has a limit of detection if ~1 µM.[63] Later iterations of this sensor design had more consistent sensitivity across different RSNO's with improved overall limit of detection (~0.1 µM) and employed dialysis membranes modified with functionalized polyethyleneimine (PEI) containing organoselenium[62] or organotelluride[64] catalysts.

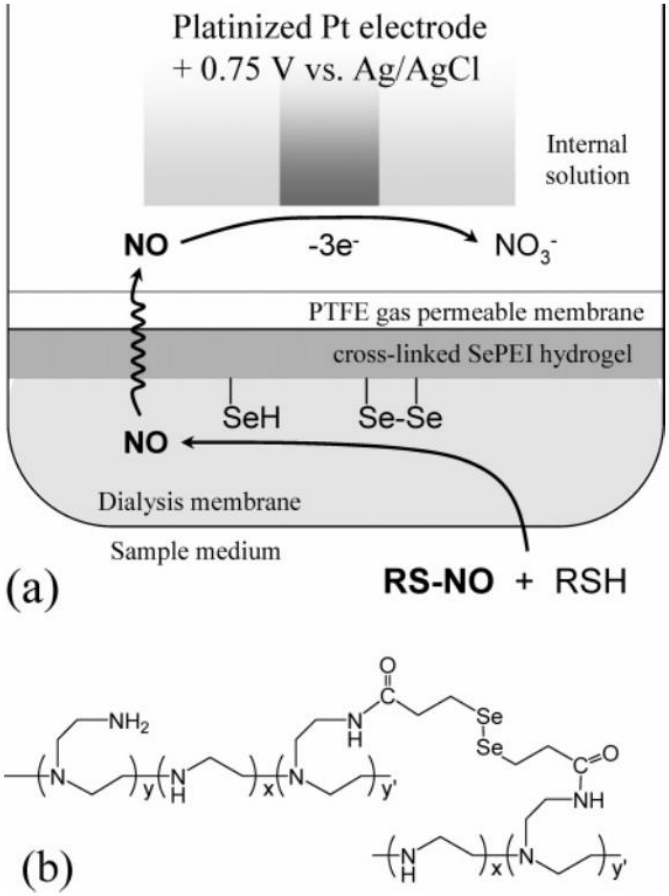

Figure 1.5. (a) Amperometric detection scheme of RSNO sensor based on catalytic RSe-PEI hydrogel.(b) Structure of cross-linked RSe-PEI hydrogel layer.[62] Reprinted (adapted) with permission from Langmuir, 22 (25), 10830–10836. Copyright 2006 American Chemical Society.

One of the challenges associated with RSNO sensors based on the Shibuki-design is response time; the additional dialysis membrane limits diffusion of NO to the working electrode surface and as a result, reduces temporal resolution. Another concern is leaching of free catalyst into the bulk sample, which would lead to homogeneous catalytic release of NO, which would then be scavenged by other species such as oxyhemoglobin and superoxide. More recent strategies for amperometric RSNO detection have employed photolytic decomposition of RSNO's using narrow band visible LED's in proximity to the working electrode surface (that detects liberated NO) in microfluidic devices.[65] The advantage of this arrangement is the fact that photolytic decomposition does not require synthesis of catalytic membranes and can be modulated at will. The sensor in this microfluidic system is not a Shibuki-design NO sensor, and will be described in greater details in the following section.

1.2.2 Needle-type Amperometric Microsensors

Around the same time that Shibuki developed the adapted Clark-style NO sensor (Shibuki-design), Malinski *et al.* developed an electropolymerized porphyrinic film, nickel(II) tetrakis(3-methoxy-4-hydroxy-phenyl)porphyrin, or Ni(II)TMHPP, with enhanced oxidative electrocatalysis properties[66] and subsequently demonstrated its application in detecting NO from single cells.[67,68] While the film was shown to be adherent to several electrode materials (Pt, Au, and glassy carbon),[66] the sensor was fashioned from a thermally sharpened carbon fiber (Figure 1.6). Ni(II)TMHPP was electropolymerized on the surface of the fiber potentiodynamically and dip-coated with a layer of Nafion as a permselective membrane.

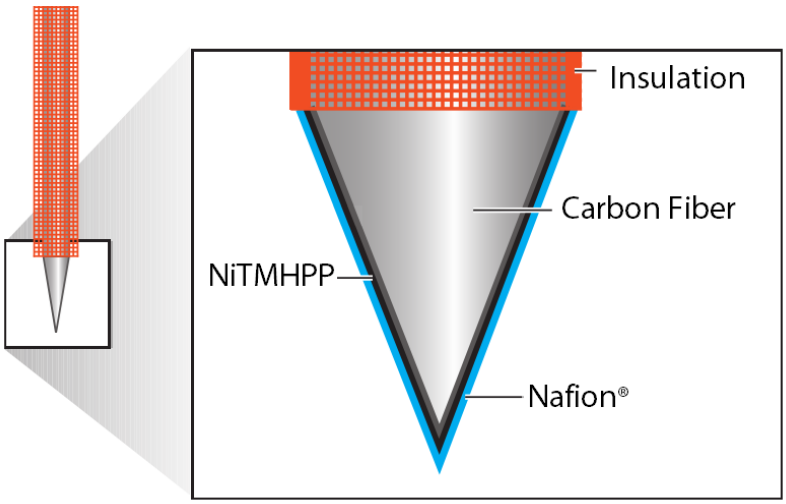

Figure 1.6. Schematic of amperometric NO microsensor with electropolymerized NiTMHPP as catalytic enhancement layer and Nafion permselective coating.

Nafion is a tetrafluoroethylene copolymer with sulfonate functional groups (Figure 1.7) and is widely used a cationic exchange material in research fields and in applications ranging from hydrogen fuel cells to synthetic organic catalysis. In the field of electrochemical sensors, it serves as a hydrophilic membrane and solid-polymer electrolyte (SPE) with permselective properties that impart selectivity against anionic interfering species, which are generally the most susceptible to electro-oxidation. Another key advantage to this sensor was the spatial resolution it could achieve by virtue of its size. A disadvantage is the exposed external reference electrode, which is susceptible to fouling and changes in reference potential.

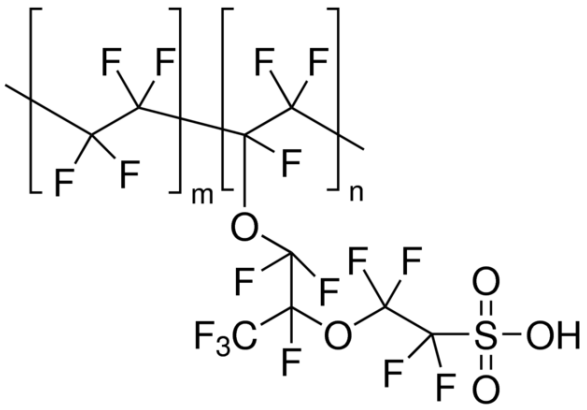

Figure 1.7. Structure of Nafion monomer unit in proton form; note the cationic exchange site (hydroxyl).

The porphyrinic microsensor saw substantial impact and employment in early biological NO studies but lacked selectivity vs. carbon monoxide (CO). As mentioned in section 1.2.1, CO selectivity is a relevant and warranted concern in amperometric NO sensing of biological systems. Because Nafion is permeable to gases, CO is not excluded and may contribute to artificially high NO estimates. In 2005, Ho *et al.* developed a sol-gel based fluoropolymer (xerogel), which was used in a coating containing up to 17% Nafion, for the preparation of needle-type NO microsensors.[69] The resulting sensor exhibited high selectivity vs. nitrite and good limits of detection for NO (25 μM). Further developments of the xerogel formulation led to the application of a Nafion-free membrane with very high selectivity vs. anionic interfering species as well as impressive exclusion of CO ($\log K_{NO,CO}$ = -1.3 or ~5% of NO sensitivity).

A xerogel coating has also been employed in microfluidic devices for the determination of RSNO's in blood plasma[65] by reducing the background currents generated by interfering species. The coating was applied to a Pt electrode patterned on a PDMS microfluidic device via evaporative sputtering. The sensor had impressive limits of detection towards LMW RSNO's and estimated total plasma RSNO from porcine blood to be 1.5 ± 1.0 μM, which is within the range of RSNO concentrations previously reported using other techniques.[65]

1.2.3 Solid-Polymer Electrolyte based Amperometric Gas Sensors

While aqueous-phase NO research accounts for the greater part of the physiological NO sensing literature, there has been recent increased interest in gas-phase NO measurements, especially in regards to (fractional) exhaled nasal NO or "FeNO". Exhaled nasal NO has been shown to correlate with the onset of several physiological conditions and diseases (including asthma,[70,71] chronic rhinosinusitis,[72] cystic fibrosis,[71,73] and primary ciliary dyskinesia[58]), which makes it a measurement of diagnostic and clinical value. FeNO concentrations are often in the mid to low ppb range,[74] which is theoretically beyond the capabilities of currently established Shibuki-type NO sensor designs due to instability of the thin aqueous layer between the GPM and the working electrode surface under direct gas flow[75] as well as thermodynamic constraints (i.e., equilibrium concentration of NO in the aqueous thin layer under low ppb gaseous NO flow is below detection limits achievable by the sensor).

The electrochemical detection of gas-phase NO in the low ppb range requires a highly sensitive sensor with low noise and stable response to changes in concentration. One approach to fabricating such a sensor is by utilizing a solid-polymer electrolyte, like Nafion, as a high surface area scaffold for the deposition of a porous Pt layer. The earliest academic report of this process[76] employed the Takenaka and Torikai (TT) method,[77] that calls for a solid Nafion film to be situated in a diffusion cell with a plating metal salt solution (chloroplatinic acid) on one side and reducing agent (sodium borohydride) solution on the other. As the two solutions diffuse into the membranes, Pt is plated where the two solution fronts meet. A later method, known as the impregnation-reduction (IR) method,[78] achieved Pt deposition by impregnating the Nafion membrane with Pt ions prior to placement in a diffusion cell and exposing only one side of the membrane to a reducing agent (Figure 1.8). This method produced sensors with the electrode

plated consistently close to the surface of the membrane (Figure 1.9)[78] and has been the preferred approach in many subsequent papers on the subject.

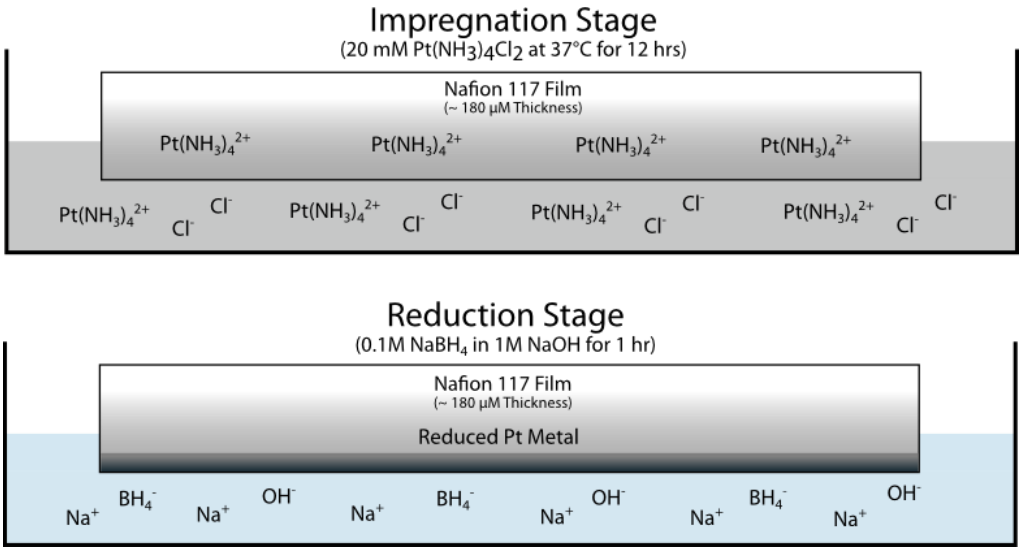

Figure 1.8. Schematic of the impregnation-reduction method for Pt deposition on Nafion 117 ion-exchange film.

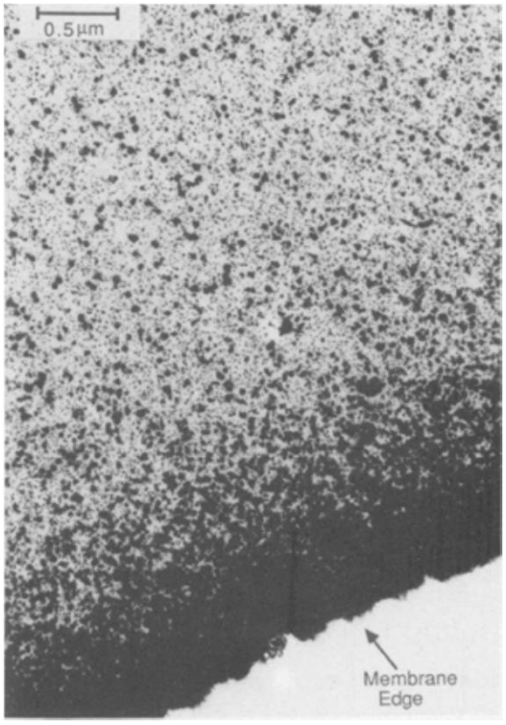

Figure 1.9. Cross-sectional transmission electron micrograph of a Nafion film platinized via IR method.[78] The blackened areas represent deposited Pt clusters. Reprinted with permission from the Journal of the Electrochemical Society, 136 (3), 899. Copyright 1989.

Once a working electrode has been plated onto the Nafion membrane, it is placed between a gas inlet/outlet chamber and an electrolyte chamber with the deposited side facing the gas inlet (Figure 1.10). A constant anodic potential is applied as gas is passed across the surface of the Pt/Nafion membrane electrode under a controlled flow rate, generating current proportional to the analyte concentration. This sensor arrangement has been employed for a number of gases including, but not limited to: NO,[79–81] NO_2,[79] ethylene,[82,83] and SO_2.[83,84] This type of sensor can achieve very low limits of detection (<20 ppb for NO) and fast response times (<5 s), often limited only by dead volume in the flow scheme plumbing. Currently, the most notable drawback of this sensor design is its inherently poor specificity across a number of different gases. NO electro-oxidation on Pt/Nafion electrodes has an optimal sensitivity at an applied potential of 1 V vs. Ag/AgCl, which is fairly high and overlaps directly with oxidative potentials for gases such as CO and other volatile organics. This presents a major obstacle in the application of SPE-based gas sensors for detection of specific gas species (such as NO) in complex sample matrices such as exhaled breath, which contains numerous volatile compounds, many of which exceed the NO concentration and cannot be discriminated at 1V.

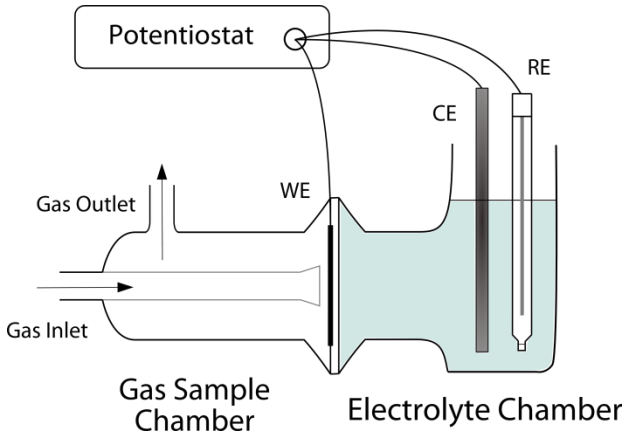

Figure 1.10. Schematic of SPE-based amperometric gas-phase NO sensor configuration.

1.2.4 Other Electrochemical NO Sensors

In addition to the methods described above, there are several other electrochemical techniques for the detection of NO. Solid-state conductometric sensors have been developed for the detection of gaseous analytes such as NO, and have been dubbed "electronic noses" or "e-noses". The basic principle behind these sensors is that the conductivity of the sensing substrate (often an extrinsic semiconductor or metal oxide semiconductor) changes when gas molecules or specific thermal products of gas molecules adsorb to the surface. The primary advantage of a conductometric sensor is that it does not require an electrolyte or additional electrodes (in fact it is barely an electrochemical cell; it is simply a single solid-phase resistor in series). Unfortunately, the response times (minutes to tens of minutes) and detection limits (low ppm) of these sensors are currently unacceptable for FeNO measurements and they require elevated operating temperatures (from several hundred to over 1000°C),[85,86] often leading to additional concerns over sensor stability.[87] While these sensors have a place in automotive and industrial emissions testing, they remain unsuitable for biological applications.

Potentiometric nitrate determination has also been investigated as an indirect method for NO detection.[88] Nitrate is formed when NO is scavenged by oxyhemoglobin (1.4) and can be detected using an anion-selective electrode. In this method, a solution of oxyhemoglobin is purged with the sample gas (NO released from polymeric films doped with SNAP or nitrite solutions catalyzed by copper complexes) and is then analyzed for nitrate. The moles of nitrate can be determined and normalized over the volume of gas used to purge the oxyhemoglobin solution to determine NO concertation. An advantage of this configuration is that it is readily compatible with flow-injection analysis. However, it has limited analytical performance (~1.5 μM detection limit for nitrate) and requires considerable time for analysis (up to 30 min per sample depending on NO flux).

Due to the current limitations of the technologies described in this section, the remainder of this dissertation will focus on the development of amperometric techniques.

1.3 Statement of Research

In this dissertation, novel materials and modifications for the electrochemical determination of NO are explored and evaluated for analytical performance, stability, and viability in research and clinical applications. The primary electrochemical method in this work is amperometry, a potentiostatic approach where current is measured in response to changes in analyte concentration.

Chapter 2 describes a novel modification to modern Shibuki-design amperometric NO sensors to improve selectivity vs. carbon monoxide (CO). A direct modification of the working electrode surface was achieved by altering the internal electrolyte from a dilute hydrochloric acid saline solution to a phosphate saline solution buffered at pH 11. The alkaline electrolyte

promotes the formation of a thin surface oxide on the Pt working electrode, which is demonstrated to inhibit CO adsorption. Prevention of this adsorption process effectively reduces CO interference on Shibuki-design sensors and was confirmed via cyclic voltammetry experiments. The stability of this modification was further assessed and the sensor performance in the presence of CO_2 was also determined since CO_2 is capable of potentially titrating the inner alkaline buffer within the electrolyte thin-film of the sensor. The findings in this chapter are published in ACS Analytical Chemistry.[89]

In Chapter 3, solid-polymer electrolyte (SPE) based amperometric gas-phase NO sensors are adapted and applied for the characterization of NO released from NO-donor biomaterials and biomedical devices. Analytical performance and surface characterization of Pt chemically deposited on Nafion was performed and reported. The NO release rates from SNAP-doped Carbosil2080A polymer films and buffered nitrite solution with homogeneous copper(II)-tri(2-pyridylmethyl)amine (CuTPMA) catalyst were characterized using the platinized Nafion-based NO gas sensors and chemiluminescence (reference method). NO release data from both methods were normalized to pmol s^{-1} and compared, showing close correlation and parity between results from the two methods. Native selectivity vs. CO was also investigated and it was determined that a conditioning period improved the selectivity considerably. The findings in this chapter are published in Analytica Chimica Acta.[90]

In Chapter 4, strategies for improving the selectivity of solid-polymer electrolyte (SPE) based amperometric gas-phase NO sensors are explored in further detail in the pursuit of a sensor capable of discriminating ppb levels of NO in complex matrices such as exhaled nasal breath. Filtration/treatment of the sample stream through carbon and Nafion-based materials were tested

along with investigations of sensor selectivity as a function of applied potential. Efforts are also described to use alkaline internal solutions much like the strategy developed in Chapter 2.

In Chapter 5, additional applications of solid-polymer electrolyte (SPE) based amperometric gas-phase NO sensors are examined. Notably, a monitoring system for a cost-effective inhaled nitric oxide therapy (INO) device is described. Nitrite and RSNO detection and calibration without the use of NO gas standards are also demonstrated as an effective application.

1.4 References

(1) Palmer, R.; Ferrige, A.; Moncada, S. *Nature* **1987**, *327*, 524.

(2) Ignarro, L.; Buga, G. *PNAS* **1987**, *84* (December), 9265.

(3) Bredt, D. S.; Hwang, P. .; Snyder, S. *Nature* **1990**, *347*, 768.

(4) Bredt, D. S.; Snyder, S. H. *Neuron* **1992**, *8* (1), 3.

(5) Radomski, M. W.; Palmer, R. M.; Moncada, S. *PNAS* **1990**, *87* (13), 5193.

(6) Kubes, P.; Suzuki, M.; Granger, D. N. *PNAS* **1991**, *88* (11), 4651.

(7) Nathan, C. F.; Hibbs, J. B. *Curr. Opin. Immunol.* **1991**, *3* (1), 65.

(8) Nathan, C.; Xie, Q. W. *Cell* **1994**, *78* (6), 915.

(9) Pollock, J. S.; Förstermann, U.; Mitchell, J. A.; Warner, T. D.; Schmidt, H. H.; Nakane, M.; Murad, F. *Proc. Natl. Acad. Sci. U. S. A.* **1991**, *88* (23), 10480.

(10) Schmidt, H. H.; Pollock, J. S.; Nakane, M.; Gorsky, L. D.; Förstermann, U.; Murad, F. *Proc. Natl. Acad. Sci. U. S. A.* **1991**, *88* (2), 365.

(11) Stuehr, D. J.; Cho, H. J.; Kwon, N. S.; Weise, M. F.; Nathan, C. F. *Proc. Natl. Acad. Sci. U. S. A.* **1991**, *88* (17), 7773.

(12) Förstermann, U.; Sessa, W. C. *Eur. Heart J.* **2012**, *33* (7), 829.

(13) Marletta, M. *Cell* **1994**, *78* (6), 927.

(14) Schmidt, H. H. H. W.; Nau, H.; Wittfoht, W.; Gerlach, J.; Prescher, K. E.; Klein, M. M.; Niroomand, F.; Böhme, E. *Eur. J. Pharmacol.* **1988**, *154* (2), 213.

(15) Palmer, R. M. J.; Ashton, D. S.; Moncada, S. *Nature* **1988**, *333* (6174), 664.

(16) McCleverty, J. A. *Chem. Rev.* **2004**, *104* (2), 403.

(17) Lundberg, J. O.; Weitzberg, E.; Gladwin, M. T. *Nat. Rev. Drug Discov.* **2008**, *7* (2), 156.

(18) Bryan, N. S. *Free Radic. Biol. Med.* **2006**, *41* (5), 691.

(19) Denninger, J. W.; Marletta, M. A. *Biochim. Biophys. Acta* **1999**, *1411* (2-3), 334.

(20) Moncada, S.; Higgs, E. A. *Eur. J. Clin. Invest.* **1991**, *21* (4), 361.

(21) Feelisch, M.; Stamler, J. *Methods in Nitric Oxide Research*; Wiley & Sons: Chichester, England, 1996.

(22) Lewis, R. S.; Deen, W. M. *Chem. Res. Toxicol.* **1994**, *7* (4), 568.

(23) Doyle, M. P.; Hoekstra, J. W. *J. Inorg. Biochem.* **1981**, *14* (4), 351.

(24) Blough, N. V.; Zafiriou, O. C. *Inorg. Chem.* **1985**, *24* (22), 3502.

(25) Liu, X.; Miller, M. J. S.; Joshi, M. S.; Sadowska-Krowicka, H.; Clark, D. A.; Lancaster, J. R. *J. Biol. Chem.* **1998**, *273* (30), 18709.

(26) Thomas, D. D.; Liu, X.; Kantrow, S. P.; Jr., J. R. L. *PNAS* **2001**, *98* (1), 355.

(27) Doctor, A.; Platt, R.; Sheram, M. L.; Eischeid, A.; McMahon, T.; Maxey, T.; Doherty, J.; Axelrod, M.; Kline, J.; Gurka, M.; Gow, A.; Gaston, B. *Proc. Natl. Acad. Sci.* **2005**, *102* (16), 5709.

(28) Grasemann, H.; Gaston, B.; Fang, K.; Paul, K.; Ratjen, F. *J. Pediatr.* **1999**, *135* (6), 770.

(29) Smith, B. C.; Marletta, M. A. *Curr. Opin. Chem. Biol.* **2012**, *16* (5-6), 498.

(30) Barnett, D. J.; McAninly, J.; Williams, D. L. H. *J. Chem. Soc. Perkin Trans. 2* **1994**, No. 6, 1131.

(31) Sexton, D. J.; Muruganandam, A.; McKenney, D. J.; Mutus, B. *Photochem. Photobiol.* **1994**, *59* (4), 463.

(32) McAninly, J.; Williams, D. L. H.; Askew, S. C.; Butler, A. R.; Russell, C. *J. Chem. Soc. Chem. Commun.* **1993**, No. 23, 1758.

(33) Brisbois, E. J.; Handa, H.; Major, T. C.; Bartlett, R. H.; Meyerhoff, M. E. *Biomaterials* **2013**, *34* (28), 6957.

(34) Gierke, G. E.; Nielsen, M.; Frost, M. C. *Sci. Technol. Adv. Mater.* **2011**, *12* (5), 055007.

(35) Chipinda, I.; Simoyi, R. H. *J. Phys. Chem. B* **2006**, *110* (10), 5052.

(36) Cosby, K.; Partovi, K. S.; Crawford, J. H.; Patel, R. P.; Reiter, C. D.; Martyr, S.; Yang, B. K.; Waclawiw, M. A.; Zalos, G.; Xu, X.; Huang, K. T.; Shields, H.; Kim-Shapiro, D. B.; Schechter, A. N.; Cannon, R. O.; Gladwin, M. T. *Nat. Med.* **2003**, *9* (12), 1498.

(37) Benjamin, N.; O'Driscoll, F.; Dougall, H.; Duncan, C.; Smith, L.; Golden, M.; McKenzie, H. *Nature* **1994**, *368* (6471), 502.

(38) Duca, M.; Kavvadia, V.; Rodriguez, P.; Lai, S. C. S.; Hoogenboom, T.; Koper, M. T. M. *J. Electroanal. Chem.* **2010**, *649* (1-2), 59.

(39) Ren, H.; Wu, J.; Xi, C.; Lehnert, N.; Major, T.; Bartlett, R. H.; Meyerhoff, M. E. *ACS Appl. Mater. Interfaces* **2014**, *6* (6), 3779.

(40) Roy, J. B.; Wilkerson, R. G. *Urology* **1984**, *23* (3), 270.

(41) Griess, P. *Berichte der Dtsch. Chem. Gesellschaft* **1879**, *12* (1), 426.

(42) Noack, E.; Kubitzek, D.; Kojda, G. *Neuroprotocols* **1992**, *1* (2), 133.

(43) Wennmalm, A.; Lanne, B.; Petersson, A. S. *Anal. Biochem.* **1990**, *187* (2), 359.

(44) Gomes, A.; Fernandes, E.; Lima, J. L. F. C. *J. Fluoresc.* **2006**, *16* (1), 119.

(45) Kojima, H.; Nakatsubo, N. *Anal. Chem.* **1998**, *70* (13), 2446.

(46) Hetrick, E. M.; Schoenfisch, M. H. *Annu. Rev. Anal. Chem.* **2009**, *2*, 409.

(47) Kikuchi, K.; Nagano, T.; Hayakawa, H.; Hirata, Y.; Hirobe, M. *Anal. Chem.* **1993**, *65* (13), 1794.

(48) Fontijn, A.; Sabadell, A.; Ronco, R. *Anal. Chem.* **1970**, *42* (6), 575.

(49) Robinson, J. K.; Bollinger, M. J.; Birks, J. W. *Anal. Chem.* **1999**, *71* (22), 5131.

(50) Bates, J. N. *Neuroprotocols* **1992**, *1* (2), 141.

(51) Shibuki, K. *Neuroprotocols* **1992**, *1* (2), 151.

(52) Shibuki, K.; Okada, D. *Nature* **1991**, *349* (24), 326.

(53) Shibuki, K. *Neurosci. Res.* **1990**, *9*, 69.

(54) Lee, Y.; Yang, J.; Rudich, S. M.; Schreiner, R. J.; Meyerhoff, M. E. *Anal. Chem.* **2004**, *76* (3), 545.

(55) Lee, Y.; Oh, B. K.; Meyerhoff, M. E. *Anal. Chem.* **2004**, *76* (3), 536.

(56) Cha, W.; Meyerhoff, M. E. *Chem. Anal.* **2006**, *949* (51), 949.

(57) Park, S. S.; Kim, J.; Lee, Y. *Anal. Chem.* **2012**, *84* (3), 1792.

(58) Horváth, I.; Loukides, S.; Wodehouse, T.; Csiszér, E.; Cole, P. J.; Kharitonov, S. a; Barnes, P. J. *Thorax* **2003**, *58* (1), 68.

(59) Wu, L.; Wang, R. *Pharmacol. Rev.* **2005**, *57* (4), 585.

(60) Kajimura, M.; Fukuda, R.; Bateman, R. M.; Yamamoto, T.; Suematsu, M. *Antioxid. Redox Signal.* **2010**, *13* (2), 157.

(61) Pfeiffer, S.; Schrammel, A.; Schmidt, K.; Mayer, B. *Anal. Biochem.* **1998**, *258* (1), 68.

(62) Cha, W.; Meyerhoff, M. E. *Langmuir* **2006**, *22* (25), 10830.

(63) Cha, W.; Lee, Y.; Oh, B. K.; Meyerhoff, M. E. *Anal. Chem.* **2005**, *77* (11), 3516.

(64) Hwang, S.; Meyerhoff, M. E. *J. Mater. Chem.* **2007**, *17* (15), 1462.

(65) Hunter, R. A.; Schoenfisch, M. H. *Anal. Chem.* **2015**, *87* (6), 3171.

(66) Malinski, T.; Ciszewski, A.; Bennett, J.; Fish, J. R.; Czuchajowski, L. *J. Electrochem. Soc.* **1991**, *138* (7), 2008.

(67) Malinski, T.; Taha, Z.; Grunfeld, S.; Burewicz, A.; Tomboulian, P.; Kiechle, F. *Anal. Chim. Acta* **1993**, *279* (1), 135.

(68) Malinski, T.; Taha, Z. *Nature* **1992**, *358*.

(69) Shin, J. H.; Weinman, S. W.; Schoenfisch, M. H. *Anal. Chem.* **2005**, *77* (11), 3494.

(70) Alving, K.; Weitzberg, E.; Lundberg, J. M. *Eur. Respir. J.* **1993**, *6* (9), 1368.

(71) Lundberg, J. O.; Nordvall, S. L.; Weitzberg, E.; Kollberg, H.; Alving, K. *Arch. Dis. Child.* **1996**, *75* (4), 323.

(72) Ragab, S. M.; Lund, V. J.; Saleh, H. a; Scadding, G. *Allergy* **2006**, *61*, 717.

(73) Grasemann, H.; Michler, E.; Wallot, M.; Ratjen, F. *Pediatr. Pulmonol.* **1997**, *24* (3), 173.

(74) Stewart, L.; Katial, R. *Immunol. Allergy Clin. North Am.* **2007**, *27* (4), 571.

(75) Knake, R.; Jacquinot, P.; Hodgson, A. W. E.; Hauser, P. C. *Anal. Chim. Acta* **2005**, *549* (1-2), 1.

(76) Katayama-Aramata, A.; Nakajima, H.; Fujikawa, K.; Kita, H. *Electrochim. Acta* **1983**, *28* (6), 777.

(77) Takenaka, H.; Torikai, E. (Japan Patent). 55-35934, 1980.

(78) Fedkiw, P. S. *J. Electrochem. Soc.* **1989**, *136* (3), 899.

(79) Jacquinot, P.; Hodgson, A.; Hauser, P. *Anal. Chim. Acta* **2001**, *443* (1), 53.

(80) Ho, K.; Hung, W.; Yang, J. *Sensors* **2003**, No. 2, 290.

(81) Ho, K.C.; Liao, J. Y.; Yang, C. C. *Sensors Actuators B Chem.* **2005**, *108* (1-2), 820.

(82) Jordan, L. R.; Hauser, P. C.; Dawson, G. A. *Anal. Chem.* **1997**, *69* (4), 558.

(83) Hodgson, A. W. E.; Jacquinot, P.; Jordan, L. R.; Hauser, P. C. *Electroanalysis* **1999**, *11*, 782.

(84) Chiou, C.Y.; Chou, T.C. *Sensors Actuators B Chem.* **2002**, *87* (1), 1.

(85) Sberveglieri, G. *Sensors Actuators B Chem.* **1995**, *23* (2-3), 103.

(86) Azad, A. M. *J. Electrochem. Soc.* **1992**, *139* (12), 3690.

(87) Korotcenkov, G.; Cho, B. K. *Sensors Actuators B Chem.* **2011**, *156* (2), 527.

(88) Zajda, J.; Crist, N. R.; Malinowska, E.; Meyerhoff, M. E. *Electroanalysis* **2016**, *28* (2), 277.

(89) Jensen, G. C.; Zheng, Z.; Meyerhoff, M. E. *Anal. Chem.* **2013**, *85*, 10057.

(90) Zheng, Z.; Ren, H.; VonWald, I.; Meyerhoff, M. E. Anal. Chim. Acta 2015, 887, 186.

CHAPTER 2

AMPEROMETRIC NITRIC OXIDE SENSORS WITH ENHANCED SELECTIVITY OVER CARBON MONOXIDE VIA PLATINUM OXIDE FORMATION UNDER ALKALINE CONDITIONS

2.1 Introduction

As discussed in Chapter 1, there is demand for effective quantitative methods of NO detection due to the importance of physiological NO to biomedical therapeutics/monitoring as well as chemical, biological, and medicinal research. While a number of techniques have been developed to quantify NO levels, most rely on indirect routes such as the Griess assay,[1] which measures nitrite spectroscopically after NO oxidation in oxygenated solutions, or by measuring methemoglobin after NO reaction with oxyhemoglobin.[2] The most direct methods for NO measurement are currently chemiluminescence[3–5] and electrochemical techniques. While chemiluminescence offers very high sensitivity and selectivity, it is expensive, has poor spatial resolution, and suffers from excessive foaming when used to analyze samples rich in protein.

Electrochemical measurement of NO via oxidation to nitrate offers a number of attractive advantages over other methods. Amperometric sensors have very low limits of detection (<1-10 nM in many cases),[6–8] good selectivity over many potential interfering species, such as nitrite and ascorbate, and can be miniaturized, granting spatial resolution for detection of local concentrations of NO. A variety of amperometric NO sensors have been developed over the last

twenty years, although most are based on either the Clark-type sensor configuration first suggested by Shibuki[9–11] or the solid microsensor scheme originally described by Malinski.[12–14]

Due to the high oxidation potentials required for NO oxidation (e.g., 0.7-0.9 V vs. Ag/AgCl), reducing electrochemical interference has become a recent focus in amperometric NO sensor design and development. Exclusion of ionic species that oxidize directly on the working electrode surface can be achieved through applying perm-selective coatings[7,13,15] or gas-permeable membranes[6,10] to the sensor assembly; however, volatile species, such as carbon monoxide (CO), remain problematic. Depending on the sample type, volatile interfering species can be a significant obstacle in the acquisition of an accurate analytical NO measurement.

Carbon monoxide is a common interfering species in a number of physiological applications of NO sensors, especially for the measurement of NO in exhaled oral and nasal air,[16,17] as well as various tissues that liberate NO. Recently, several studies have focused on overcoming this CO interference problem with amperometric NO sensors. For example, Shin *et al.* have developed a xerogel solid microsensor with CO sensitivity less than 5% of that for NO[7] while Park *et al.* have developed a Shibuki style sensor by co-depositing Fe(III) nanoparticles and Pt black on the Pt working electrode to achieve enhanced selectivity for NO over CO.[18] These efforts to discriminate CO in amperometric NO sensors have been effective to varying degrees, however, fabrication of such sensors can be complex (xerogels must be sufficiently thin and cannot be spread-cast while co-deposition of iron and Pt require additional preparation of iron nanoparticles).

In this chapter, a Shibuki-design amperometric NO sensor based on a Pt working electrode is described that exhibits improved selectivity over CO as a function of the internal electrolyte pH. Using a previously reported sensor design from our group,[6,19] we examine the

effect of internal electrolyte solution pH on the observed selectivity for NO over CO. Almost all Shibuki-design NO sensors reported to date, including the original version of our design, employ acidic internal electrolytes (pH 0-2) that form the layer between the working Pt electrode and the gas permeable membrane of the device. Herein, we examine the effect of increasing the pH to neutral and alkaline conditions on the performance and selectivity of this NO sensor configuration. It will be shown that use of a higher pH inner filling solution increases the formation of a stable platinum oxide film on the working electrode surface, which significantly decreases the oxidation of CO at the inner electrode surface without changing the efficiency of NO oxidation, thereby substantially increasing selectivity of the sensor over CO. Further, this selectivity enhancement is preserved even under neutral conditions if the oxide layer is first formed under alkaline conditions prior to sensor assembly with a neutral pH internal solution.

2.2 Experimental

2.2.1 Chemicals and Reagents.

Platinum wire (diameter 76 μm) and Ag wire (diameter 250 μm) were purchased from Sigma-Aldrich (St. Louis, MO). Borosilicate glass capillaries (outer diameter 2 mm, inner diameter 1.12 mm, length 100 mm) were obtained from World Precision Instruments Inc. (Sarasota, FL). Microporous poly(tetrafluoroethylene) (PTFE) membranes (Tetratex®, pore size 0.07 μm, thickness ~18 μm) were from Donaldson Company, Inc. (Minneapolis, MN). Teflon AF® (Grade 601-100-6) was obtained from DuPont Fluoroproducts (Wilmington, DE).

NO and CO-saturated stock solutions were prepared by bubbling deionized water with pure NO and CO gases in an airtight vessel. Gas-phase NO was generated from acidification of

$NaNO_2$ with H_2SO_4 and scrubbed of N_2O by sparging through 5% sodium hydroxide, all purchased from Sigma-Aldrich (St. Louis, MO). Carbon monoxide gas was obtained from Matheson Tri-Gas (Albuquerque, NM).

Platinizing solution (3% chloroplatinic acid, <0.1% lead acetate, water balance) was purchased from LabChem Inc. (Pittsburgh, PA). Trizma base, H_2SO_4, KCl, NaH_2PO_4, and Na_2HPO_4, $Na_2B_4O_7 \cdot 10H_2O$, HCl, and NaOH were products of Sigma-Aldrich. All solutions were prepared with 18 MΩ·cm deionized water using reagent grade compounds without further purification.

2.2.2 Fabrication of Clark-type Amperometric NO Sensors

The amperometric NO sensor was prepared as described previously[15] and is depicted in Figure 2.1. Briefly, a 76 μm Pt wire was sealed in a glass capillary and filed on one end with 600 grit carbide to expose a planar Pt disk. The Pt disk was polished with 0.3 μm alumina and rinsed with deionized water. The Pt disk was then platinized by cycling from +0.6 V to -0.3 V at 20 mV s^{-1} for 2 cycles in platinizing solution. The disk electrode was rinsed thoroughly with deionized water following platinization. The Ag/AgCl reference electrode was prepared by taking a coiled 250 μm Ag wire and cycling from 0 to 0.5 V at 100 mV s^{-1} for 30 cycles in 0.1 M HCl.

The platinized Pt disk electrode and Ag/AgCl coil reference electrode were then inserted into the sensor housing (sealed with Teflon® AF treated PTFE prior to assembly for enhanced selectivity over ammonia[20]) along with the internal electrolyte (10 mM PBS, 140 mM KCl, titrated to pH 7.4 and 11.7, 10 mM BBS titrated to pH 9.0, unbuffered 0.01 M HCl for pH 2.0, or unbuffered 0.5 M H_2SO_4 for pH 0). Sensors were then polarized in pH 7.4 PBS solution for at

least 6 h at 0.7 V vs. Ag/AgCl prior to amperometric measurements. Measurements and calibrations were performed by injecting sample or standard into a pH 7.4 PBS buffer solution, with stirring, and allowing the current to reach a steady state.

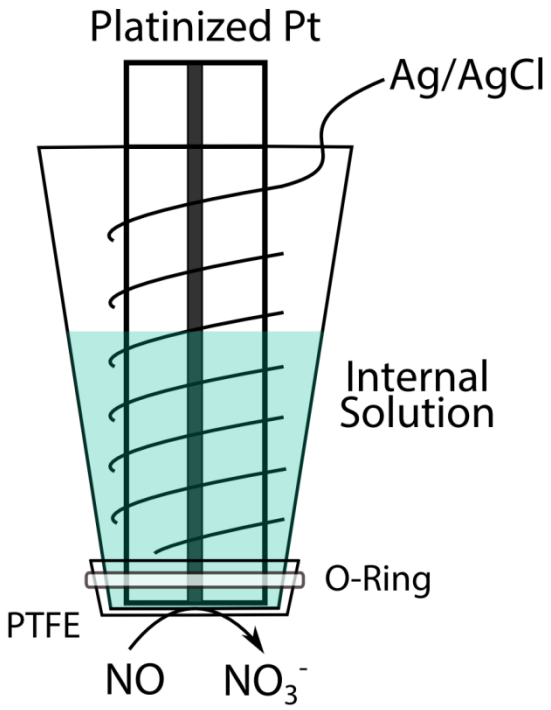

Figure 2.1. Schematic of the planar, amperometric nitric oxide sensor used in this study.

2.2.3 Cyclic Voltammetry of Pt Electrode Surface

All CV experiments were performed in N_2-purged pH 2.0 (10 mM HCl, 130 mM KCl) and pH 11.7 (10 mM PBS, 138 mM NaCl, 2 mM KCl) solutions using clean and oxidized Pt surfaces. The oxidized surface was prepared by taking a platinized Pt electrode and applying a constant potential of +0.7 V in the given internal solution being investigated. Cyclic voltammetry measurements involved cycling from -0.6 to 0.8 V in pH 11.0 internal solution and

from -0.1 to 1.1 V in pH 2.0 internal solution at 10 mV/sec. For CO stripping experiments, CO was adsorbed onto the working electrode by immersing the Pt disk electrode for 10 min in a CO-saturated internal solution of the type under investigation.

2.2.4 Evaluation of Selectivity Stability in High CO_2 Environments

In consideration of potential real-world applications for this sensor, we also investigated the effect of high CO_2 sampling environments on the pH in the thin film of internal electrolyte behind the GPM. High levels of CO_2 may titrate the thin electrolyte layer and overwhelm the buffer capacity of such a small volume (Figure 2.2). To probe the electrolyte thin film, we emulated the sensor configuration using an ammonia gas sensor (Thermo Scientific 9512HPBNWP), which is comprised of a glass pH probe housed behind a fluoropolymer gas-permeable membrane that is identical to that used in assembling the NO sensors described here and is in intimate contact with the pH probe. The ammonia sensing internal solution is swapped for the internal solution examined in the NO sensors. The probe is then placed in N_2 and 10% CO_2 (in N_2 balance) purged PBS solutions and monitored for changes in pH.

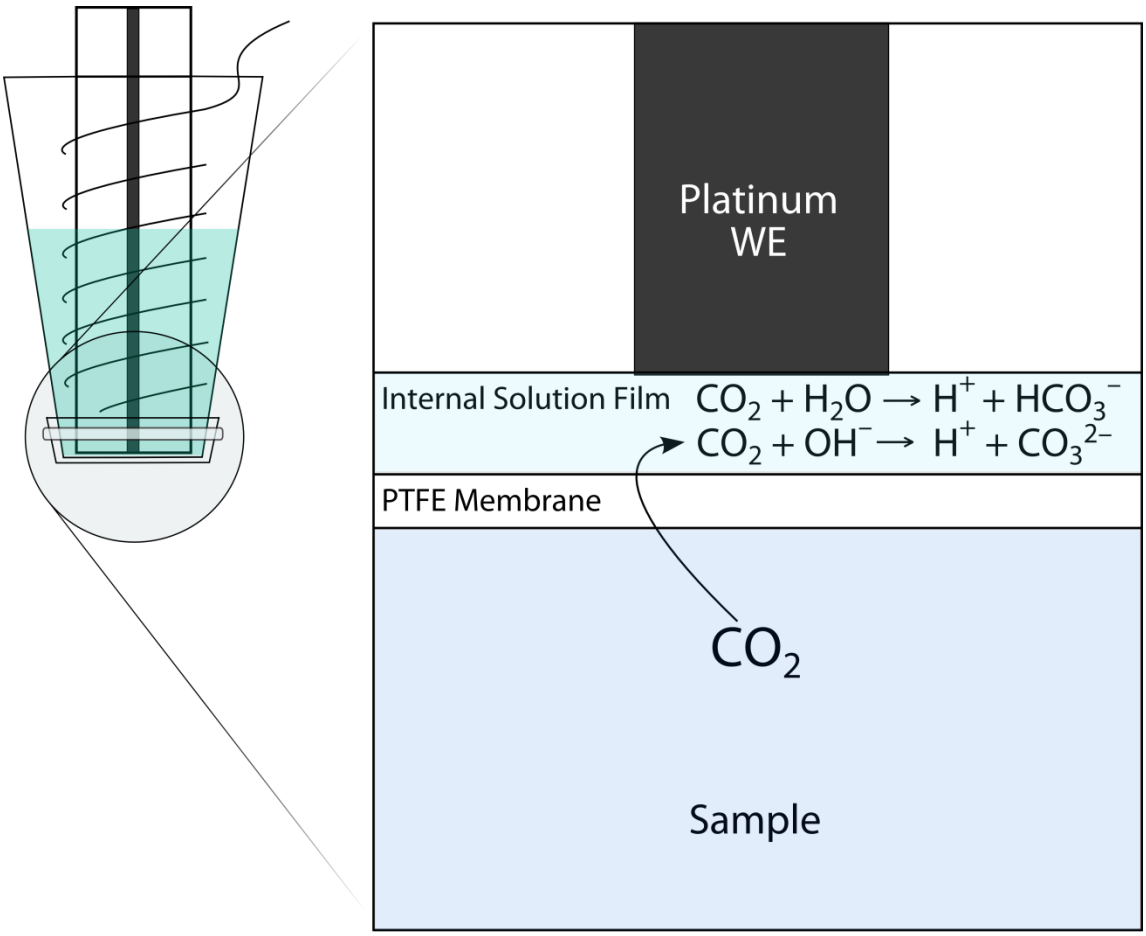

Figure 2.2. Diagram of internal arrangement near the sensor distal tip showing potential for CO_2 titration of the internal electrolyte solution of the NO sensor.

In a separate experiment, the inner working electrode of the sensor was polarized at +0.700 V vs. Ag/AgCl for 10 min in pH 11.7 internal solution, then used to assemble an NO sensor containing a pH 7.4 inner solution. The selectivity of this sensor was then evaluated and compared to the selectivity of a sensor assembled with a neutral pH internal solution without prior oxide formation under alkaline conditions. We also conducted NO and CO calibrations for both the sensors (with and without pre-oxide formation in pH 11.7 solution) under a 10% CO_2 purged environment. Long-term stability of the oxide layer was performed over a 17 day period where selectivity is measured every day under ambient conditions.

2.3 Results and Discussion

2.3.1 Characterization of Reversible Amperometric NO Sensor Selective over CO

Amperometric signals of NO sensors in response to standard additions of CO and NO are shown in Figure 2.3 for the Shibuki style sensors assembled using pH 2.0 and pH 11.7 internal solutions. NO sensitivity is comparable between sensors assembled using acidic vs. basic inner solutions; however, there is significantly lower response to CO from sensors assembled using an alkaline internal solution, suggesting improved selectivity over CO. Selectivity is defined by the following equation:[18]

$$\log K_{\mathrm{NO},j} = \log\left(\frac{\Delta I_j / c_j}{\Delta I_{\mathrm{NO}} / c_{NO}}\right) \quad (2.1)$$

where ΔI_{NO} and ΔI_j are the measured currents for NO and interfering species (in this case, j = CO) and c_{NO} and c_j are the concentrations of NO and interfering species, respectively. Similar experiments were also conducted using a series of internal solutions of varying pH values (pH 0, 2.0, 7.4, 9.0, and 11.7). A summary of the selectivity coefficients determined as a function of internal solution pH is shown in Figure 2.4. Selectivity against CO is improved substantially as a function of increasing internal electrolyte solution pH. Based on the amperometric data, it is clear that enhanced selectivity for NO over CO can be achieved by increasing the alkalinity of the internal electrolyte solution. This sensor modification allows for the composition of the outer gas permeable membrane to remain unchanged, retaining the selectivity over other common interfering species in biological samples, such as nitrite, ascorbate, and ammonia. Any differences in the response times of the sensors are primarily due

irreproducibility in the thickness of the porous Teflon membrane® or the thickness of the inner electrolyte layer between the platinum working electrode and this Teflon outer membrane.

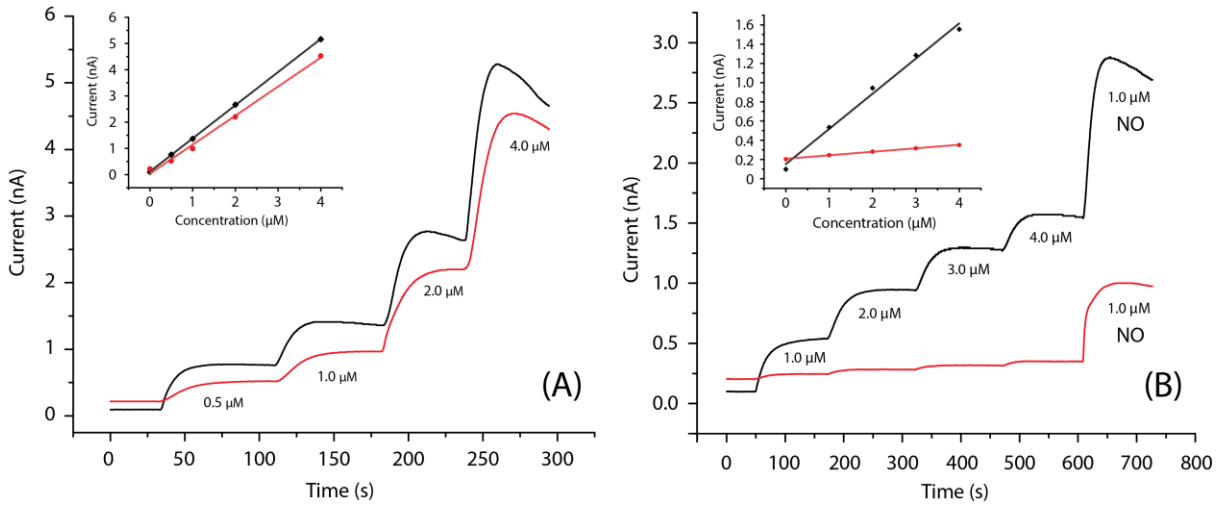

Figure 2.3. Amperometric response to standard additions of (A) NO and (B) CO of sensors assembled with pH 11.7 (red) and pH 2.0 (black) internal filling solution (10 mM PBS, 138 mM NaCl, 2 mM KCl).

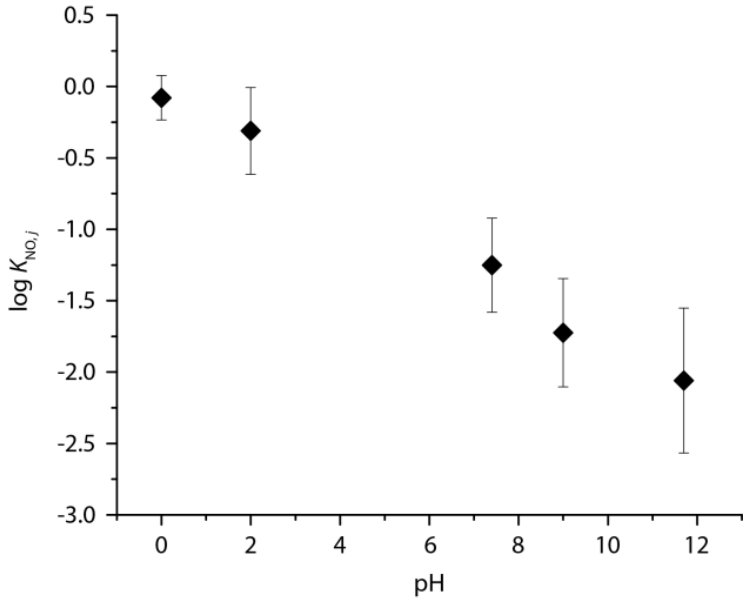

Figure 2.4. log $K_{NO,j}$ of sensors assembled using internal solutions of varying pH.

2.3.2 Preliminary Study of CO Selectivity Mechanism

A secondary goal of this work was to investigate how the use of a high pH internal electrolyte solution improves selectivity for NO over CO. We hypothesize that an increase in the internal electrolyte pH may lead to a more extensive oxidized Pt layer on the inner working electrode surface when polarized at anodic potentials, passivating the surface towards CO oxidation. This behavior has been previously suggested by Tsceng and Yang[21] in their development of a CO sensor and later observed by Ho *et al.*[22] in the development of a solid polymer electrolyte-based NO sensor for kinetic studies. This phenomenon was not previously investigated in detail and was offered only as speculation in this earlier work. In 1957, Anson *et al.*[23] found that Pt electrodes, while generally considered "noble", form oxide films under sufficiently anodic potentials, even under acidic conditions. A number of subsequent studies have since confirmed this finding, although the exact composition of the oxide film remains unclear.[24]

In a bimolecular surface reaction, such as the oxidation of CO to CO_2 on Pt, the two major possible reaction mechanisms are the Langmuir-Hinshelwood (LH) mechanism, where two reactants adsorb independently and subsequently react on the surface, and the Eley-Rideal (ER) mechanism, where one of the reactants adsorbs to the surface while the other reacts with the adsorbed species without itself adsorbing (Figure 2.5). In both the LH and ER mechanisms, CO must be adsorbed to the electrode surface for oxidation to proceed, and the dominant mechanism for CO oxidation on Pt is generally accepted to be an LH mechanism.[25] In either case, CO must first adsorb to the electrode surface in order for oxidation to occur. There is a lack of previous work relating to CO adsorption and subsequent oxidation on electrochemically

oxidized polycrystalline Pt. Investigations of CO adsorption and oxidation in the literature have been primarily performed using un-oxidized single-crystal Pt.[26]

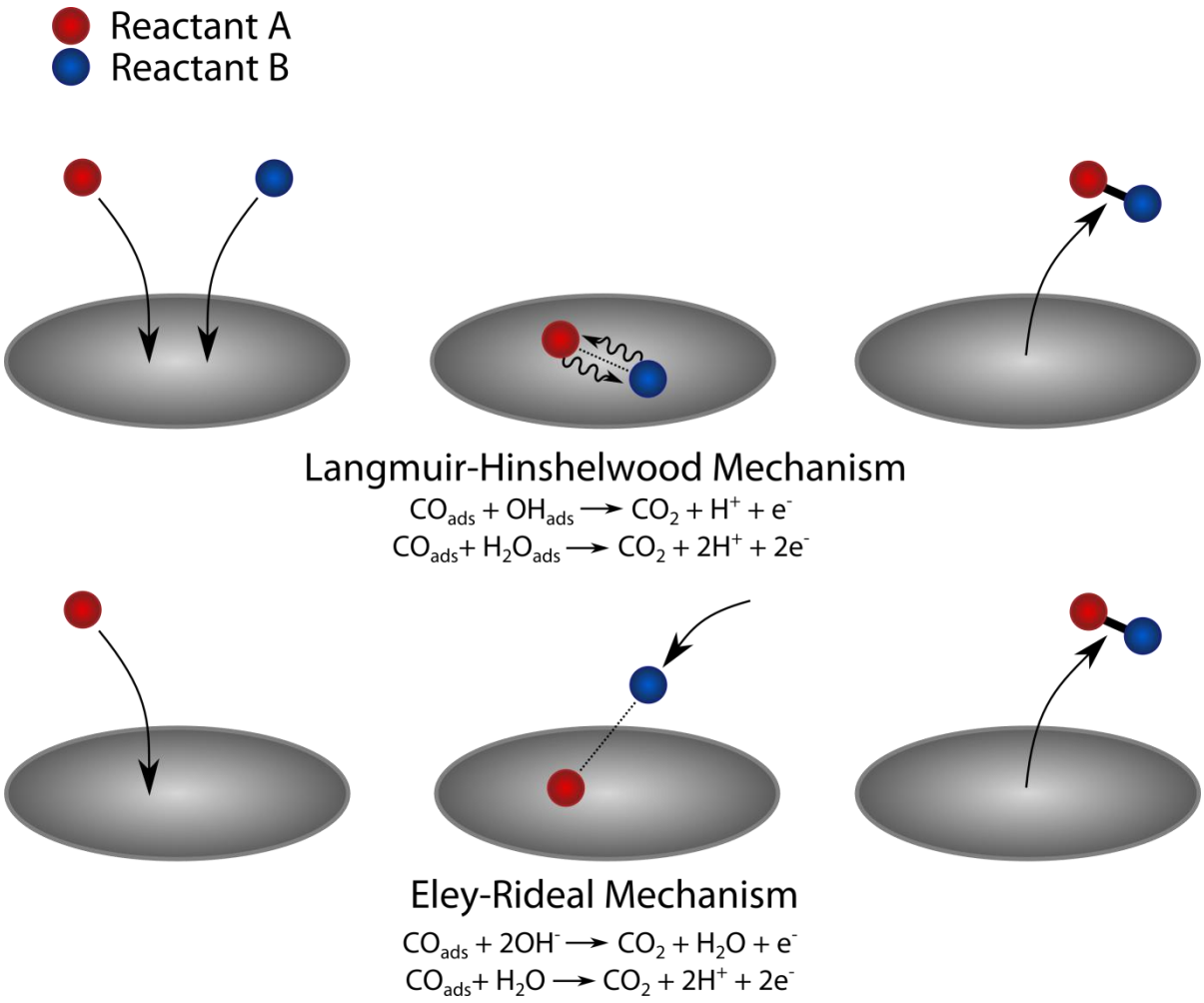

Figure 2.5. Langmuir-Hinshelwood and Eley-Rideal mechanisms of heterogeneous bi-molecular reactions.

We hypothesize that the increased pH of the internal solution results in the formation of a more extensive film of oxidized platinum during polarization of the sensor when a constant anodic potential of +0.7 V vs. Ag/AgCl is applied for long periods of time. Pourbaix diagrams for polycrystalline Pt also suggest that pH has a profound effect on the formation and

composition of oxidized platinum films, with increasing pH favoring oxide formation.[27] It is conceivable that greater coverage of oxidized Pt on the electrode surface may prevent adsorption of CO, hence passivating the surface towards CO oxidation. Thus, clean and oxidized Pt electrode surfaces were placed in bulk "internal" solutions of pH 11.7 and pH 2.0 and anodically stripped of previously adsorbed CO in order to probe the behavior of the electrode surface in acidic and basic environments. Corresponding CV's for NO oxidation at clean and oxidized Pt surfaces may also be useful although it has been shown that NO does not adsorb to a great extent on polycrystalline platinum.[25,28] Instead, NO oxidation is suggested to occur primarily in bulk solution and not as an adsorbate, making adsorption an unnecessary step in the overall mechanism.[28] Furthermore, the oxidation of NO appears to be largely independent of the electrode material, suggesting weak interactions with the electrode surface. In Figure 2.6, a diagram of the postulated mechanism of CO adsorption inhibition is shown.

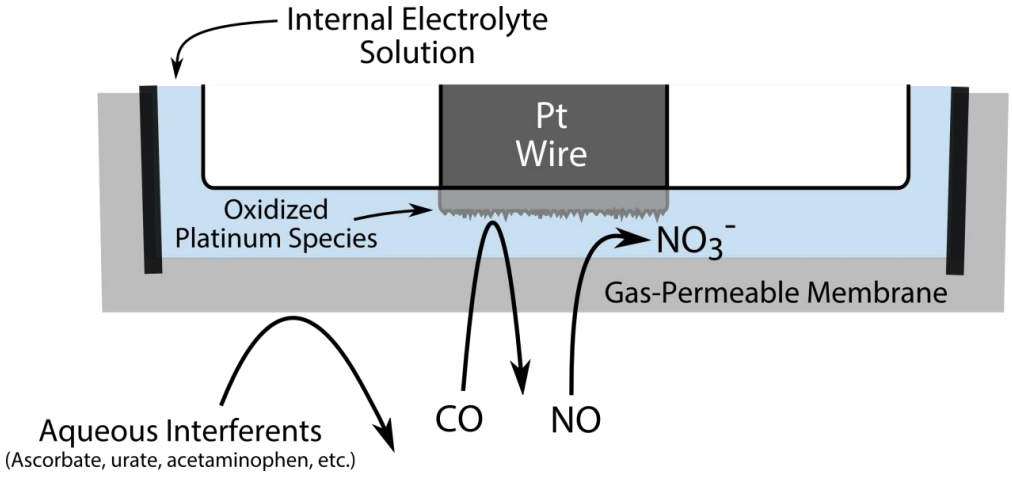

Figure 2.6. Schematic of amperometric Shibuki-design sensor tip details illustrating hypothesized CO selectivity mechanism.

In order to elucidate the mechanism of inhibition of electrochemical CO oxidation, cyclic voltammetry was employed to probe the behavior of CO at platinum electrode surfaces. Background CV's are shown in Figure 2.7 with oxide reduction from -0.2 to -0.4 V in pH 11.7 solution and oxide reduction from +0.3 to +0.5 V in pH 2.0 solution. Note that no oxide reduction occurs on the initial negative sweep, confirming that the reduction peak on the second cycle is likely the oxide formed during the anodic sweep. The oxide formed also appears more extensive when the Pt electrode is oxidized under basic conditions, as hypothesized, with an 11-fold increase in total charge passed during reduction (molar quantity cannot be determined due to the ambiguity of the exact oxide layer composition).

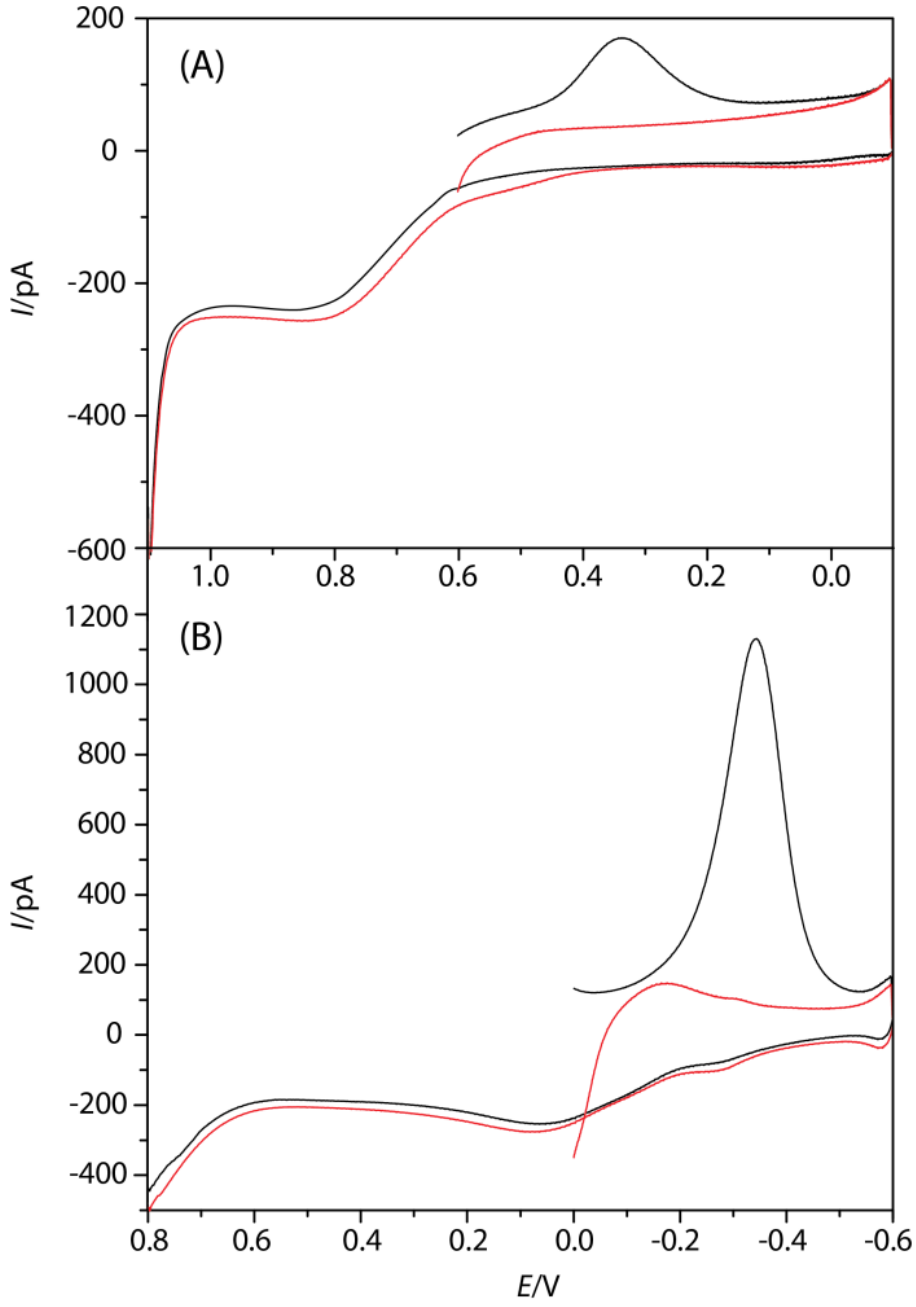

Figure 2.7. Background cyclic voltammograms of clean (red) and oxidized (black) Pt disk electrodes in (A) pH 2.0 solution and (B) pH 11.7 solution.

Carbon monoxide oxidation occurs over a potential range of +0.45 to +0.5 V in pH 2.0 solution and -0.2 to -0.3 V in pH 11.7 solution, as shown in Figure 2.8. Under acidic conditions, there is little difference in the CO adsorption and oxidation behavior between a clean Pt surface and one that had been pre-oxidized. Under basic conditions, however, there is no CO stripping current during the initial positive sweep for the oxidized Pt, suggesting that CO does not adsorb to the oxidized electrode surface, while a very clear feature is seen for the clean Pt surface. Without adsorption to the surface, it is unlikely that CO would be oxidized to a great extent via a bimolecular surface reaction. Nitric oxide adsorption on polycrystalline Pt has been attempted by previous investigators without consistent observation of an adsorbed species; it has been suggested that NO adsorption is not critical to NO oxidation in bulk aqueous solutions.[28]

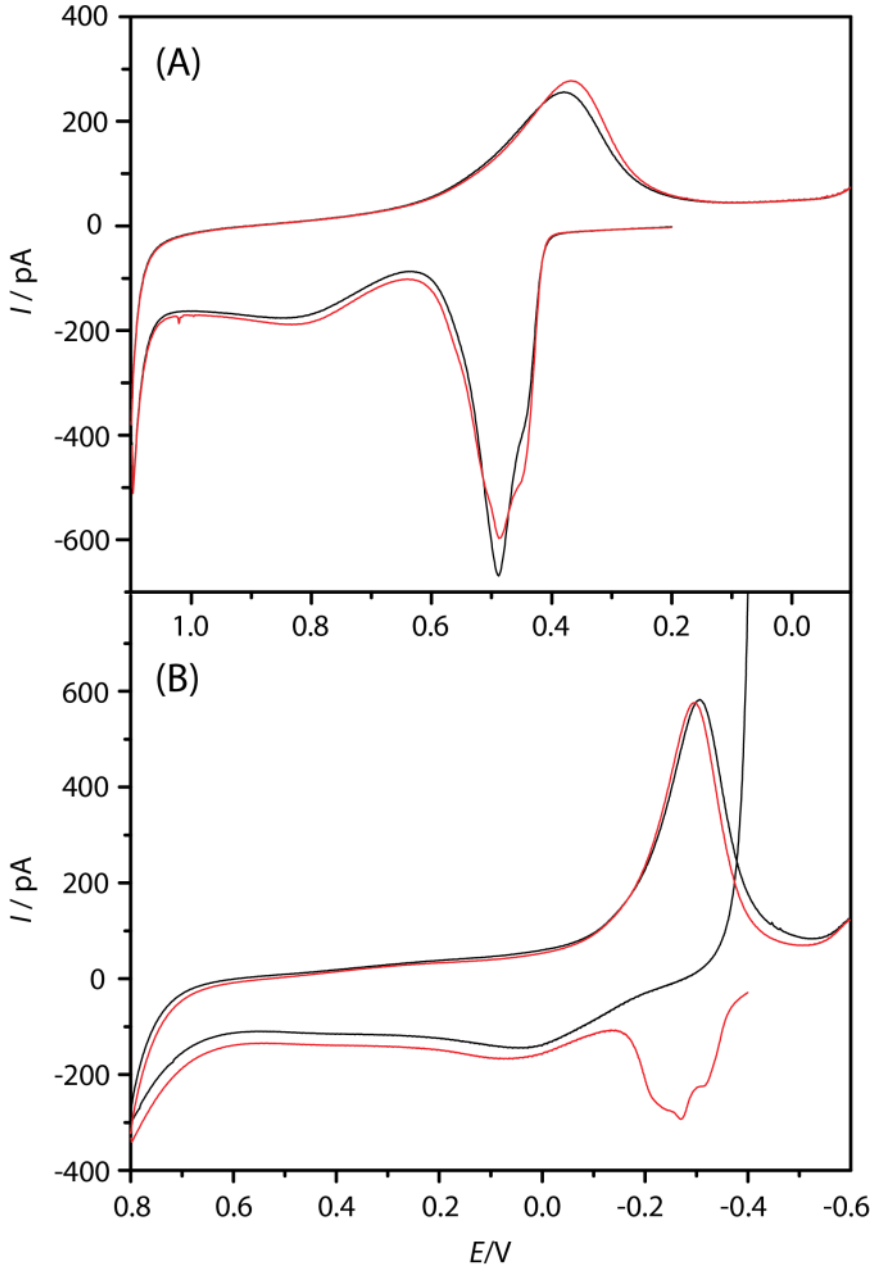

Figure 2.8. CO stripping cyclic voltammograms of clean (red) and oxidized (black) Pt disk electrodes in (A) pH 2.0 solution and (B) pH 11.7 solution.

2.3.3 Stability of CO Selectivity in High CO_2 Environments

In our electrolyte thin-film pH studies, a significant change in the sensor thin film pH occurs within 20 min of sparging the bulk pH 7.4 PBS solution with 10% CO_2 gas, but the pH remains stable at pH 6.6 thereafter (Figure 2.9). While the pH drops noticeably, we find that the NO response of the sensor is not compromised and the selectivity of the sensor remains intact even after exposure to high CO_2 levels. We have also conducted NO and CO calibrations under a 10% CO_2 purged environment and demonstrated that selectivity is maintained compared to ambient conditions (see Figure 2.10). Indeed the inner working electrode of the sensor was polarized at +0.700 V vs. Ag/AgCl for 10 min in the high pH internal solution, then used to assemble an NO sensor using a neutral pH inner solution. The sensitivity to NO and selectivity over CO remained the same as when assembling and with a high pH inner electrolyte solution only (Figure 2.11).

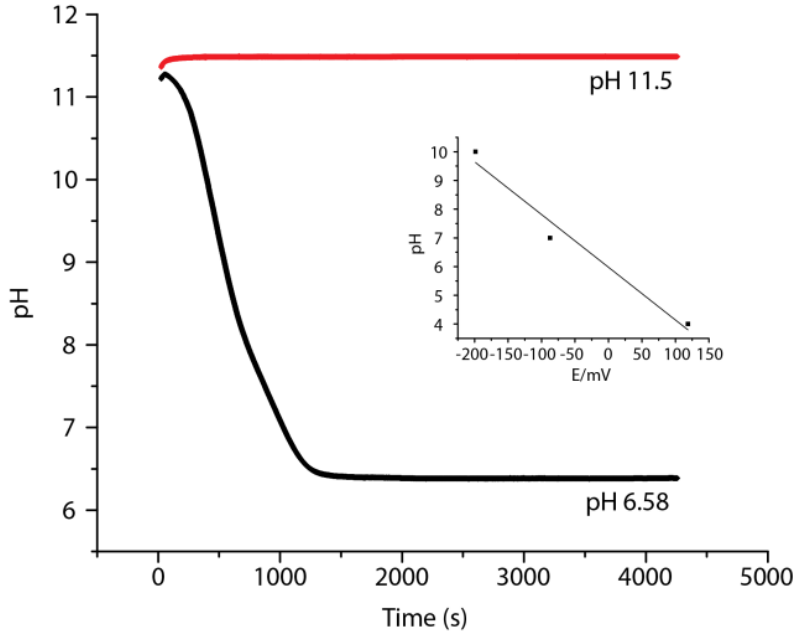

Figure 2.9. Change in internal electrolyte solution pH in an N_2 purged (red) and 10% CO_2 purged (black) pH 7.4 phosphate buffered saline solution. Inset shows calibration of pH sensor.

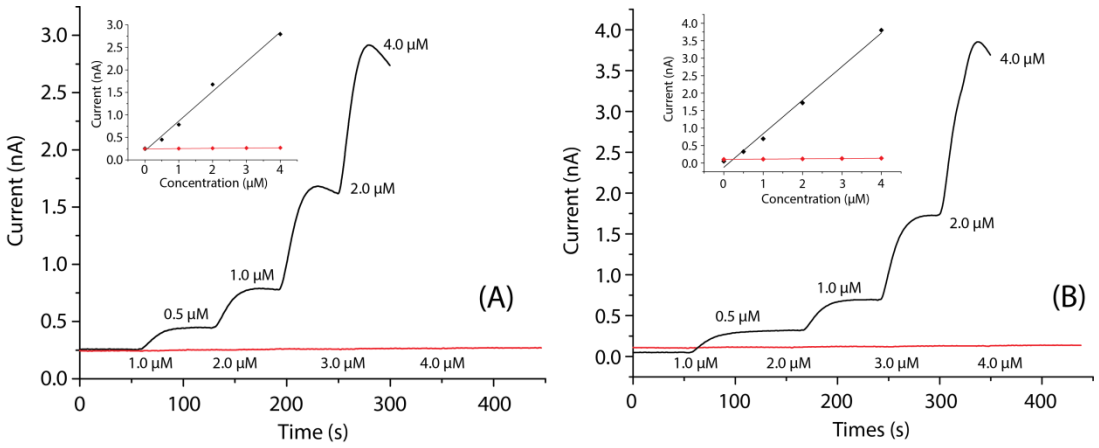

Figure 2.10. Amperometric response to standard additions of NO (black) and CO (red) of the same sensor under (A) ambient and (B) 10% CO_2 environments.

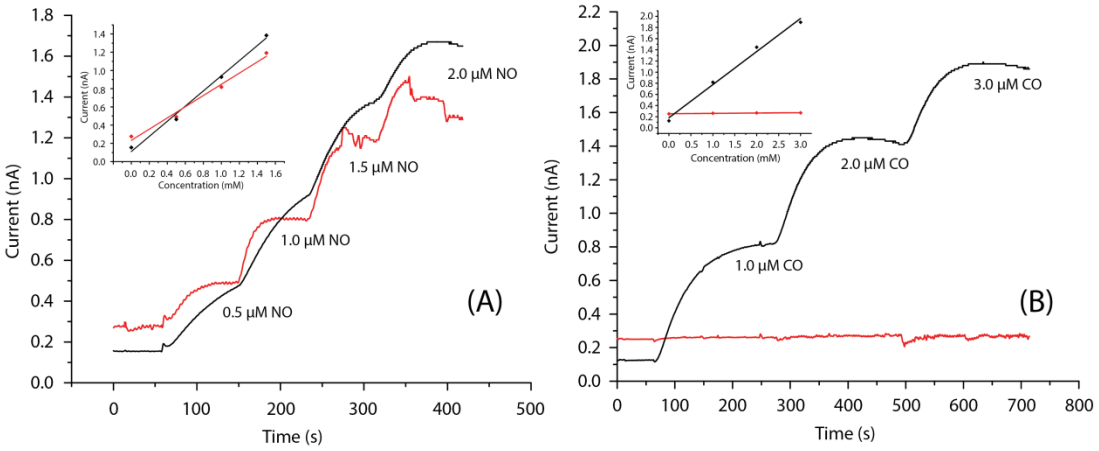

Figure 2.11. Amperometric response to standard additions of (A) NO and (B) CO of sensors with working electrodes pre-polarized in basic (red) and acidic (black) solutions prior to assembly and operation in neutral (pH 7.4) internal solutions.

Sensors were first tested for selectivity under ambient conditions, then purged for 24 h under 10% CO_2 and retested under high CO_2 conditions. We also found that the stability of the oxide layer was maintained over a 17-day experiment where selectivity was measured every day under ambient conditions; average selectivity ($\log K_{\mathrm{NO},j}$) across 3 sensors assembled using pH 11.7 internal solution under ambient conditions was -1.71 on day 1 and -1.73 on day 17.

2.4 Conclusions

An amperometric, planar NO sensor with high sensitivity for NO and high selectivity over CO has been developed and characterized. The sensor is a Shibuki-type device with internal filling solution and internal Ag/AgCl reference electrode housed with a platinum working electrode behind a gas permeable membrane. Selectivity over CO in such a sensor configuration can be achieved, without compromising sensitivity towards NO, by elevating the internal solution pH. A basic internal solution lowers the potential for forming an oxidized Pt layer on the Pt working surface, that inhibits CO adsorption as shown via cyclic voltammetry. Carbon monoxide adsorption is observed on clean Pt surfaces as well as surfaces oxidized in the traditional acidic internal solution, while such adsorption is inhibited on a Pt surface pre-oxidized in a basic internal solution. Carbon monoxide oxidation on a Pt surface requires CO adsorption to the electrode surface; the oxidized Pt layer is responsible for greatly reducing CO interference in the proposed sensor configuration. By using a basic internal solution, a more extensive oxidized Pt layer is formed on the working electrode surface, which precludes CO adsorption to a significant extent. It is likely that this new improved-selectivity NO sensor can be readily applied for biomedical measurements, such as measurement of NO released from explanted tissues and exhaled nasal breath, where CO interference was previously an obstacle[16]

2.5 References

(1) Griess, P. *Berichte der Dtsch. Chem. Gesellschaft* **1879**, *12* (1), 426.

(2) Noack, E.; Kubitzek, D.; Kojda, G. *Neuroprotocols* **1992**, *1* (2), 133.

(3) Fontijn, A.; Sabadell, A.; Ronco, R. *Anal. Chem.* **1970**, *42* (6), 575.

(4) Bates, J. N. *Neuroprotocols* **1992**, *1* (2), 141.

(5) Robinson, J. K.; Bollinger, M. J.; Birks, J. W. *Anal. Chem.* **1999**, *71* (22), 5131.

(6) Lee, Y.; Oh, B. K.; Meyerhoff, M. E. *Anal. Chem.* **2004**, *76* (3), 536.

(7) Shin, J. H.; Privett, B. J.; Kita, J. M.; Wightman, R. M.; Schoenfisch, M. H. *Anal. Chem.* **2008**, *80* (18), 6850.

(8) Hetrick, E. M.; Schoenfisch, M. H. *Annu. Rev. Anal. Chem.* **2009**, *2*, 409.

(9) Shibuki, K. *Neurosci. Res.* **1990**, *9*, 69.

(10) Shibuki, K.; Okada, D. *Nature* **1991**, *349* (24), 326.

(11) Shibuki, K. *Neuroprotocols* **1992**, *1* (2), 151.

(12) Malinski, T.; Taha, Z.; Grunfeld, S.; Burewicz, A.; Tomboulian, P.; Kiechle, F. *Anal. Chim. Acta* **1993**, *279* (1), 135.

(13) Malinski, T.; Taha, Z. *Nature* **1992**, *358*.

(14) Malinski, T.; Ciszewski, A.; Bennett, J.; Fish, J. R.; Czuchajowski, L. *J. Electrochem. Soc.* **1991**, *138* (7), 2008.

(15) Shin, J. H.; Weinman, S. W.; Schoenfisch, M. H. *Anal. Chem.* **2005**, *77* (11), 3494.

(16) Horváth, I.; Loukides, S.; Wodehouse, T.; Csiszér, E.; Cole, P. J.; Kharitonov, S. a; Barnes, P. J. *Thorax* **2003**, *58* (1), 68.

(17) Yamaya, M.; Sekizawa, K. *Am. J. Respir. Crit. Care. Med.* **1998**, No. 12, 1.

(18) Park, S. S.; Kim, J.; Lee, Y. *Anal. Chem.* **2012**, *84* (3), 1792.

(19) Lee, Y.; Yang, J.; Rudich, S. M.; Schreiner, R. J.; Meyerhoff, M. E. *Anal. Chem.* **2004**, *76* (3), 545.

(20) Cha, W.; Meyerhoff, M. E. *Chem. Anal.* **2006**, *949* (51), 949.

(21) Tsceng, K.I.; Yang, M. C. *J. Electrochem. Soc.* **2003**, *150* (7), H156.

(22) Ho, K.C.; Liao, J. Y.; Yang, C. C. *Sensors Actuators B Chem.* **2005**, *108* (1-2), 820.

(23) Anson, F.; Lingane, J. *J. Am. Chem. Soc.* **1957**, *1315* (13), 4901.

(24) Birss, V.; Chang, M.; Segal, J. *J. Electroanal. Chem.* **1993**, *355*, 181.

(25) Dahlstrøm, P. K.; Harrington, D. a.; Seland, F. *Electrochim. Acta* **2012**, *82*, 550.

(26) Madix, R.; Benziger, J. *Annu. Rev. Phys. Chem.* **1978**, No. Lee D, 285.

(27) Pourbaix, M. *Atlas of Electrochemical Equilibria in Aqueous Solutions*, 2nd ed.; National Association of Corrosion Engineers: Houston, 1974.

(28) Devooys, A. C. .; Beltramo, G.; Vanriet, B.; Vanveen, J.; Koper, M. *Electrochim. Acta* **2004**, *49* (8), 1307.

CHAPTER 3

HIGHLY SENSITIVE AMPEROMETRIC PLATINUM-NAFION GAS PHASE NITRIC OXIDE SENSOR: PERFORMANCE AND APPLICATION IN CHARACTERIZING NITRIC OXIDE-RELEASING BIOMATERIALS

3.1 Introduction

As discussed in the Chapters 1 and 2, nitric oxide (NO) has been studied extensively since its discovery as the endothelial-derived relaxing factor in 1987[1,2] and has since been shown to play critical roles in a number of other physiological functions such as inhibition of platelet activation/adhesion,[3,4] neurotransmission,[5,6] and as a potent antimicrobial agent.[7] Local changes in NO concentration *in vivo* are often important indicators of physiological and biochemical phenomena. For example, exhaled gas phase NO concentrations (either oral or nasal) may be useful in diagnosing asthma and other respiratory diseases such as chronic rhinosinusitis (CRS),[8,9] that affects 13-14% of Americans.[10,11]

Due to the attractive antithrombotic and antimicrobial properties of NO, investigations of synthetic NO-donor molecules, such as *S*-nitrosothiols (RSNO)[12,13] and diazeniumdiolates,[12] incorporated into medical-grade polymers (e.g., silicone rubber, polyurethanes, and block co- or tri-polymers of these and other polymers[14]), have been undertaken in order to improve the biocompatibility of catheters and other implantable medical devices. Currently, the rates of NO release from these materials are usually characterized by ozone-based chemiluminescence.[15] Similar chemiluminescence measurements are also the gold standard for measurement of NO in

exhaled oral and nasal breath samples.[16–18] While chemiluminescence is highly sensitive (with a purported limit of detection of 0.5 ppb)[19] and high selectivity for NO, it remains costly as a workhorse analytical-research technique and is relatively impractical as a near-patient diagnostic tool due to its complexity and size.

Amperometric NO sensing is inexpensive, compact, and quite facile to integrate into devices, making it an attractive alternative to chemiluminescence. For gas phase NO measurements, semiconductor[20–22] and solid-polymer electrolyte (SPE)-based sensors [23–27] have been reported. While conductivity-based sensors have good stability, they often require high operating temperatures and fall short of the requisite response times and limits of detection for detecting NO from exhaled breath (10 - 500 ppb)[18] and from NO-donor doped materials (5 ppb - 100 ppm).[12,14]

SPE-based sensors utilize ion-exchange membranes such as Nafion 117 as both a high surface area scaffold for the deposition of a metal working electrode and as an ion conductive pathway for the electrochemical cell. Prior SPE-based NO sensors reported in the literature [23,27,28] have been based on platinized Nafion and report limits of detection of <10 ppb, with fast response times and large dynamic linear ranges. Despite the promising initial characterizations of amperometric Pt-Nafion NO sensors, no studies have been conducted to demonstrate their potential biomedical/biomaterials-research applications or to establish a correlation between data obtained using Pt-Nafion amperometric NO sensors versus that of the gold standard for gas phase NO detection, chemiluminescence.

In this work, an optimized gas-phase amperometric Pt-Nafion SPE type NO sensor is described and applied for determining the rates of NO released from RSNO-doped polymer films as well as NO generated electrochemically via copper(II)-tri(2-pyridylmethyl)amine (CuTPMA)

mediated reduction of inorganic nitrite within $NaNO_2$ solutions.[29] The RSNO and polymer of choice in this work are *S*-nitroso-*N*-acetylpenicillamine (SNAP) and CarboSil2080A, respectively. Replicate samples of the same NO release materials are also analyzed for NO release rates via chemiluminescence measurements and the results are compared to those obtained via the new amperometric sensing approach. While selectivity concerns are minimal for NO generated from NO-donor materials/devices, preliminary selectivity experiments are also described for the SPE NO sensor with respect to carbon monoxide (CO), a known potential interfering species in exhaled breath.

3.2 Experimental

All chemicals used were commercially obtained from Sigma-Aldrich (St. Louis, MO) unless otherwise specified and were reagent grade without further purification or modification. All gases used for the calibration of the Pt-Nafion sensors were obtained from Cryogenic Gases (Detroit, MI). Aqueous solutions were prepared using water (18.2 MΩ·cm) purified through a Milli-Q system (Millipore, Bedford, MA). Sensor cell assembly and sample cells were prepared by Glass-blowing Services, Department of Chemistry, University of Michigan (Ann Arbor, MI). All potentials reported herein are versus Ag/AgCl (saturated KCl), which is +0.197 V vs. SHE.

3.2.1 Sensor Fabrication

The general design and fabrication of the Pt-Nafion working electrode have been described in previous reports,[25,28,30,31] with minor changes described in this section. Briefly, Nafion 117 (DuPont, Wilmington, DE) was cut into 1 cm dia. circles and cleaned of impurities

by boiling in 3 M nitric acid for 1 h followed by boiling in deionized water for 1 h. The membranes were then incubated in 20 mM $Pt(NH_3)_4Cl_2$ at 37 °C for 6 h before mounting between two glass cells with 0.94 cm dia. openings (0.88 cm^2 exposed geometric area) with one side of the ionomer membrane exposed to 50 mM $NaBH_4$ in 1 M NaOH. Chemical reduction was allowed to proceed for 90 min. The Pt-Nafion membrane was then boiled in DI water for 1 h to remove any remaining Pt complex and reducing agent. It should be noted that after the completion of this work, we determined that performing the impregnation on a single side and conducting the reduction step at 37°C resulted in a marked improvement in reproducibility and decrease in fabrication failure rate without adversely affecting the performance of the sensor. It is thus preferable to follow the single-side impregnation followed by single-side reduction at 37°C.

The working electrode lead was a 10 mm x 2 mm piece of 50 µm thick Au foil secured between the SPE membrane electrode and the gas inlet/outlet section of the sensor (made out of glass). A single junction Ag/AgCl (saturated KCl) reference electrode and bare Pt auxiliary electrode were used along with a 0.5 M H_2SO_4 internal electrolyte in the final sensor assembly (see Figure 3.1). A CHI800B potentiostat (CH Instruments, Austin, TX) was used to polarize the working electrode and record sensor output currents. Note that in all measurements, the metallic side of the membrane electrode faces the gas phase. 2x MC-200SCCM mass flow controllers (Alicat Scientific, Tucson, AZ) operated in tandem via a BB9-USB signal distribution box (Alicat Scientific, Tucson, AZ) and FlowVision SC software (Alicat Scientific, Tucson, AZ) were used for mixing of calibration gas (1 ppm NO in N_2 balance and 10 ppm CO in N_2 balance) and delivery of nitrogen into sample cells (with RSNO doped films or electrochemical NO generation from nitrite) to advance the NO released from the samples to the gas phase sensor.

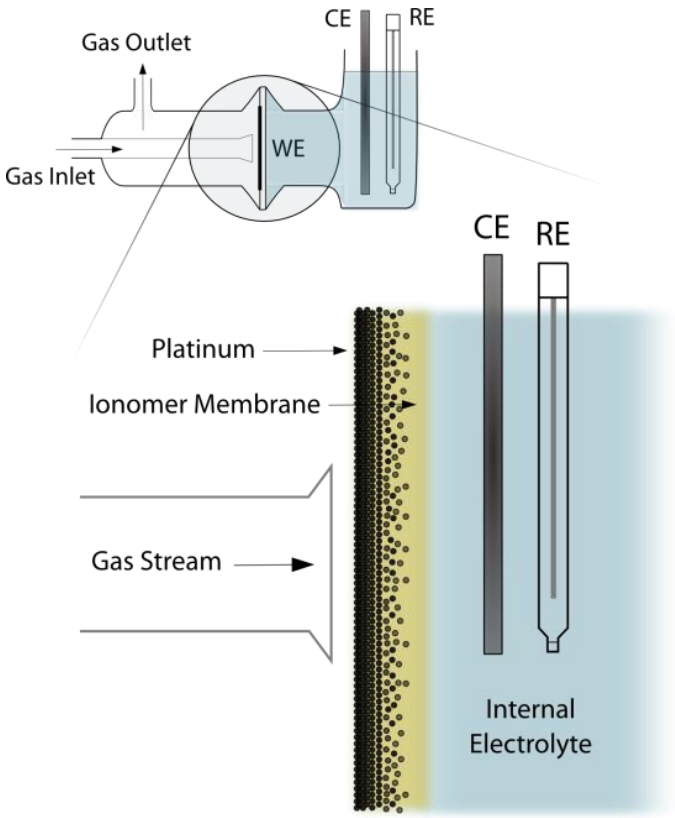

Figure 3.1. Schematic of amperometric SPE-based NO Sensor. WE = Pt-Nafion; CE = bare Pt; RE = single-junction Ag/AgCl in saturated KCl; internal electrolyte = 0.5 M H_2SO_4.

3.2.2 NO-Release Film Preparation and Characterization

The general concept for the preparation of the SNAP-doped CarboSil2080A (DSM Biomedical Inc., Berkley, CA) films has been described in a previous work[14] although, in that earlier work, the polymer of choice was E2As, not Carbosil2080A. Further, unlike this earlier report,[14] no silicone rubber topcoat was utilized in this work. Additionally, SNAP was synthesized from *N*-acetyl-DL-penicillamine (NAP) via a high-yield/high-purity one-step synthesis,[14] which is facile and more economical than purchasing SNAP commercially. To prepare the NO release polymer films, 180 mg of CarboSil2080A was dissolved in 3 mL of

tetrahydrofuran by gently agitating the mixture for 1 h. Then, 20 mg of SNAP was dissolved in the CarboSil2080A solution and the mixture was poured into a Teflon mold (1 inch dia., 0.25 inch depth). The film was allowed to cure overnight before cutting into 8 mm dia. circles and then dried under vacuum for 24 h. The NO-release rate was evaluated via chemiluminescence (Sievers 280i Nitric Oxide Analyzer) and the amperometric Pt-Nafion sensor using an arrangement as shown in Figure 3.2. NO-release from the SNAP-doped polymeric films was modulated via light (S-NO bond is photolytically cleaved at 590 nm)[14] using a broad visible-spectrum fiber-optic ring (DCR II, Schott-Fostec LLC) as the source. The light source has arbitrary light intensity settings that are marked from 0-100; settings of 100, 85, 75, 70, and 65 were used in the modulation of NO release from the SNAP/Carbosil2080A films.

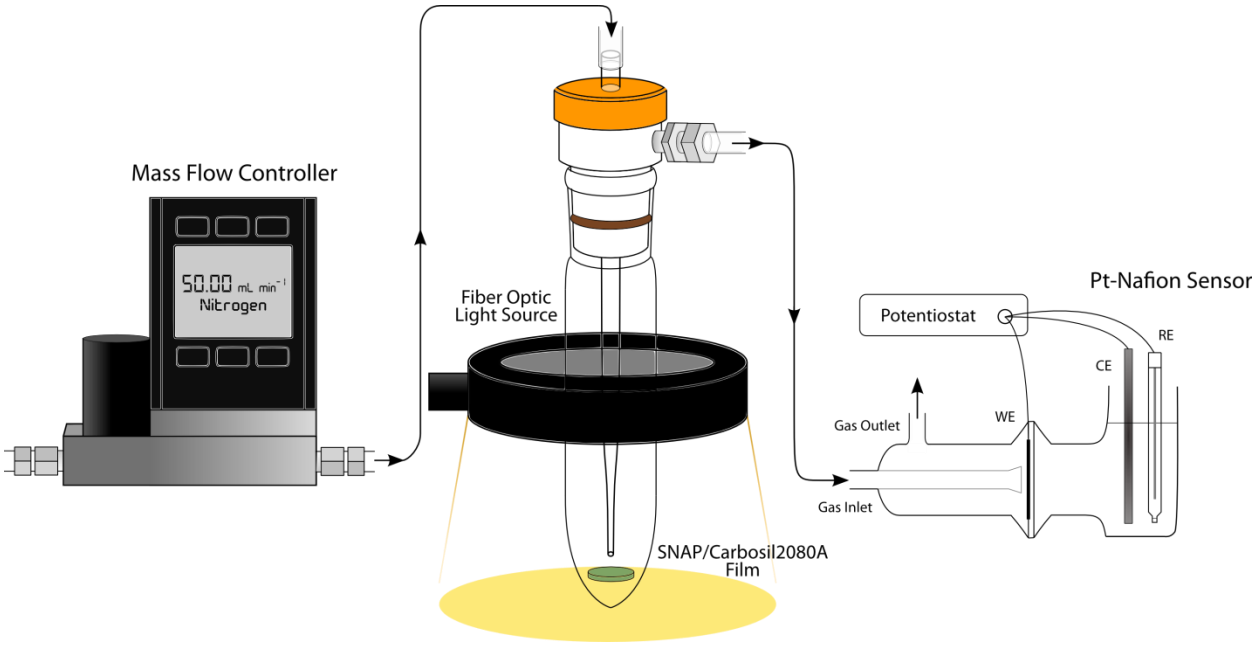

Figure 3.2. Sensing configuration employed for the determining the rates of NO release from SNAP-Carbosil2080A films by photolysis reaction at different intensities of light.

3.2.3 Electrochemically Modulated NO Release Characterization

In a separate work from our group,[29] a novel method to electrochemically modulated NO release was developed and characterized using chemiluminescence. Sodium nitrite in the presence of a copper(II)-complex (CuTPMA), serving as an electron transfer mediator, can be electrochemically reduced to NO at various rates depending on applied potential to a Pt, Pt-Ir alloy, Au or stainless steel working electrode. This technique has the potential to be employed in the development of NO sources for NO inhalation therapy[32,33] as well as intravascular catheters with a separate lumen for electrochemical generation of NO in order to enhance biocompatibility and reduce the risk of catheter-associated infections. In this work, the Pt-Nafion gas phase NO sensor was utilized to characterize the rate of NO produced from a bulk solution of sodium nitrite via the CuTPMA-mediated electro-reduction reaction of nitrite and the results were compared to the rates determined under the exact same conditions using chemiluminescence detection of the liberated NO.

The NO-generating solution was composed of 1 mM CuTPMA, 0.3 M $NaNO_2$, 0.3 M NaCl, and 0.5 M HEPES (buffered to pH 7.2). A CHI1206B potentiostat (CH Instruments, Austin, TX) was employed to modulate the NO generation by applying a constant potential vs. Ag/AgCl (single junction saturated KCl) across a range of potentials. The working electrode was a 6 cm long, 127 µm dia. Teflon-coated Pt-Ir alloy wire (A-M Systems, Sequim, WA) with an exposed length of 2 cm (~0.08 cm^2 exposed surface area). The counter electrode was a 10 cm long, 127 µm dia. Teflon-coated Pt-Ir alloy wire (A-M Systems, Sequim, WA) with an exposed length of 4 cm (~0.16 cm^2 exposed surface area), which was coiled around the unexposed section

of the working electrode to reduce the space occupied in the sample cell. The experimental configuration for these electrochemical NO generation experiments is shown in Figure 3.3.

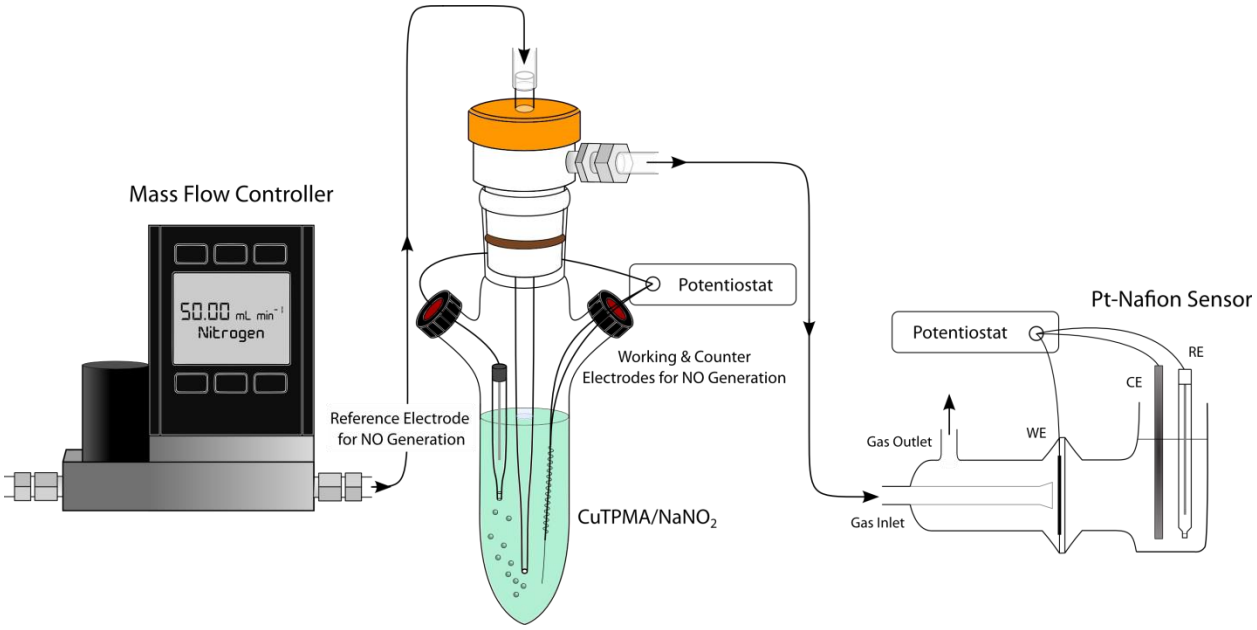

Figure 3.3. Sensing configuration employed for determining the rate of NO generated using electrochemical reduction of nitrite via use of CuTPMA as the electron transfer mediator.

3.3 Results and Discussion

3.3.1 Sensor Characterization

The Pt-Nafion membrane electrode was characterized by cyclic voltammetry to confirm Pt character and to estimate electrochemical surface area via hydrogen adsorption.[34] The hydrogen adsorption region spans from -0.200V to + 0.150 V upon the anodic scan and the Pt oxide reduction is observed between + 0.650 V to 0.0.20 V upon the cathodic scan (Figure 3.4). Applied potential (Figure 3.5) and flow rate (Figure 3.6) studies were performed to evaluate

optimal sensor parameters. An electrochemical surface area of 34 ± 9 cm^2 was determined for n = 3 electrodes prepared as described in the Experimental Section.

Previous studies[25,28] on the effect of flow rate suggests that flow rates above 100 mL min^{-1} provide diminishing returns with regard to sensitivity (reaction rate is no longer mass transport limited), which we have confirmed for our sensors as well (see Figure 3.6). Furthermore, from a practical standpoint, lower flow rates conserve calibration standard gas and reduce splashing, which can contaminate the system plumbing. The optimal applied potential was found to be about approx. 1V, which is in agreement in previous studies[25,28] as well.

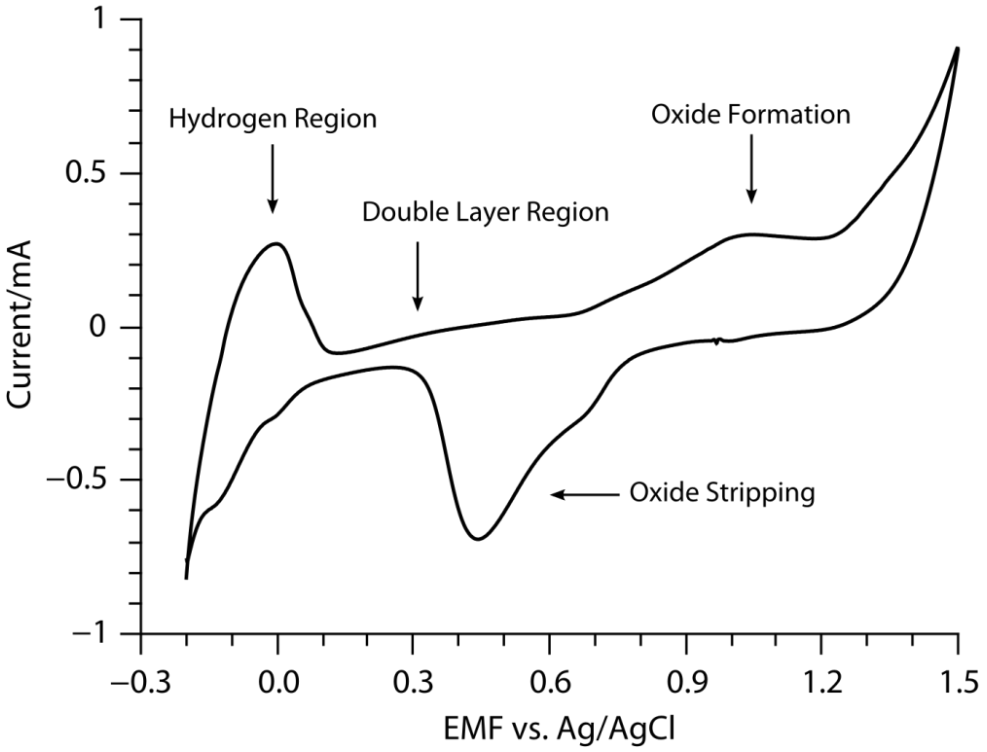

Figure 3.4. Cyclic voltammogram of Pt-Nafion membrane in gas sensor configuration. A 0.5 M H_2SO_4 internal solution was used; scan rate = 20 mV s^{-1}, N_2 flow rate = 50 ml min^{-1}.

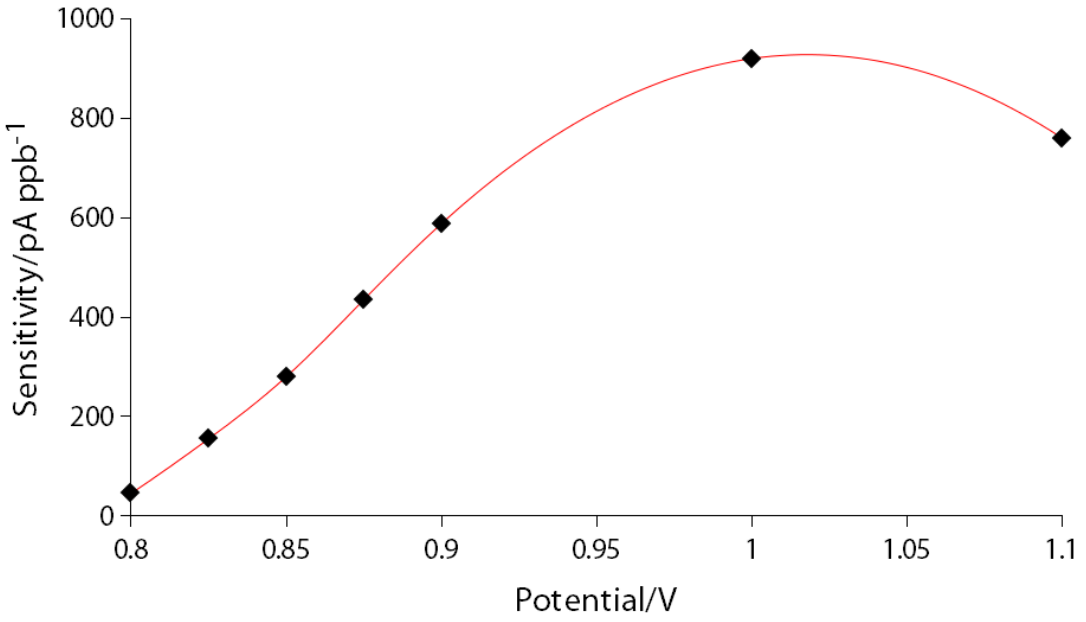

Figure 3.5. NO sensitivity dependence on applied potential for amperometric Pt-Nafion sensors. Operating at constant flow rate of 50 mL min^{-1}. Red line represents best fit curve.

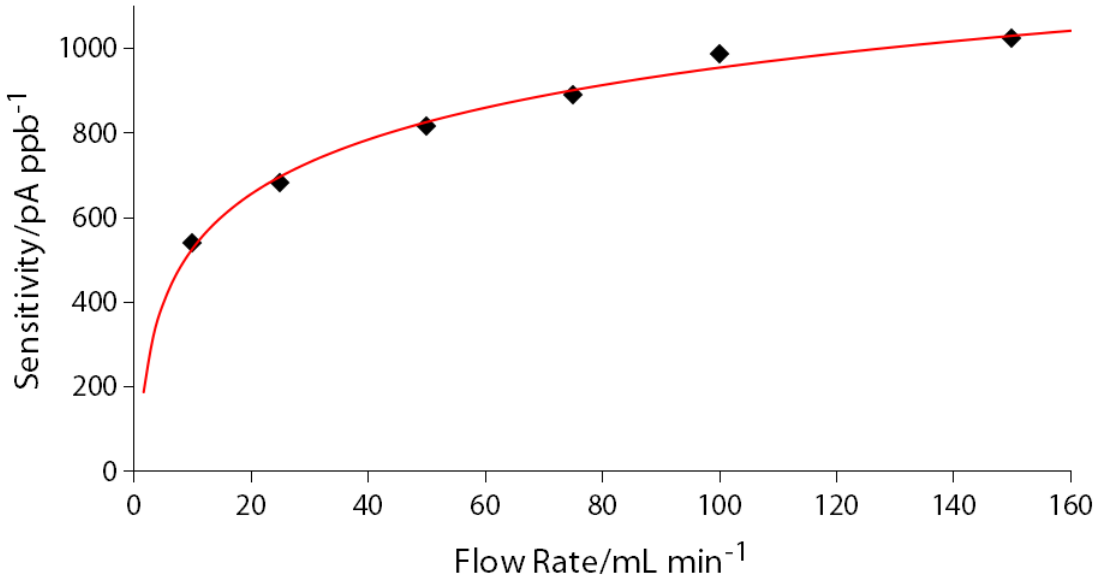

Figure 3.6. NO sensitivity dependence on flow rate for amperometric Pt-Nafion sensors. Operating potential of 1 V vs. Ag/AgCl. Red line represents best fit curve.

Scanning electron microscope (SEM) images of the membrane electrode surface (Figure 3.7) were obtained on an AMRAY 1910 Field Emission SEM; no sputter-coating was required as Pt is already highly conductive. Samples were mounted and conductivity was established with the sample stub using carbon tape. These images indicate that the surface has a considerable number of cracks and pores to provide ionic conductivity into the underlying ionomer membrane.

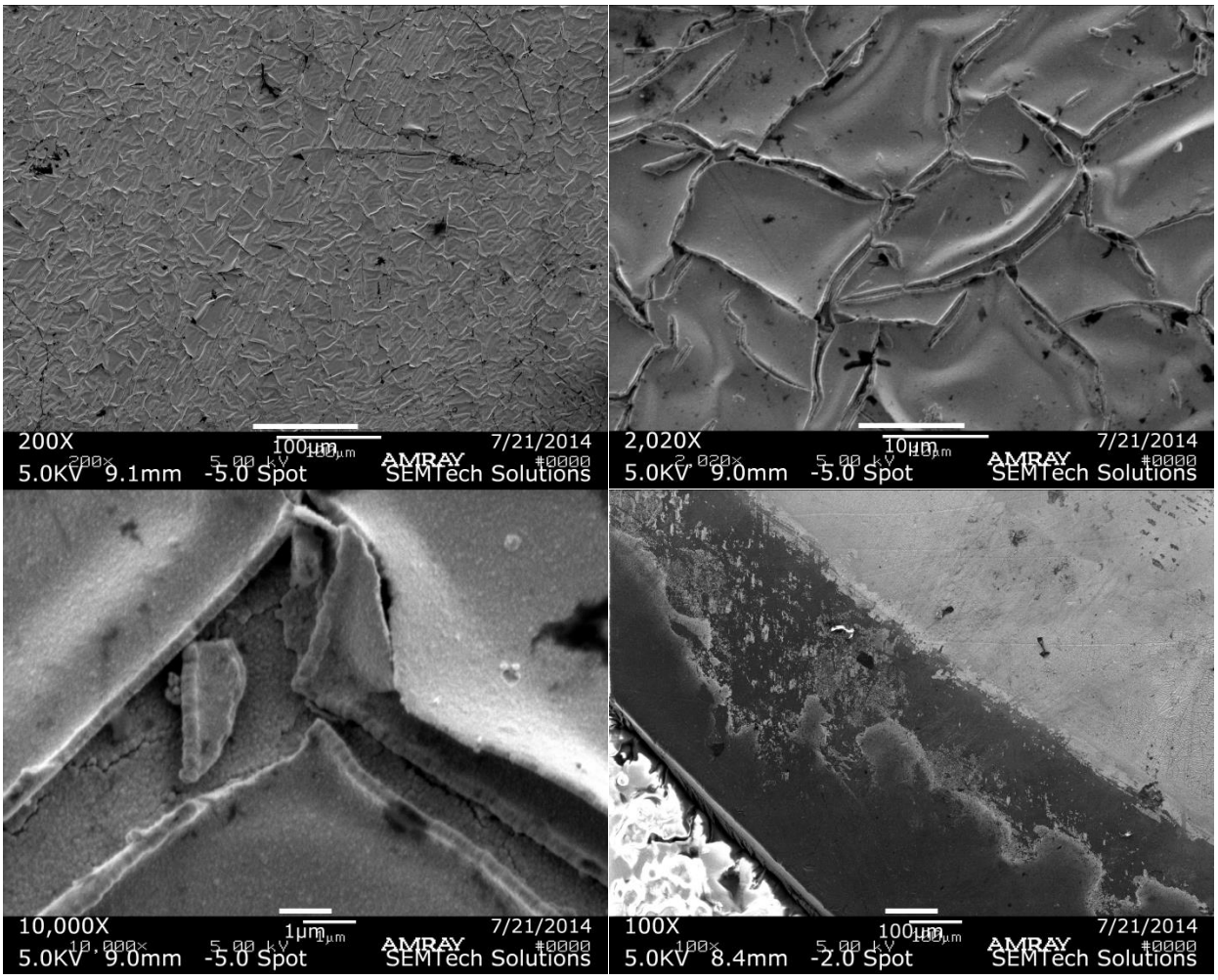

Figure 3.7. (a) (Top Left) Pt-Nafion electrode surface at 200x magnification. (b) (Top Right) Pt-Nafion electrode surface at 2020x magnification. (c) (Bottom Left) Pt-Nafion electrode surface at 10,000x magnification. (d) **(**Bottom Right) Pt-Nafion electrode film edge at 100x magnification. Note that the redundant scale bars are the result of bugged image export software at the time of acquisition; the integrity of the image itself remains unaffected.

Amperometric NO sensing performance was evaluated via calibration using a 1 ppm NO standard gas (commercial cylinder of NO) and diluting with nitrogen using mass flow controllers to achieve total flow rates of 50 mL min^{-1} over the surface of the sensor (Figure 3.8). The response time is quite rapid (<5 s) and the sensitivity is favorable (880 ± 60 pA ppb^{-1}), with limits of detection (LOD) of 4.3 ± 1.1 ppb based on S/N ratio of 3. The sensor response is also highly reversible and reproducible.

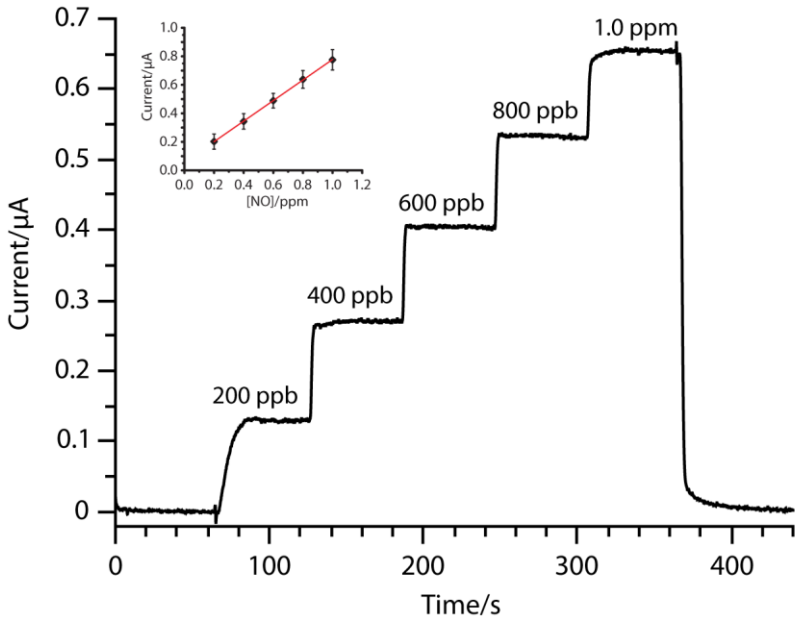

Figure 3.8. Representative amperometric response of Pt-Nafion sensor to NO standard gas (in N_2 background) in 200 ppb increments. A constant total flow rate of 50 mL min^{-1} of the standard gas mix was used. Linear regression of calibrations with error (n = 5) is shown in the inset.

While concern over interfering species is minimal in connection with using the Pt-Nafion sensor to quantitate NO release rates from NO-releasing materials, future concerns regarding the sensor's utility in determining NO levels in exhaled breath requires cross-sensitivity evaluation versus carbon monoxide (CO), which is present in exhaled breath at low ppm concentrations.[35] Preliminary findings suggest relatively poor native selectivity for NO vs. CO, which is in

disagreement with a previous report;[27] however, the selectivity, expressed as log$K_{NO,CO}$ where $K_{NO,CO}$ is the ratio of CO sensitivity to NO sensitivity, can easily be improved by conditioning the sensor in the presence of CO (Figure 3.9). Conditioning involves applying the operating potential to the sensor while under a stream of CO gas (at 10 ppm in N_2). By performing this conditioning for 2 h at a flow rate of 50 mL min^{-1}, selectivity is improved significantly to a log$K_{NO,CO}$ value of -2.22, which indicates a CO sensitivity that is < 0.6% of the NO sensitivity. The effectiveness of this treatment likely stems from the passivation or blocking of the electrochemically-active sites on the Pt-Nafion electrode towards CO oxidation by the oxidation products of CO (namely, adsorbed CO_2 or CO_2 adsorption products with co-adsorbed species such as H_{ads} to form $COOH_{ads}$).[36,37] Because CO oxidation is generally agreed to follow a Langmuir-Hinshelwood reaction mechanism,[36,38] impedance to its adsorption to the working electrode surface will impede its oxidation (see also Chapter 2). This hypothesis requires further investigation of the Pt-SPE type NO gas phase sensing design to fully confirm.

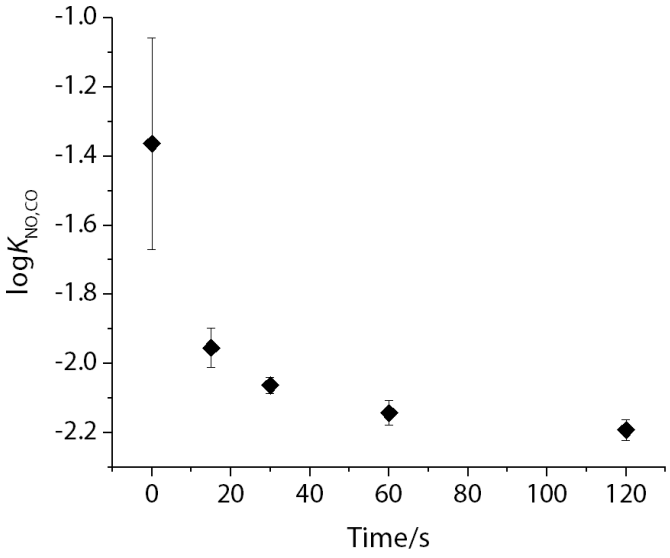

Figure 3.9. Selectivity of Pt-Nafion sensor vs. CO as a function of conditioning time in presence of 10 ppm CO at a flow rate of 50 mL min^{-1} (n = 3).

Anionic exchange membranes (AEM) may also be used to fabricate SPE-based NO sensors for use with an alkaline internal solution, which would promote oxide formation and potentially improve CO selectivity even further.[39,27] However, AEM commercial availability is limited, and most available products are fabric-reinforced, which is not acceptable for the chemical deposition of metal electrodes. One strategy for promoting oxide formation is to use a higher potential, such as 1.2 V, during the polarization of the sensor before bringing the sensor back to 1.0 V. This strategy, however, greatly reduced the NO sensitivity in our experiments while offering no notable decrease in CO sensitivity. This may be due to the intended oxides blocking the "triple" interfacial sites where the Nafion, Pt, and NO phases meet and where the NO undergoes electrochemical oxidation.[24] Further investigation into this phenomenon is required to gain a clearer understanding of the inability of oxide coatings to enhance NO to CO selectivity with this specific type of sensor compared to what was achievable in the solution phase Shibuki design described in Chapter 2.

3.3.2 Determination of NO Released from SNAP/Carbosil2080A Films

When using the Pt-Nafion gas phase NO sensor to quantitate the photolytic release of NO from SNAP-doped CarboSil polymeric films, the amperometric response of the SPE NO sensor (Figure 3.10a) closely matches that of chemiluminescence, the reference method for the determination of NO release rates (Figure 3.10b). This can be attributed to the similarly fast response times (~1 s and < 5 s for chemiluminescence and the SPE sensor, respectively) and low limits of detection as well as the near-identical sampling methods. When NO release rates from identical films are compared between both methods, not only was strong correlation found (R = 0.999), but the results were close to parity (m = 0.999) (Figure 3.11). Both methods are

calibrated to measure in ppb levels of NO; however, due to the presence of the nitrogen "sweep" gas, the stream in both chemiluminescence and the amperometric Pt-Nafion sensor systems are diluted to different degrees (the Sievers chemiluminescence analyzer system draws a vacuum and operates at a different flow rate that is not optimal for the Pt-Nafion sensor). This makes it difficult to accurately compare ppb measurements from one system to another to report NO release rates. Therefore, in this work, NO-release is reported in absolute pmol s^{-1}, which is independent of sample stream dilution effects.

Accounting for the nitrogen dilution involves the derivation of release constants with units of mol ppb^{-1} s^{-1} used to convert ppb to NO-release units of mol s^{-1}, which are independent of nitrogen dilution. The chemiluminescence NO-release constant, $\boldsymbol{k_C}$, is obtained by acidifying a known quantity of nitrite, which converts almost completely to NO, and integrating the response curve (Figure 3.12).

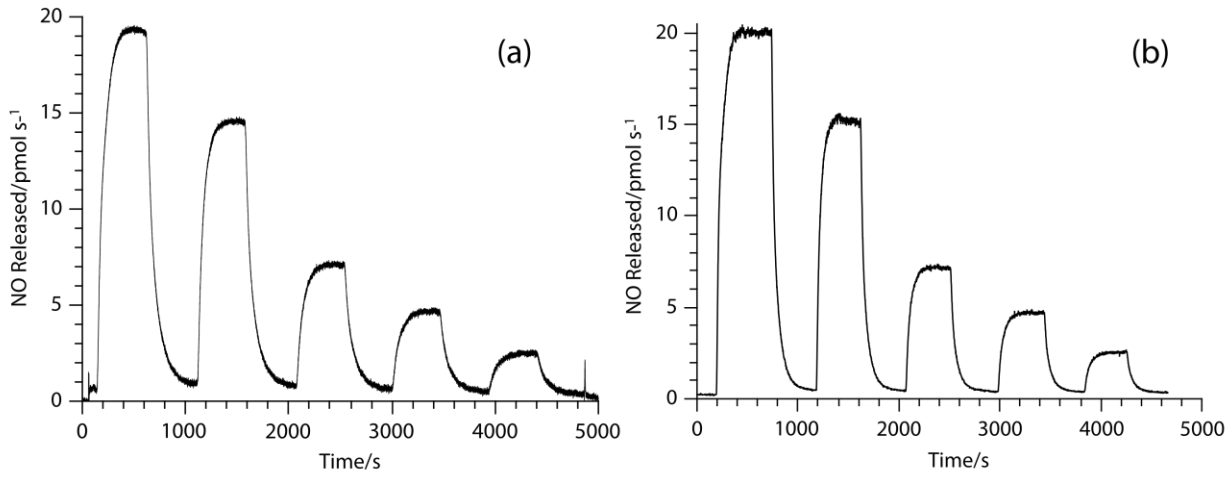

Figure 3.10. (a) Amperometric Pt-Nafion sensor response to photolysis induced NO release from SNAP/Carbosil2080A films at varying light intensities. (b) Chemiluminescence response to NO released from SNAP/Carbosil2080A films at varying light intensities. The same light intensity settings were used for both techniques.

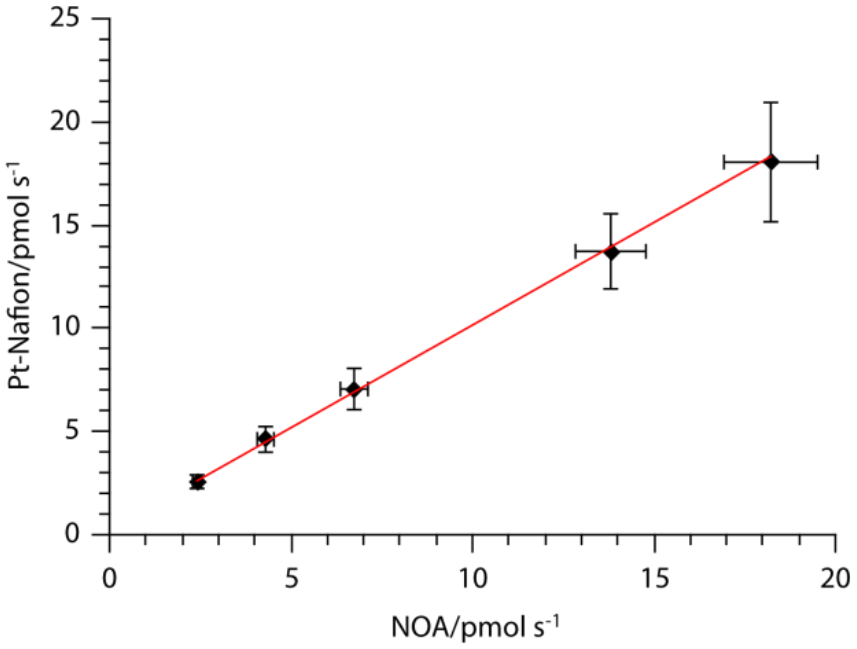

Figure 3.11. Correlation between SNAP/Carbosil2080A NO-release measured via amperometric Pt-Nafion sensing vs. chemiluminescence. Absolute error bars are shown representing standard deviation (n = 6, R = 0.999, m=0.999).

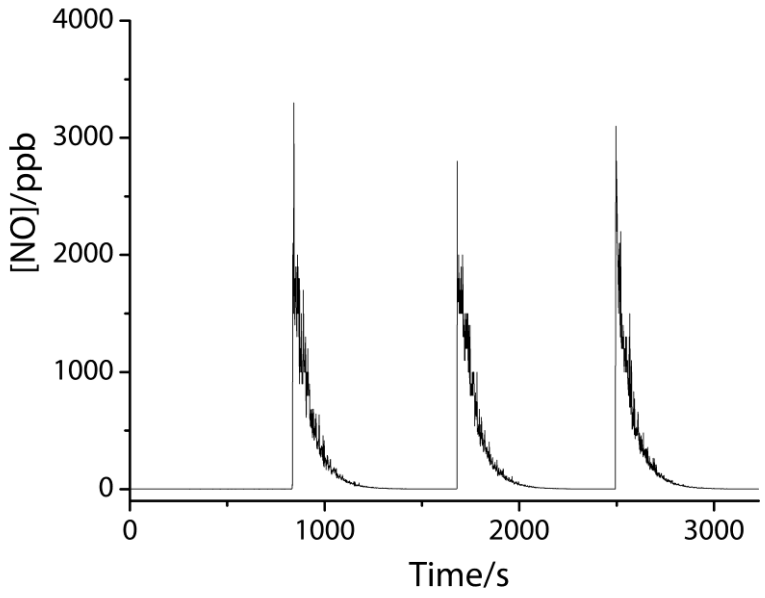

Figure 3.12. Representative chemiluminescence response to NO generated from acidified $NaNO_2$ and corresponding sample determination NO-release constant $\boldsymbol{k_C}$.

The SPE NO-release constant, $\boldsymbol{k_{SPE}}$, is obtained using the flow rate (Q), density of NO (ρ_{NO}), and molar mass of NO (M_{NO}). See sample $\boldsymbol{k_{SPE}}$ computed using a flow rate of 50 mL min^{-1}:

$$\boldsymbol{k_{SPE}} = \frac{\rho_{NO} Q}{M_{NO}} * \text{ppb} = \frac{\frac{1.34E-3\ g}{mL} * \frac{50\ mL}{min}}{\frac{30.02\ g}{mol}} * \left(\frac{min}{60\ s}\right) * \frac{1}{1E9} = \boldsymbol{3.723E-14\ mol\ ppb^{-1} s^{-1}} \qquad (3.1)$$

3.3.3 Determination of Electrochemically Modulated NO Release from CuTPMA/$NaNO_2$ Solutions

To employ the Pt-Nafion NO sensor to monitor NO release from solutions where NO is generated via electrochemical reduction through CuTMPA mediated electron transfer, the solution phase is purged with a constant flow of nitrogen (at 50 mL min^{-1}) and this gas phase is then flowed into the amperometric sensor (or into the chemiluminescence analyzer to obtain correlation data). The amperometric response of the Pt-Nafion NO sensor (Figure 3.13a) shows a similar profile compared to that of chemiluminescence measurements (Figure 3.13b) when the applied voltage to the Pt-Ir working electrode is varied, although the noise level was significantly lower for the new electrochemical sensor method. This may be due to the larger diameter tubing used in the plumbing of the Pt-Nafion system compared to that of the chemiluminescence system. Larger diameter tubing may promote mixing/homogeneity of gases when running liquid samples since the bubbling of the solution produces tight bursts of NO that manifest as concentration spikes. Another explanation is that aerosol droplets, which are formed during aqueous sample purging, are carried into the reaction cell and scatter the photons detected at the photomultiplier tube of the NOA instrument but have no effect on the electrochemical sensor measurements. The NO-released measured by both methods showed very good correlation (R = 0.999) and overall agreement in value (m = 0.938) (see Figure 3.14). As expected, as the voltage applied is made more cathodic, the rate of generation of Cu(I)TMPA at the electrode surface increases, and this increases the rate of NO generation from inorganic nitrite ions in the solution adjacent to the working electrode surface.[29]

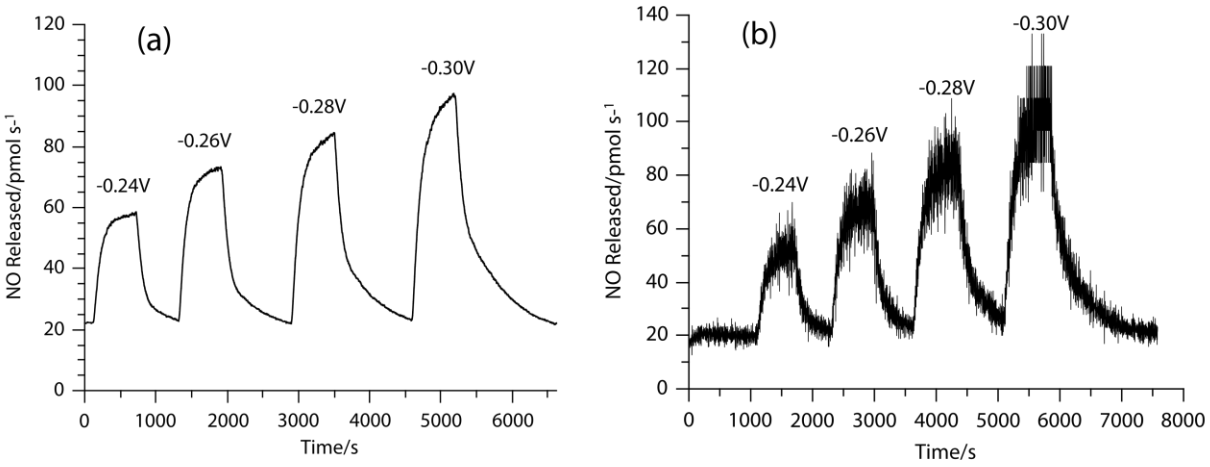

Figure 3.13. (a) Amperometric Pt-Nafion sensor response to electrochemically generated NO formed via the CuTPMA-mediated reduction of nitrite ions in solution at various applied cathodic potentials in 4 mL of solution containing 1 M $NaNO_2$ and 0.3 M CuTMPA. The working electrode was a Teflon-coated Pt-Ir alloy wire with an exposed surface area of 0.08 cm^2 (b) Chemiluminescence response to NO released from the same solution described in (a). The same potentials were used for both gas phase measurement techniques.

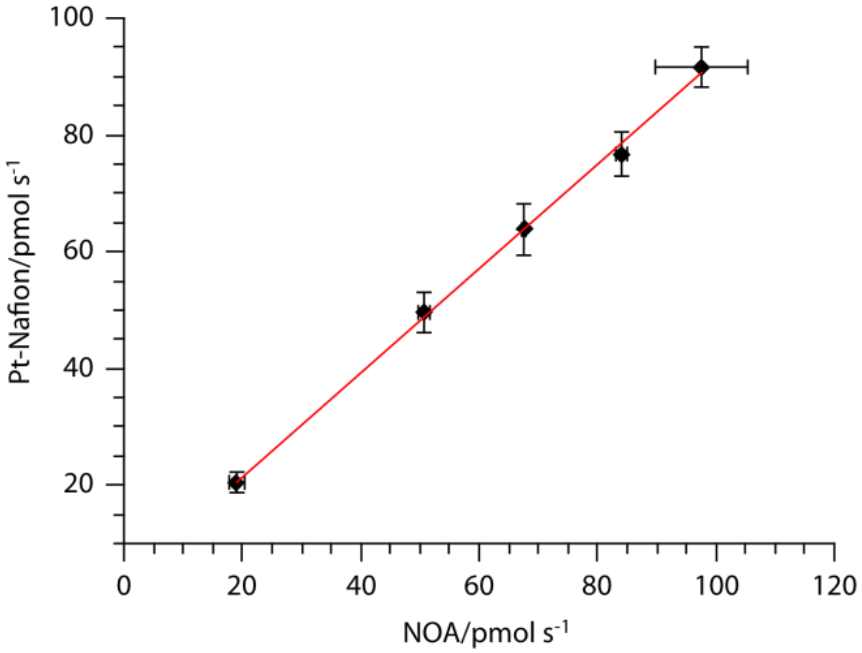

Figure 3.14. Correlation between NO release rates measured from electrochemical generation of NO from solution of CuTPMA and $NaNO_2$ by the amperometric Pt-Nafion sensing vs. chemiluminescence measurements under the exact same conditions. Absolute error bars are shown representing standard deviation (n = 3, R = 0.999, m=0.938)

3.4 Conclusions

An improved amperometric Pt-Nafion sensor has been demonstrated as a viable and competitive alternative to chemiluminescence for the characterization of NO generation/release rates from NO-donor biomaterials and devices. The gas phase sensor is highly sensitive (880 ± 60 pA ppb^{-1}) with low limits of detection (4.3 ± 1.1 ppb) and a fast response time (<5s). These amperometric Pt-Nafion SPE sensors generate results in close agreement with chemiluminescence in two distinctly different biomaterials-research applications.

Selectivity remains a major challenge for use of the amperometric NO gas sensors for diagnostic purposes. However, with proper conditioning and/or use of optimized applied potentials, we have demonstrated that selectivity over CO can be greatly enhanced. Additional strategies for improving the selectivity of Pt-Nafion NO sensors, such as sample treatment (filtration/scrubbing) and applied potential studies are explored in Chapter 4 of this dissertation.

While further selectivity improvements are needed before applying the sensor configuration described here for measuring NO in exhaled breath (especially enhancing the selectivity over ammonia using a coating over the sensor and/or a trap to remove ammonia), it is certainly possible to use this optimized SPE-based NO sensor at this stage of development for monitoring NO in the gas streams used for NO inhalation therapy within hospital settings (INO-therapy).[32,33] With amperometric gas-phase NO sensors of the type described here, it may also be possible to combine electrochemical NO generation[29] and electrochemical NO detection within a new integrated INO system/device that does not require expensive and unstable tanks of compressed NO gas. Proof-of-concept for NO monitoring in such an INO system, as well as safety concerns, are addressed in Chapter 5 of this dissertation.

3.5 References

(1) Ignarro, L.; Buga, G. *PNAS* **1987**, *84* (December), 9265.

(2) Palmer, R.; Ferrige, A.; Moncada, S. *Nature* **1987**, *327*, 524.

(3) Moncada, S.; Higgs, E. *N. Engl. J. Med.* **1993**, *329*, 2002.

(4) Radomski, M. W.; Palmer, R. M.; Moncada, S. *PNAS* **1990**, *87* (13), 5193.

(5) Bredt, D. S.; Hwang, P.; Snyder, S. *Nature* **1990**, *347*, 768.

(6) Vincent, S. R. *Prog. Neurobiol.* **1994**, *42* (1), 129.

(7) Nathan, C. F.; Hibbs, J. B. *Curr. Opin. Immunol.* **1991**, *3* (1), 65.

(8) Naraghi, M.; Deroee, A. F.; Ebrahimkhani, M.; Kiani, S.; Dehpour, A. *Am. J. Otolaryngol. - Head Neck Med. Surg.* **2007**, *28*, 334.

(9) Ragab, S. M.; Lund, V. J.; Saleh, H. A.; Scadding, G. *Allergy* **2006**, *61*, 717.

(10) Benson, V.; Marano, M. A. *Natl. Heal. Surv. Vital Heal. Stat.* **1998**, No. 199, 1.

(11) Adams, P. F.; Hendershot, G. E.; Marano, M. A. *Natl. Heal. Surv. Vital Heal. Stat.* **1999**, No. 200, 1.

(12) Wang, P. G.; Xian, M.; Tang, X.; Wu, X.; Wen, Z.; Cai, T.; Janczuk, A. J. *Chem. Rev.* **2002**, *102*, 1091.

(13) Williams, D. L. H. *Acc. Chem. Res.* **1999**, *32* (10), 869.

(14) Brisbois, E. J.; Handa, H.; Major, T. C.; Bartlett, R. H.; Meyerhoff, M. E. *Biomaterials* **2013**, *34* (28), 6957.

(15) Fontijn, A.; Sabadell, A.; Ronco, R. *Anal. Chem.* **1970**, *42* (6), 575.

(16) Alving, K.; Weitzberg, E.; Lundberg, J. M. *Eur. Respir. J.* **1993**, *6* (9), 1368.

(17) Grasemann, H.; Michler, E.; Wallot, M.; Ratjen, F. *Pediatr. Pulmonol.* **1997**, *24* (3), 173.

(18) Kharitonov, S.; Alving, K.; Barnes, P. J. *Eur. Respir. J.* **1997**, *10* (7), 1683.

(19) Technologies, G. W. & P. GE Analytical Instruments 2010, p 11.

(20) Tomchenko, A. A.; Khatko, V. V.; Emelianov, I. L. *Sensors Actuators B Chem.* **1998**, *46*, 8.

(21) Chen, L.; Tsang, S. C. *Sensors Actuators B Chem.* **2003**, *89* (x), 68.

(22) Wetchakun, K.; Samerjai, T.; Tamaekong, N.; Liewhiran, C.; Siriwong, C.; Kruefu, V.; Wisitsoraat, A.; Tuantranont, A.; Phanichphant, S. *Sensors Actuators B Chem.* **2011**, *160* (1), 580.

(23) Ho, K.; Hung, W.; Yang, J. *Sensors* **2003**, No. 2, 290.

(24) Hodgson, A. W. E.; Jacquinot, P.; Jordan, L. R.; Hauser, P. C. *Electroanalysis* **1999**, *11*, 782.

(25) Knake, R.; Jacquinot, P.; Hodgson, A. W. E.; Hauser, P. C. *Anal. Chim. Acta* **2005**, *549* (1-2), 1.

(26) Opekar, F.; Štuli • k, K. *Anal. Chim. Acta* **1999**, *385*.

(27) Ho, K.C.; Liao, J. Y.; Yang, C. C. *Sensors Actuators B Chem.* **2005**, *108* (1-2), 820.

(28) Jacquinot, P.; Hodgson, A.; Hauser, P. *Anal. Chim. Acta* **2001**, *443* (1), 53.

(29) Ren, H.; Wu, J.; Xi, C.; Lehnert, N.; Major, T.; Bartlett, R. H.; Meyerhoff, M. E. *ACS Appl. Mater. Interfaces* **2014**, *6* (6), 3779.

(30) Fedkiw, P. S. *J. Electrochem. Soc.* **1989**, *136* (3), 899.

(31) Jordan, L. R.; Hauser, P. C.; Dawson, G. A. *Anal. Chem.* **1997**, *69* (4), 558.

(32) Rossaint, R.; Falke, K. J.; Lopez, F.; Slama, K.; Pison, U.; Zapol, W. M. *N. Engl. J. Med.* **1993**, *328*, 399.

(33) The Neonatal Inhaled Nitric Oxide Group. *N. Engl. J. Med.* **1997**, *336*, 597.

(34) Doña Rodríguez, J. M.; Herrera Melián, J. A.; Pérez Peña, J. *J. Chem. Educ.* **2000**, *77* (9),

1195.

(35) Yamaya, M.; Sekizawa, K. *Am. J. Respir. Crit. Care. Med.* **1998**, No. 12, 1.

(36) McClure, S. M.; Goodman, D. W. *Chem. Phys. Lett.* **2009**, *469* (1-3), 1.

(37) Sobkowski, J.; Czerwinski, A. *J. Phys. Chem.* **1985**, *89* (24), 365.

(38) Dahlstrøm, P. K.; Harrington, D. A.; Seland, F. *Electrochim. Acta* **2012**, *82*, 550.

(39) Jensen, G. C.; Zheng, Z.; Meyerhoff, M. E. *Anal. Chem.* **2013**, *85*, 10057.

CHAPTER 4

FUNDAMENTAL STUDIES OF SELECTIVITY IN AMPEROMETRIC PT-NAFION GAS PHASE NITRIC OXIDE (NO) SENSORS

4.1 Introduction

As discussed throughout this dissertation, amperometric methods for the detection of nitric oxide provide compact, cost-effective, and sensitive alternatives to more costly and immobile instrumentation (e.g., chemiluminescence). Solid-polymer electrolyte (SPE) based amperometric sensors can detect a wide array of gaseous analytes including volatile organics (such as ethylene[1]) as well as inorganic gases (NO,[2–5] NO_2,[5–7] SO_2,[2,8,9] CO[10,11]). The ability to discriminate between these different analytes, however, has proven to be a defining limitation of amperometric SPE sensing in its current state. Enhancing selectivity is a critical element for improving the analytical performance and applicability of amperometric sensing for biomedical applications such as exhaled nasal NO detection. There are over 1800 volatile organic compounds (VOC) present in the human exhalate,[12,13] as well as inorganic gases. While the potential number of relevant interfering species may seem daunting, it is prudent and worthwhile to first investigate and address some of the more prevalent perpetrators, such as NH_3 (100-1000 ppb in human breath)[12] and CO (1-5 ppm in human breath),[14] and approach this problem incrementally. The oxidation products of carbon monoxide and NH_3 are primarily CO_2 and N_2, respectively.

Attempts to improve the selectivity of amperometric SPE sensors in the literature are sparse and the selectivity required to perform exhaled breath analysis remains elusive. Several electrode materials (e.g., Pt, Au, C)[10,15] have been used to fabricate SPE membrane electrodes with varying degrees of selectivity towards particular analytes; however, no single sensor has proven sufficiently selective for NO or any other specific analyte. For example, Au[1,5] and carbon[2] based SPE sensors have been shown to have impressive inherent selectivity vs. CO but lack selectivity vs. SO_2. Use of a highly acidic (10 M H_2SO_4) internal solution has been shown to improve selectivity over SO_2 ten-fold on both Au and carbon working electrodes, but negatively impacts NO sensitivity on carbon.[1,2] Sensor sensitivity is also adversely affected by changes in relative humidity on Au,[5] but does not affect sensitivity on Pt or carbon. Reports of selectivity are also often inconsistent between studies, suggesting that performance and behavior are sensitive to fabrication parameters.[16]

One approach to imparting greater selectivity to SPE-based sensors is to employ permselective outer membranes or coatings, which have been used in other types of amperometric NO sensors to impart selectivity vs. aqueous interfering species, but have generally been less effective vs. dissolved gases and gas-phase samples. Nafion itself has been employed extensively to coat needle-type microsensors[17,18] (discussed in Chapter 1) but does not exclude gas phase interfering species to any significant extent. More recent developments in the area of permselective barriers have made strides towards better discrimination against gas-phase interferents such as ammonia via Teflon AF[19] and CO via Xerogels.[20,21] However, these materials are difficult to work with in context to SPE sensors for a number of reasons. First, both materials are fluoropolymers that become brittle upon curing and are ionically non-conductive if the coating is too thick or is non-uniform. Dip coating of needle-type microsensors produces a

thin and mostly uniform coating, but spread-casting is woefully inadequate for uniformly coating planar electrodes such as those deposited on SPE materials. We have also found that permselective coating solutions generally utilize fluorinated solvents and organic solvents, both of which lead to solvent interactions with the SPE membranes that inactivate the membrane electrodes. Discrete permselective membranes represent an alternative and may appear to be viable options for providing protection from interfering species in the absence of solvent interactions. However, extremely thin layers are required, as thicker layers lead to poor sensitivity and dramatically lengthened response times, especially if diffusion of NO through these phases is unfavorable. Furthermore, it is exceedingly difficult to achieve intimate contact between a discretely cast permselective membrane and the SPE membrane electrode due to a slight concave geometry that forms on electrodes deposited on SPE membranes.

Other explorations of selectivity improvement in this dissertation have been briefly discussed in earlier chapters. In Chapter 2, it was demonstrated that modifying the Pt electrode surface with a simple change in the internal electrolyte pH could improve selectivity vs. carbon monoxide dramatically.[22] This approach is briefly examined in this chapter as it relates to its compatibility with the platinized Nafion membrane electrodes and is shown to suffer from lack of ionic conductivity between the electrolyte solution and the SPE phase due to the cationic exchange properties of Nafion vs. the anionic nature of hydroxide in more alkaline electrolytes. In Chapter 3, it was demonstrated that selectivity vs. carbon monoxide could be markedly improved by conditioning the sensor under a high concentration of CO for up to 2 h.[23] This same approach does not show significant improvement as it pertains to other interfering species (such as NH_3 and NO_2, both eliciting steady responses from the sensor within 60 s of contact as opposed to 2 h).

This chapter primarily describes strategies to improve NO selectivity of the SPE sensor described in Chapter 3 involving on-line sample pretreatment via filtration and scrubbing of the gas stream. Gas stream filtration and "cleaning" are common industrial processes and have been employed for decades; however, NO has generally been regarded as a pollutant and its removal from the gas stream is viewed as desirable, leaving very little incentive for the development of a process that preserves NO while selectively removing other gaseous components. Although sample pre-treatment is generally a less desirable approach to achieving selectivity versus an electrode surface modification or permselective membrane, it generally serves as a more universal solution for a wide array of analytes. Filtration and scrubbing materials studied herein include activated carbon materials (activated charcoal, carbon clothe, proprietary activated carbon fiber) and acidic materials (solid citric acid, Nafion polymer pellets, Nafion tubing, and sulfuric acid scrubbing). As will be reported here, modest improvements in selectivity vs. NH_3 are observed with sample pre-treatment using citric acid, Nafion, and sulfuric acid scrubbing, while carbon cloth and activated charcoal are found to be overly aggressive and remove all relevant gases including NO. The activated carbon fiber filter (extracted from a NIOX MINO proprietary sensor) is shown to yield an improvement in selectivity for NO vs. both CO and ammonia although the mechanism remains unclear.[24]

4.2 Experimental

4.2.1 Materials & Reagents

All chemicals used were commercially obtained and were reagent grade without further purification or modification unless otherwise specified. All gases used for the calibration of the Pt-Nafion sensors were obtained from Cryogenic Gases (Detroit, MI). Aqueous solutions were prepared using water

(18.2 MΩ·cm) purified through a Milli-Q system (Millipore, Bedford, MA). Sensor cell assembly, sample cells, and filter housing parts were prepared by Glass-blowing Services, Department of Chemistry, University of Michigan (Ann Arbor, MI). All applied potentials reported herein are versus Ag/AgCl (saturated KCl), which is +0.197 V vs. SHE. Note that current in this chapter is expressed in Δi, which is a baseline subtracted value of net current change.

4.2.2 Sensor Fabrication

The general design and fabrication of the Pt-Nafion working electrode are described in Chapter 3. Briefly, Nafion 117 (DuPont, Wilmington, DE) was cut into 1 cm dia. circles and cleaned of impurities by boiling in 3 M nitric acid for 1 h followed by boiling in deionized water for 1 h. The membranes were then placed in a diffusion cell with one side exposed to 20 mM $Pt(NH_3)_4Cl_2$ at 37 °C for 6 h followed by exposure to 50 mM $NaBH_4$ in 1 M NaOH for at 37 °C 90 min. The Pt-Nafion membrane was then boiled in DI water for 1 h to remove any remaining Pt complex and reducing agent.

A single junction Ag/AgCl (saturated KCl) reference electrode and bare Pt auxiliary electrode were used along with a 0.5 M H_2SO_4 internal electrolyte in the final sensor assembly (see Figure 3.1). A CHI800B potentiostat (CH Instruments, Austin, TX) was used to polarize the working electrode and record sensor output currents. 2x MC-200SCCM mass flow controllers (Alicat Scientific, Tucson, AZ) operated in tandem via a BB9-USB signal distribution box (Alicat Scientific, Tucson, AZ) and FlowVision SC software (Alicat Scientific, Tucson, AZ) were used for mixing of calibration gas (1 ppm NO in N_2 balance and 10 ppm CO in N_2 balance).

4.2.3 Filtration & Scrubbing

The Pt-Nafion sensor was operated at 1 V with a constant total gas flow rate of 50 ml min^{-1}. For filtration through solid particles, a glass column with inlet and outlet was packed (Figure 4.1) and placed immediately upstream from the sensor gas inlet. Activated charcoal

(Sievers, Boulder, CO), Nafion beads (DuPont, Wilmington, DE), and solid citric acid were prepared and tested in this fashion.

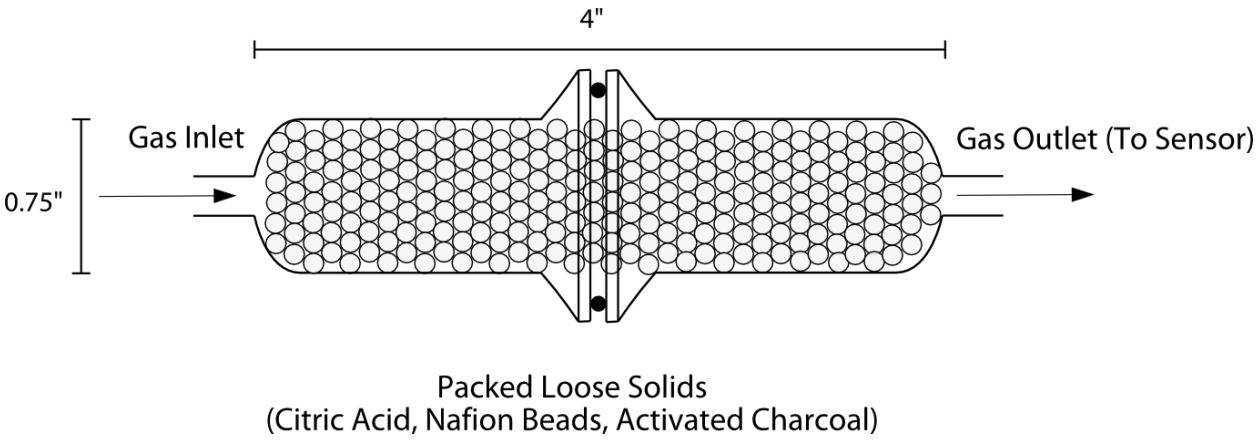

Figure 4.1. Schematic of filtration assembly packed with loose solids.

For sulfuric acid liquid scrubbing, a glass cell (Figure 4.2) was filled with 1.5 mL of scrubbing solution (0.5 M H_2SO_4) and purged with nitrogen through fritted glass (medium coarseness) prior to experiments.

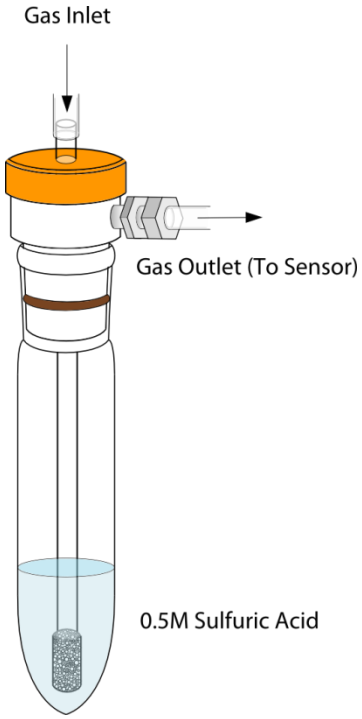

Figure 4.2. Schematic of liquid ammonia scrubbing system.

Filtration through carbon fiber cloth (Charcoal House LLC, Crawford, NE) and proprietary activated carbon fiber (ACF) thin filters (Aerocrine, Solna, Sweden) was performed by placing the filter material between two glass cells (Figure 4.3) and passing sample gas through. The edges of the thin filters were sealed off by o-rings.

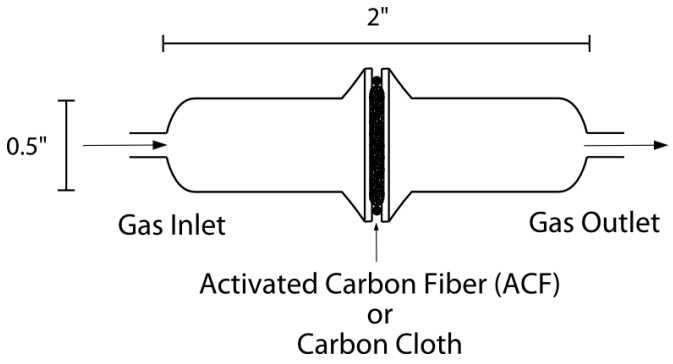

Figure 4.3. Schematic of ACF and carbon cloth filter assemblies.

Sample treatment through Nafion tubing was performed by passing sample gas through 2 m of 1/16" diam. Nafion tubing (PermPure LLC, Lakewood, NJ) (Figure 4.4) immersed in 0.5 M H_2SO_4.

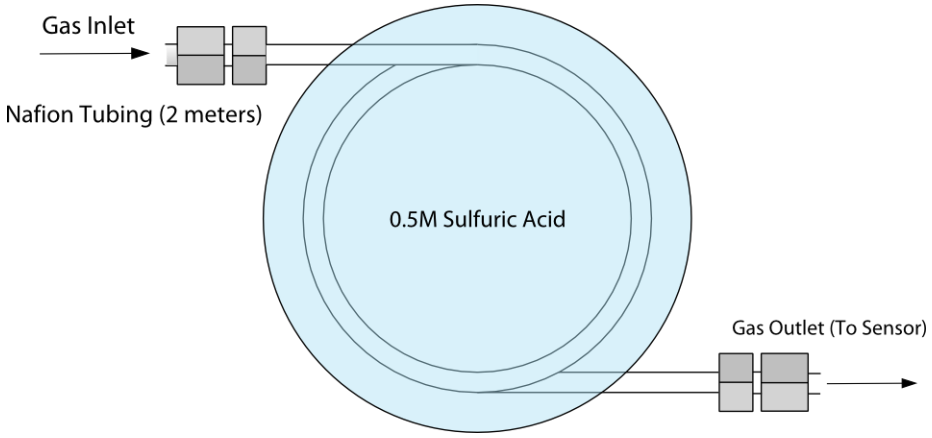

Figure 4.4. Schematic of Nafion tubing gas sample treatment system. The tubing is immersed in 0.5M H_2SO_4

4.3 Results and Discussion

4.3.1 Sensor Selectivity (vs. NH_3 and CO) as a Function of Applied Potential

The sensitivity of Pt-Nafion NO sensors towards various gases is dependent on the applied potential. It is conceivable that selectivity might be improved by electing to use a potential where the sensor is considerably more sensitive to NO than it is towards relevant interfering species, such as CO or NH_3.

NO, CO, and NH_3 calibrations were performed at varying potentials over the range where sensor sensitivity to NO is greatest (0.8-1.2V). The selectivity of the sensor vs. CO and NH_3 were determined at each examined potential and plotted (Figures 4.5-4.6). The sensor was conditioned under 10 ppm CO for 1 h prior to testing.

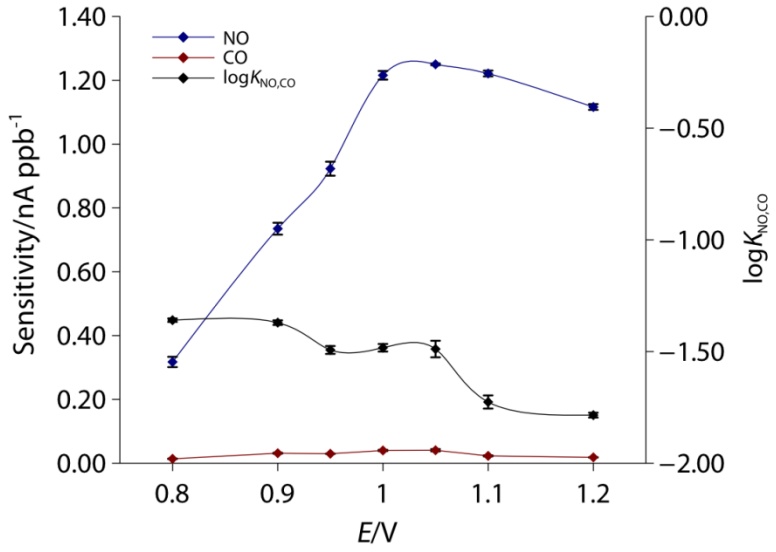

Figure 4.5. Sampled selectivity (black, right axis) of Pt-Nafion NO sensor vs. CO with sensitivities of NO (blue) and CO (red) as a function of applied potential.

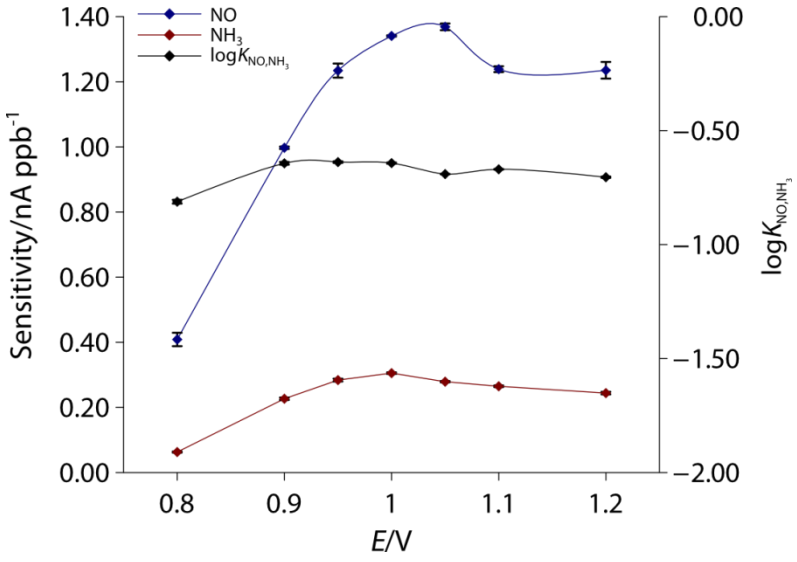

Figure 4.6. Sampled selectivity (black, right axis) of Pt-Nafion NO sensor vs. NH_3 with sensitivities of NO (blue) and NH_3(red) as a function of applied potential.

The sensor exhibits good selectivity towards CO after just an hour of conditioning and may further improve with 2 h of conditioning (as suggested in Chapter 3, where it was determined that CO selectivity improves with up to 2 h of conditioning). However, no significant gain in selectivity is observed at different applied potentials in the range of 0.8-1.2 V. Ammonia selectivity is poorer overall (Figure 4.6) and also does not appear to benefit greatly from different applied potentials in the range of 0.8-1.2 V. Both CO and NH_3 show significant overlap in their optimal sensitivity ranges with NO, rendering selectivity enhancement via judicious choice of an applied potential of minimal benefit. For simple applications of Pt-Nafion NO sensors, applying a 1 V potential is still the optimal condition in the absence of NH_3 or CO in order to maximize sensitivity towards NO while maintaining low limits of detection.

4.3.2 Removal of CO and NH_3 using Carbon-based Materials

A proprietary activated carbon fiber (ACF) filter was previously identified[24] as a potentially useful and effective gas filter for removing NH_3 and CO from gas streams. The ACF filter was extracted from a commercial fractional exhaled NO (FeNO) sensor housing and used in our filter assembly (Figure 4.3) without further modification. While there is some loss of NO (-14±7%) on this filter, a modest amount of NH_3 is removed and a significant amount of CO is also removed from the gas stream (Figure 4.7). The final CO selectivity coefficient after filtration was -1.84±0.01, while that of NH_3 was -0.44±0.01. The selective removal of NH_3 and CO from the gas stream is promising although the resulting selectivity remains insufficient for confident determination of NO in exhaled breath.

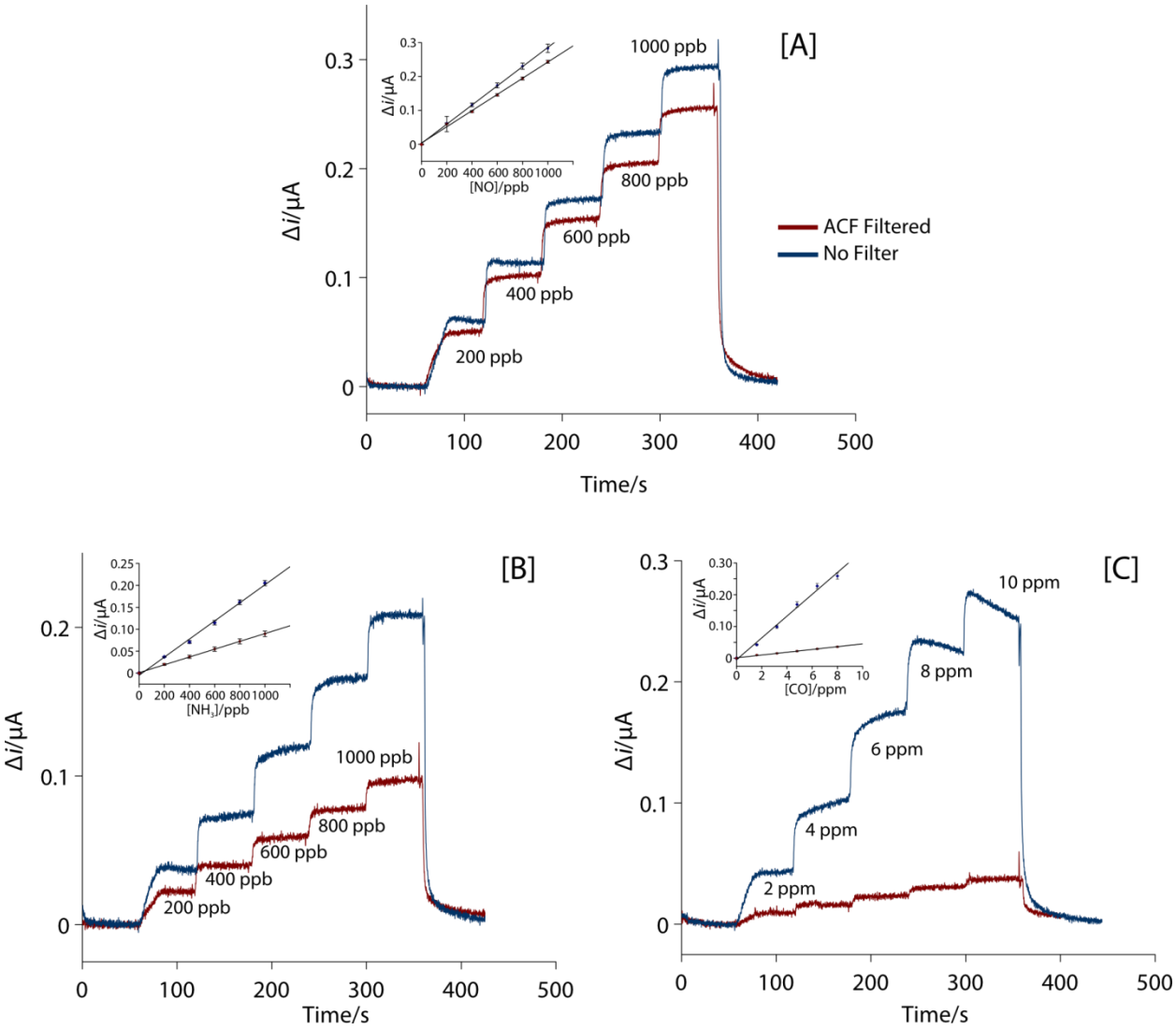

Figure 4.7. Pt-Nafion sensor current responses to increasing concentrations of [A] NO, [B] NH_3, and [C] CO with and without the use of ACF filter. Calibration curves are shown in insets with standard deviation as error bars (n=3).

If the activated carbon is indeed selectively removing CO and NH_3, other forms of activated carbon may be of use with similar performance. Activated charcoal (as a loose solid) has a number of attractive properties that make it an ideal filtration material for liquid and gas streams. It is has a very high surface area due to high porosity and is quite inexpensive. Due to the promising performance of the proprietary ACF filter, we elected to perform filtration experiments through activated charcoal. NO, CO, and NH_3 calibrations were performed on the same sensor with and without the use of a glass column packed with activated charcoal (Figure 4.8).

While interfering species CO and NH_3 were removed almost completely, NO was also removed by activated charcoal (94±1% loss of NO). Activated charcoal does not discriminate between removal of NO, CO, and NH_3, which makes it a great overall gas cleaner, but a poor filtration material for NO gas sensing applications. The calculations suggest significant improvements in selectivity, but the error is also quite significant at such low sensitivity values (see summary Tables 4.1-4.2); furthermore, a 94% loss of NO sensitivity is unacceptable.

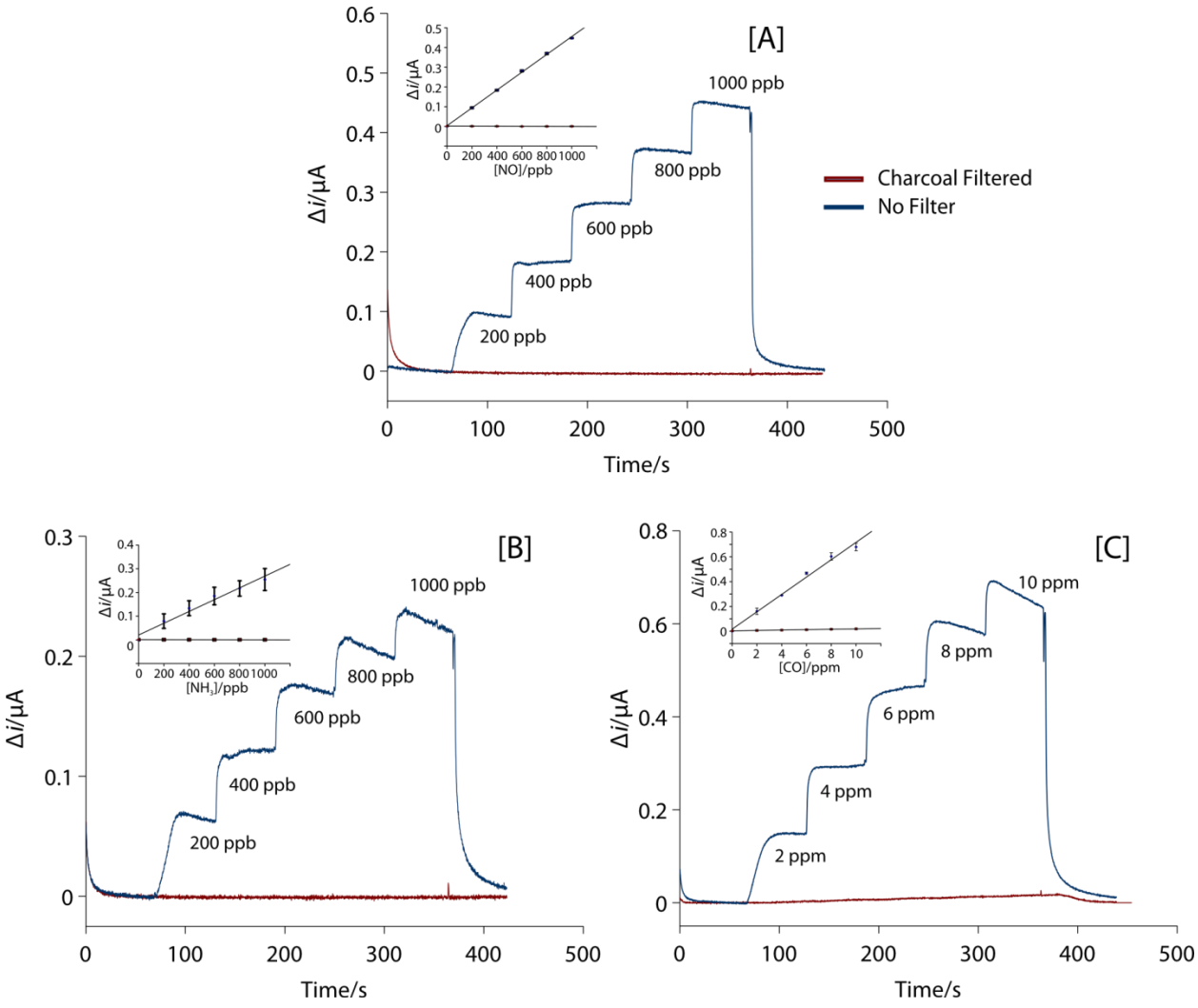

Figure 4.8. Pt-Nafion sensor current responses to increasing concentrations of [A] NO, [B] NH_3, and [C] CO with and without the use of activated charcoal filter. Calibration curves are shown in insets with standard deviation as error bars (n=3).

Carbon cloth/weave is a material similar to activated charcoal particle and is woven from carbon fibers. It is often used in conjunction with traditional textiles for a wide array of applications. Carbon cloth is also inexpensive, and easy to work with. Due to the similarity in thickness and overall geometry with the ACF filter, it was expected to have equivalent performance. However, the carbon cloth performed more similarly to the packed activated charcoal; it removed all electroactive gas species from the sample stream (Figure 4.9) including

our analyte of interest, NO (93±1% loss). This makes carbon cloth unsuitable in its current form for use in improving gas phase selectivity of the Pt-Nafion NO sensors.

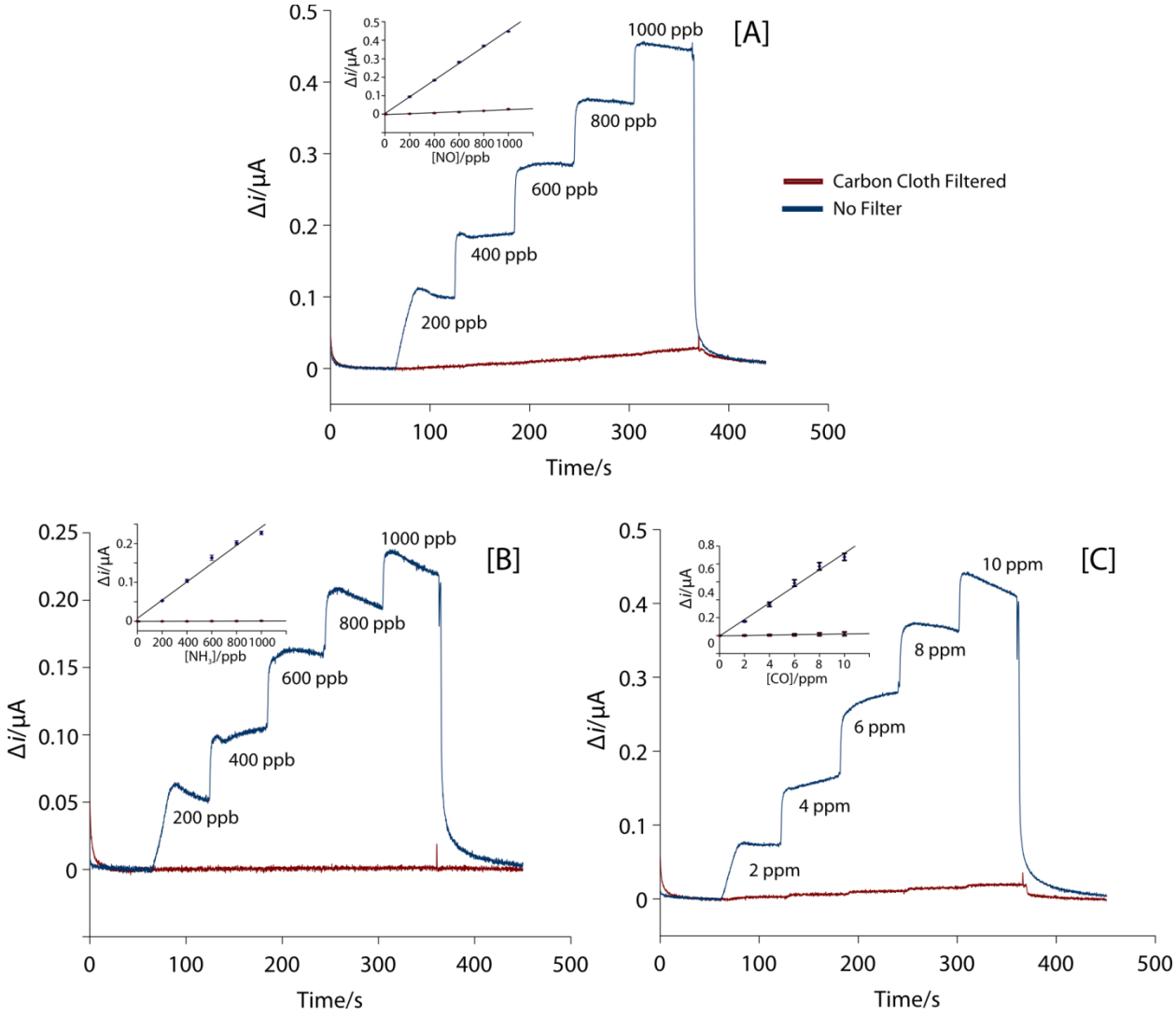

Figure 4.9. Pt-Nafion sensor current responses to increasing concentrations of [A] NO, [B] NH_3, and [C] CO with and without the use of carbon cloth filter. Calibration curves are shown in insets with standard deviation as error bars (n=3).

With both activated charcoal and carbon cloth filters failing to match the performance of the proprietary ACF filter, the data suggests that selective retention of CO and NH_3 is either dependent on the form of the activated carbon or the ACF filter has other modifications or components in addition to activated carbon that allows it to selectively retain CO and NH_3 while leaving NO largely unaffected. Elemental analysis and perhaps surface characterization of the ACF filter may shed additional light on the discrepancy.

4.3.3 Removal of NH_3 using Nafion-based Materials

Nafion has proven to be a versatile material that is chemically robust and highly effective as an ionically conductive material. Due to its proton-exchanging properties, it can be hydrated/protonated and used as a solid acid. Nafion in the form of raw polymer beads was soaked in 0.5 M sulfuric acid overnight prior to being drained and packed in a glass column. It was further dried by passing nitrogen through for 10 min prior to use in NO and NH_3 calibrations (Figure 4.10). The use of Nafion beads resulted in substantial removal of NH_3 although a modest loss of NO was also observed (24±6% loss). The net improvement in selectivity vs. NH_3 was -0.35±0.03 resulting in a selectivity coefficient of -0.67±0.02. This final selectivity coefficient is insufficient for the purpose of NO determination in exhaled breath.

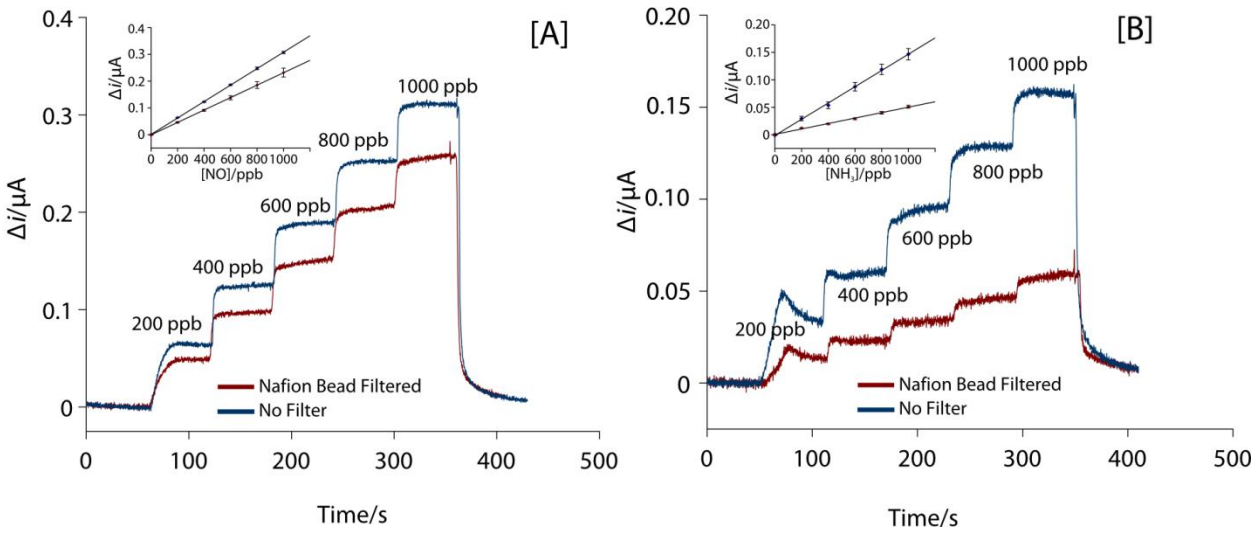

Figure 4.10. Pt-Nafion sensor current responses to increasing concentrations of [A] NO and [B] NH_3, with and without the use of Nafion bead filter. Calibration curves are shown in insets with standard deviation as error bars (n=3).

Another use of Nafion is for drying gas streams as a tubing that absorbs and exchanges water vapor with a drying gas as a jacket. However, the tubing is advertised as able to remove ammonia and several other gases when it is protonated. Using 2 meters of Nafion tubing, sample gas was passed through the tubing sitting in a 0.5 M solution of sulfuric acid (Figure 4.11). The performance of Nafion tubing is worse compared to the packed column of Nafion beads and demonstrates only minor improvement in NH_3 selectivity (coefficient change of -0.19±0.04 for a final selectivity coefficient of -0.59±0.04) at the cost of NO sensitivity (30±8%). Nafion as a solid acid template shows generally unremarkable performance when used for NO gas sensing applications in the raw form of beads or tubing.

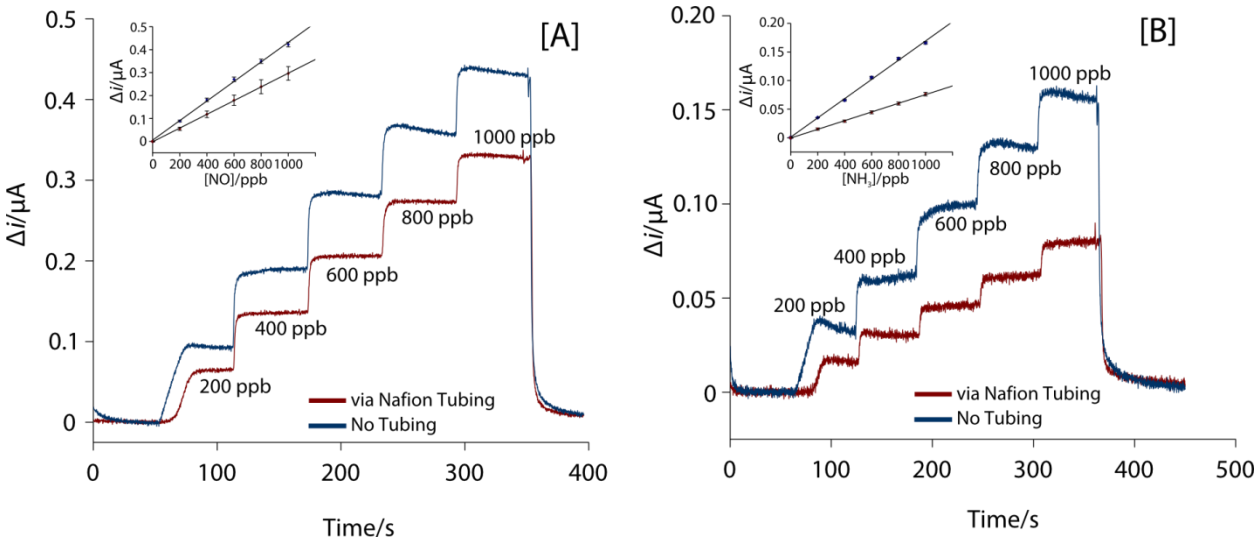

Figure 4.11. Pt-Nafion sensor current responses to increasing concentrations of [A] NO and [B] NH_3, with and without the use of Nafion tubing treatment. Calibration curves are shown in insets with standard deviation as error bars (n=3).

4.3.4 Removal of NH_3 using Acid Traps

Gas scrubbing in industrial operations often involves using sulfuric acid to neutralize and capture ammonia and other compounds that act as bases when dissolved in liquid. This process was emulated by using a glass cell containing 0.5 M sulfuric acid and passing the sample gas through the solution with a fritted glass sparger.

The scrubbing removed a significant amount of ammonia from the gas stream with some NO loss (24±2%). Overall, the net improvement in selectivity was significant (coefficient change of -1.06±0.08) resulting in a final selectivity coefficient of -1.37±0.08, which might be sufficient (~5% interference) to combat NH_3 in exhaled breath determination of NO.

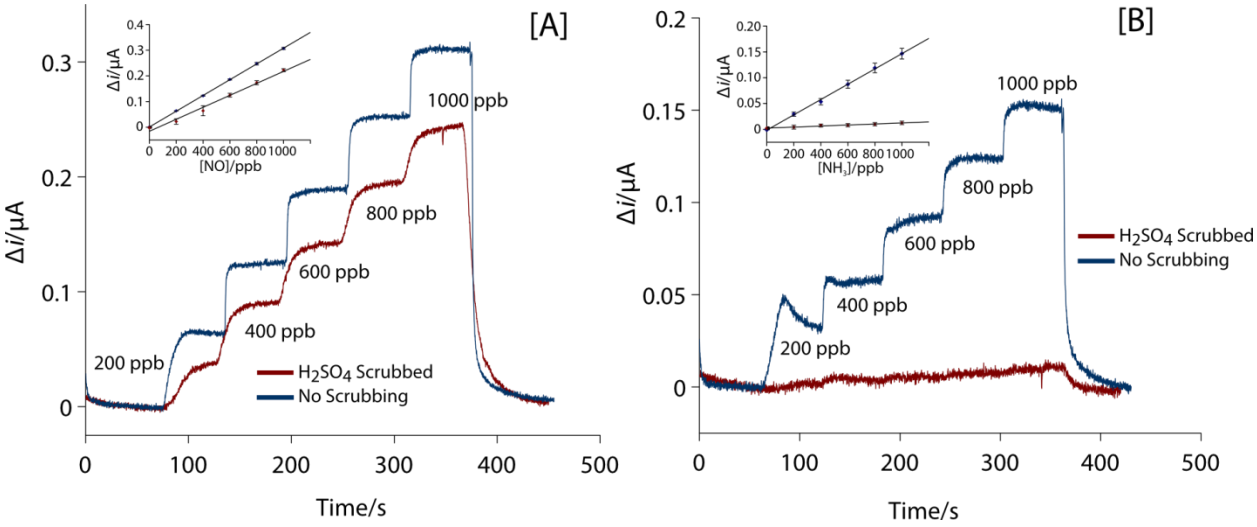

Figure 4.12. Pt-Nafion sensor current responses to increasing concentrations of [A] NO and [B] NH_3, with and without sulfuric acid scrubbing. Calibration curves are shown in insets with standard deviation as error bars (n=3).

An alternative to liquid scrubbing approach is to use crystalline organic acids packed as a loose solid. Citric acid is an inexpensive solid organic acid and almost completely ignores NO (loss of 1±3%). It removes a modest amount of ammonia from the gas stream resulting in a selectivity coefficient improvement of -0.30±0.03 for a final selectivity coefficient of -0.62±0.02, which is insufficient for reliable NO determination in exhaled breath.

A summary of selectivity changes and NO loss for each sample treatment method is provided in Table 4.1-4.2.

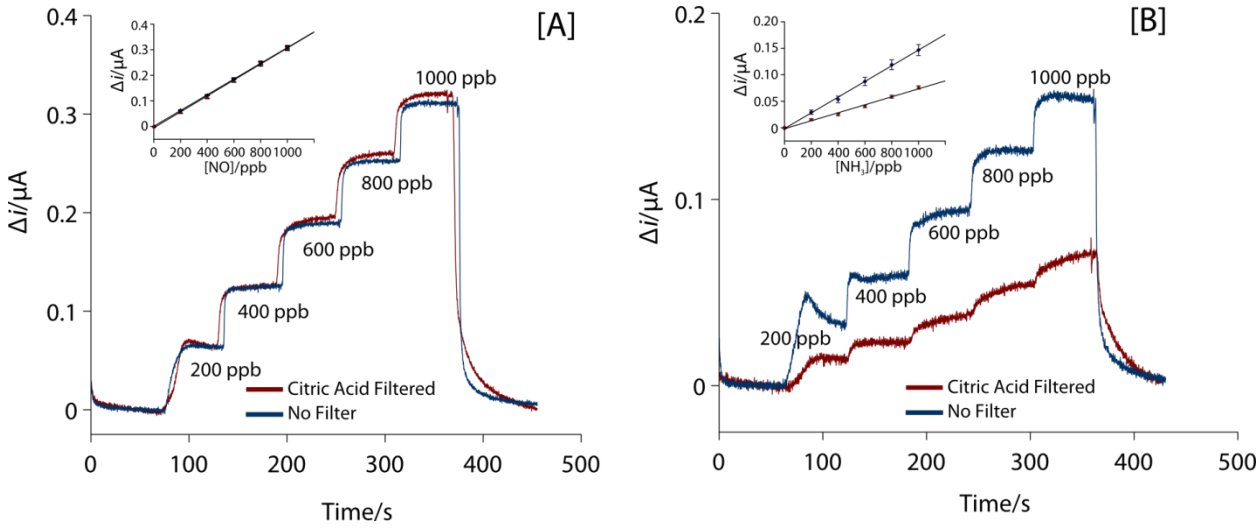

Figure 4.13. Pt-Nafion sensor current responses to increasing concentrations of [A] NO and [B] NH_3, with and without the use of citric acid filter. Calibration curves are shown in insets with standard deviation as error bars (n=3).

Table 4.1. Summary of gas sample ammonia treatment results.

Sample Treatment Method/Material	Change in Selectivity $\Delta\log K_{NO,NH3}$	Loss of NO Sensitivity
Activated Charcoal	-1.0±0.6	94±2%
Carbon Cloth	-0.9±0.6	93±2%
ACF	-0.30±0.01	14±7%
Nafion Polymer Beads	-0.35±0.03	24±6%
Nafion Tubing	-0.19±0.04	30±8%
Citric Acid (Solid)	-0.30±0.03	1±3%
Sulfuric Acid (0.5 M)	-1.06±0.08	24±2%

Table 4.2. Summary of gas sample carbon monoxide treatment results.

Sample Treatment Method/Material	Change in Selectivity $\Delta\log K_{NO,CO}$	Loss of NO Sensitivity
Activated Charcoal	-0.38±0.04	94%±2%
Carbon Cloth	-1.3±0.6	93%±2%
ACF	-0.84±0.002	14±7%

4.3.5 Selectivity vs. CO using of Alkaline Internal Electrolyte Solutions pH 7 PBS, pH 11 PBS

Our findings from Chapter 2 suggest that using a more alkaline internal electrolyte promotes the formation of Pt oxides, which are shown to inhibit CO adsorption and subsequent oxidation on Pt. This principle was tested on Pt-Nafion sensors with no such improvement in selectivity. In fact, the sensor response to NO is significantly reduced at internal electrolyte pH of 7.4 with virtually no response to NO with internal electrolyte of pH 11.7 (Figure 4.14). The ion-exchange properties of Nafion do not extend to anions, which are in fact repelled by the polymer. This leads to poor ionic conductivity towards hydroxide ions as well as nitrite and nitrate ions, which are the products of NO oxidation. This incompatibility not only discourages the formation of Pt oxides, it passivates the Pt working electrode towards NO oxidation. An anionic exchange membrane may be required for the use of alkaline internal solutions. Such a material was once available commercially as Morgane-ADP (Solvay, France), a perfluorinated polymer analogous to Nafion, but with tertbutylammonium sites instead of sulfonate sites granting anionic conductivity. This material is no longer available commercially and in-house synthesis or modifications to Nafion may be required.

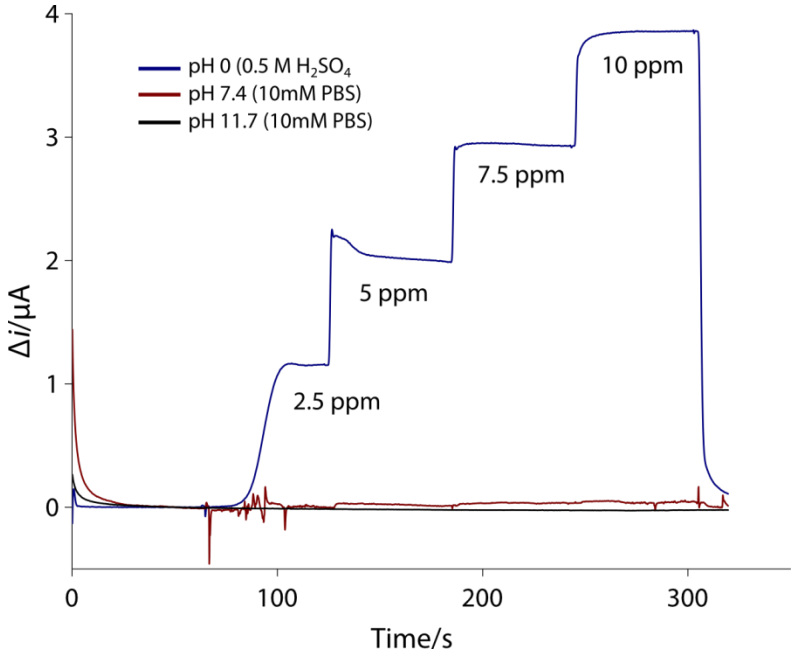

Figure 4.14. Current response of Pt-Nafion sensors filled using internal electrolytes of pH 0, 7.4, and 11.7 towards increasing concentrations of NO.

4.4 Conclusions

In order to address the poor selectivity of unmodified Pt-Nafion sensors towards various inorganic interfering species relevant to biological measurements (such as exhaled breath), strategies such as sample filtration and more alkaline internal solutions have been examined in this Chapter. It was found that acid-scrubbing of gas streams is an effective approach for trapping ammonia although the resulting selectivity is still unacceptable for exhaled breath measurement of NO, especially when there are other interfering species to contend with. Both citric acid solids and liquid sparging in sulfuric acid exhibited considerable ammonia removal capabilities with minor losses of NO, resulting in a substantive net gain in NH_3 selectivity.

Similar to traditional acid scrubbers, Nafion-based materials can trap ammonia through neutralization and were also examined for NH_3 removal efficacy. Due to the proton exchange properties of Nafion, materials made from Nafion can be hydrated and loaded with protons,

which allows the material to act as a solid acid. Treatment of gas streams using both Nafion tubing and Nafion polymer pellets showed minor improvements in overall NH_3 selectivity, but are not as effective as using acid traps and result in greater losses in NO. Nafion, while generally inexpensive considering its use in sensor fabrication and permselective coating applications, is expensive relative to traditional acid traps for the purpose of removing NH_3. For these reasons, our initial findings suggest Nafion to be a poor NH_3 trap in tubing or pellet form.

Carbon-based materials such as activated charcoal, carbon cloth and a proprietary activated carbon fiber (ACF) filter were highly effective at removing relevant electroactive species from gas streams although only the ACF filter did not retain NO. Activated charcoal and carbon cloth materials both removed significant amounts of NO (93-94%), which made them unsuitable as filtration materials.

Overall, the findings in this Chapter suggest that enhanced selectivity may be achieved through fairly simple methods such as gas scrubbing and filtration. Moreover, other aspects of sample filtration such as particle size (for packed solid filtration materials), column length and gas flow rate (standing time) all represent opportunities to further improve our understanding of potential methods for treating gas samples and optimizing the effectiveness of filtration and scrubbing. Whether or not filtration alone can provide the needed selectivity for NO determination in exhaled breath remains unclear and will require additional investigation.

4.5 References

(1) Jordan, L. R.; Hauser, P. C.; Dawson, G. A. *Anal. Chem.* **1997**, *69* (4), 558.

(2) Sun, J.; Hauser, P.; Zhelyaskov, V. *Electroanalysis* **2004**, *16* (20), 1723.

(3) Ho, K.C.; Liao, J.Y.; Yang, C. C. *Sensors Actuators B Chem.* **2005**, *108* (1-2), 820.

(4) Ho, K.; Hung, W.; Yang, J. *Sensors* **2003**, No. 2, 290.

(5) Jacquinot, P.; Hodgson, A.; Hauser, P. *Anal. Chim. Acta* **2001**, *443* (1), 53.

(6) Lin, C.Y.; Hung, W.T.; Wu, C.T.; Ho, K.C. *Sensors Actuators B Chem.* **2009**, *136* (1), 32.

(7) Ho, K.; Hung, W. *Sensors Actuators B Chem.* **2001**, *79* (2), 11.

(8) Chiou, C.Y.; Chou, T.C. *Sensors Actuators B Chem.* **2002**, *87* (1), 1.

(9) Hodgson, A. W. E.; Jacquinot, P.; Hauser, P. C. *Anal. Chem.* **1999**, *71* (14), 2831.

(10) Stetter, J. R.; Li, J. *Chem. Rev.* **2008**, *108* (2), 352.

(11) Tsceng, K.I.; Yang, M.C. *J. Electrochem. Soc.* **2003**, *150* (7), H156.

(12) Wang, T.; Pysanenko, A.; Dryahina, K.; Spaněl, P.; Smith, D. *J. Breath Res.* **2008**, *2* (3), 037013.

(13) de Lacy Costello, B.; Amann, A.; Al-Kateb, H.; Flynn, C.; Filipiak, W.; Khalid, T.; Osborne, D.; Ratcliffe, N. M. *J. Breath Res.* **2014**, *8* (1), 014001.

(14) Yamaya, M.; Sekizawa, K. *Am. J. Respir. Crit. Care. Med.* **1998**, No. 12, 1.

(15) Hodgson, A. W. E.; Jacquinot, P.; Jordan, L. R.; Hauser, P. C. *Electroanalysis* **1999**, *11*, 782.

(16) Liu, R.; Her, W. H.; Fedkiw, P. S. *J. Electrochem. Soc.* **1992**, *139* (1), 15.

(17) Malinski, T.; Taha, Z. *Nature* **1992**, *358*.

(18) Malinski, T.; Taha, Z.; Grunfeld, S.; Burewicz, A.; Tomboulian, P.; Kiechle, F. *Anal. Chim. Acta* **1993**, *279* (1), 135.

(19) Cha, W.; Meyerhoff, M. E. *Chem. Anal.* **2006**, *949* (51), 949.

(20) Shin, J. H.; Weinman, S. W.; Schoenfisch, M. H. *Anal. Chem.* **2005**, *77* (11), 3494.

(21) Shin, J. H.; Privett, B. J.; Kita, J. M.; Wightman, R. M.; Schoenfisch, M. H. *Anal. Chem.* **2008**, *80* (18), 6850.

(22) Jensen, G. C.; Zheng, Z.; Meyerhoff, M. E. *Anal. Chem.* **2013**, *85*, 10057.

(23) Zheng, Z.; Ren, H.; VonWald, I.; Meyerhoff, M. E. *Anal. Chim. Acta* **2015**, *887*, 186.

(24) Gatty, H. K.; Stemme, G.; Roxhed, N. *J. Micromechanics Microengineering* **2015**, *25* (10), 105013.

CHAPTER 5

ADDITIONAL ANALYTICAL APPLICATIONS OF AMPEROMETRIC PT-NAFION NITRIC OXIDE SENSORS: NITRITE/RSNO DETECTION AND MONITORING OF A COST-EFFECTIVE NITRIC OXIDE INHALATION THERAPY SYSTEM

5.1 Introduction

While the selectivity of amperometric SPE-based sensors is currently insufficient to reliably and confidently determine NO in complex biological samples such as exhaled breath, there are a number of valuable applications that leverage the strengths of SPE-based sensors (sensitivity, linearity, response time) without being limited by its shortcomings (selectivity). In this chapter, additional novel analytical applications of amperometric Pt-Nafion NO sensors are described.

5.1.1 Determination of RSNO's and Nitrite

As discussed in Chapters 1 and 3, NO-releasing compounds such as *S*-nitrosothiols (RSNOs) and nitrite represent important reservoirs[1,2] of NO in both clinical research as well as the development of NO-releasing materials. Nitrite is also highly relevant to other fields of study such as environmental chemistry and food chemistry.

The determination of nitrite and RSNOs in solution is generally performed by conversion to NO and detecting the released NO via chemiluminescence, which is expensive, lacks

portability, and requires considerable maintenance. For example, chemiluminescence requires calibration gas (NO), purge gas (N_2), sweep gas (N_2) and ozone (generated from an O_2 source). In the determination of gaseous NO release from NO-donor materials and other NO-releasing implements, amperometric Pt-Nafion sensors require calibration using a gas standard; aqueous phase determination of NO (as an equimolar proxy for RSNO and nitrite) can be performed using simple and inexpensive aqueous standards without the need for a pre-mixed cylinder, which can be expensive and cumbersome.

As part of this chapter, simple and robust determination of RSNO and nitrite in solution via amperometric Pt-Nafion NO sensors without the need of gas standards is demonstrated.

5.1.2 Cost-Effective Inhaled Nitric Oxide Therapy via Electrochemically Modulated NO Release from Nitrite and Electrochemical NO Monitoring/Detection

Among the many functions of nitric oxide, vasodilation, and anti-thrombotic effects are of particular interest to the biomedical field.[3,4] Respiratory diseases and disorders are often characterized by compromised vascular function and increased microbial proliferation in the lungs. Direct inhalation of controlled quantities of NO (or "inhaled nitric oxide", INO)[5,6] has been used by medical professionals for the last 20 years to relieve pulmonary hypertension and lower pulmonary vascular resistance[7] in patients with lung failure.

Currently, INO therapy is administered through pre-mixed compressed gas cylinders, which are expensive to fill, transport, and maintain, costing facilities millions of dollars each year; the University of Michigan Hospital spends up to 3000USD a day per patient with a total expenditure of ~4.8M USD per year.[8] Despite this cost, INO remains a popular treatment option and is still considered cost-effective relative to alternatives by reducing the need for

extracorporeal membrane oxygenation (ECMO) and preventing neonatal fatalities that result from pulmonary hypertension.[6,9] Compressed NO gas cylinders must be filled with NO diluted down to the ppm range and quality tested. Because the NO is under high pressure, the disproportionation of NO to NO_2 and N_2O is accelerated, necessitating maintenance of fresh supply lines and the inability to store quantities of gaseous NO for extended periods of time. Compressed gas cylinders also present a large physical footprint and are cumbersome to handle.

With all of the logistical and practical constraints associated with NO delivery via pre-calibrated compressed gas cylinders, INO is largely inaccessible to most patients and is offered in only a select number of medical and clinical facilities across the country. A more compact, convenient, inexpensive, and low-maintenance alternative source of ppm-range NO gas would make INO therapy more accessible for clinical and even supervised home use. A current alternative is a commercial product developed by a startup company, GeNO Inc., and consists of a liquid NO_2/N_2O_4 reservoir that is catalytically converted to NO.[10] The primary limitation of this product is the toxic nature of the starting material (NO_2/N_2O_4) for NO generation, which raises relevant concerns over device failure situations.

An emerging alternative to pre-mixed NO sources is to electrochemically generate NO from nitrite solutions using a copper(II)-complex catalyzed reaction,[11] which was described and demonstrated briefly in Chapter 3.[12] Preferential generation of NO from an inexpensive salt like nitrite is made possible by utilizing Cu(II)-ligand complexes such as copper(II)-tri(2-pyridylmethyl)amine (CuTPMA) and copper(II)-1,4,7-trimethyl-1,4,7-triazacyclononane ($CuMe_3TACN$),[13] which are biomimetics of nitrite reductase enzymes that contain copper active sites. To achieve the high rates of NO generation required to produce ppm-range concentrations for INO therapy, large surface area mesh electrodes are used that can generate well over 100

ppm NO when current is passed and the solution is purged with an inert sweep gas such as N_2.[13] The NO can then be mixed with relevant concentrations of O_2 and passed to the patient.

As part of this chapter, a cost-effective INO system with electrochemical generation of NO from nitrite and subsequent electrochemical detection by amperometric Pt-Nafion NO sensors is described and characterized. Concerns over potential NO_2 formation between NO and O_2 are also addressed.

5.2 Experimental

5.2.1 Materials & Reagents

All chemicals used were commercially obtained and were reagent grade without further purification or modification unless otherwise specified. All gases employed for the calibration of the Pt-Nafion sensors were obtained from Cryogenic Gases (Detroit, MI). Aqueous solutions were prepared using water (18.2 MΩ·cm) purified through a Milli-Q system (Millipore, Bedford, MA). Sensor cell assembly, sample cells, and filter housing parts were prepared by Glass-blowing Services, Department of Chemistry, University of Michigan (Ann Arbor, MI). All potentials reported herein are versus Ag/AgCl (saturated KCl), which is +0.197 V vs. SHE.

5.2.2 Sensor Fabrication

The general design and fabrication of the Pt-Nafion working electrode are described in Chapter 3. Briefly, Nafion 117 (DuPont, Wilmington, DE) was cut into 1 cm dia. circles and cleaned of impurities by boiling in 3 M nitric acid for 1 h followed by boiling in deionized water for 1 h. The membranes were then placed in a diffusion cell with one side exposed to 20 mM $Pt(NH_3)_4Cl_2$ at 37 °C for 6 h followed by

exposure on the same side to 50 mM $NaBH_4$ in 1 M NaOH for at 37 °C 90 min. The Pt-Nafion membrane was then boiled in DI water for 1 h to remove any remaining Pt complex and reducing agent.

A single junction Ag/AgCl (saturated KCl) reference electrode and bare Pt auxiliary electrode were used along with a 0.5 M H_2SO_4 internal electrolyte in the final sensor assembly. A CHI800B potentiostat (CH Instruments, Austin, TX) was used to polarize the working electrode and record sensor output currents. 2x MC-200SCCM mass flow controllers (Alicat Scientific, Tucson, AZ) operated in tandem via a BB9-USB signal distribution box (Alicat Scientific, Tucson, AZ) and FlowVision SC software (Alicat Scientific, Tucson, AZ) were used for mixing gas standards and delivery of nitrogen into sample cells to deliver the NO released from the samples to the gas phase sensor.

5.2.3 Detection of RSNO and Nitrite

A Pt-Nafion NO sensor was poised at 1V with MFC's passing a total flow rate of 50 mL min^{-1}. The sample cell was filled with 5 mL of 30 μM $CuCl_2$ in 10 mM pH 7.4 PBS along with 2 ng of cysteine as a reducing agent (Figure 5.1). The sample cell solution was then purged with N_2 at 50 mL min^{-1}. *S*-nitrosoglutathione (GSNO) standards in the μM concentration range were prepared with 100 μM EDTA in 10 mM pH 7.4 PBS. Injections of varying volumes (5, 10, 15, 20, 25 μL) of GSNO standard solution were made to the sample cell where NO is released by a Cu(II/I) catalytic reaction and detected at the Pt-Nafion sensor. The areas of the obtained peaks were integrated and used to establish a calibration curve.

For the detection nitrite, standards in the mM concentration range were prepared with distilled water (final concentration in cell will be in the μM range). The sample cell was filled with 2 mL of 0.6 M KI (reducing agent) in 0.25 M H_2SO_4 (Figure 5.1). Injections of varying

volumes (5, 10, 15, 20, 25 µL) of nitrite standard solution were made and the resulting amperometric peaks were integrated to establish a calibration curve.

In order to perform nitrite detection on a practical sample, municipal water was analyzed by purging a 2 mL aliquot of tap water with N_2 for 5 minutes and injecting 100 µL of 0.25 M H_2SO_4 in 0.6 M KI to convert any nitrite in the sample to NO. The determination was repeated using chemiluminescence instrumentation using the same sample cell and purging a 2 mL aliquot of tap water with N_2 for 5 minutes before injecting 100 µL of 0.25 M H_2SO_4 in 0.6 M KI to convert any nitrite in the sample to NO.

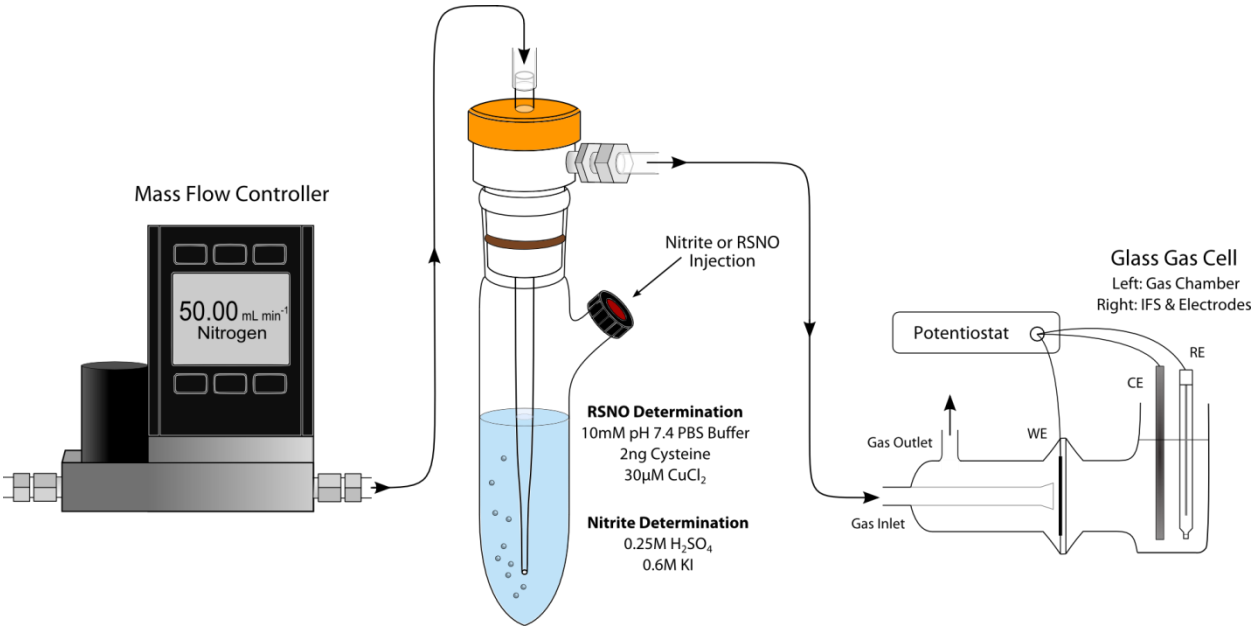

Figure 5.1. Schematic of nitrite and RSNO detection system using the Pt-Nafion sensor as detector. Nitrite is converted to NO via acidification in H_2SO_4 (KI as reducing agent). RSNOs are converted to NO catalytically via $CuCl_2$ (using cysteine as a reducing agent).

5.2.4 Inhaled Nitric Oxide System

An INO system must generate sufficient concentrations of NO, which are then mixed with a relevant concentration of O_2 prior to delivery to the patient. In order to generate NO in the ppm range, a two electrode cell consisting of large surface area Pt mesh electrodes (Figure 5.2) was used. The NO-generating solution consisted of an 80 mL aliquot of 7 mM $CuMe_3TACN$ in 0.5 M pH 7.9 HEPES and 1 M $NaNO_2$. The vessel containing the Pt mesh electrodes and the NO-generating solution will henceforth be referred to as the "INO cell". Nitrogen gas was used to purge the INO solution at 2 L min^{-1}, moving NO from the INO cell to be mixed with the desired concentration of O_2 (flowing at 0.50 L min^{-1} for 20% O_2). A fraction of the final NO/O_2 mix was peeled off from the main stream and fed to the Pt-Nafion sensor at a flow rate of 50 mL min^{-1}. The Pt-Nafion sensor was polarized and calibrated prior to use in these INO monitoring application experiments. The N_2 flow rate through the INO cell was 2 L min^{-1} across all experiments and experimental conditions because the NO concentration of the gas stream exiting the INO cell is dependent on the purge rate.[13]

In order to maintain fairly consistent rate of NO generation, a constant current was applied to the INO cell (0-5 mA) instead of a constant potential (used in the demonstration of CuTPMA-catalyzed NO release from nitrite in Chapter 3), where the current often drops off as substrate is consumed and catalyst is degraded (especially at high rates of NO generation in the INO system). A galvanostatic approach ensures that the applied potential varies as needed in order to maintain a constant level of NO generation over time.

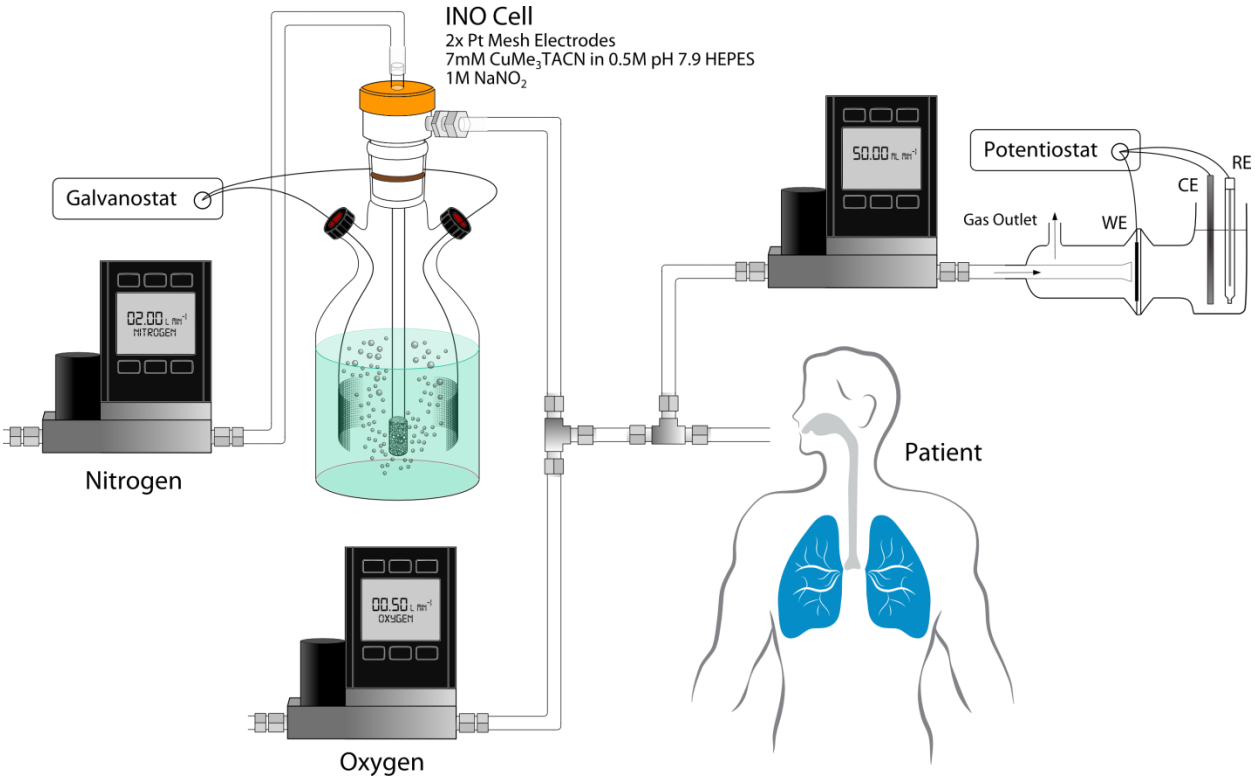

Figure 5.2. Schematic of inhaled nitric oxide system with galvanostatic NO generation from nitrite (mediated by $CuMe_3TACN$) and amperometric detection of NO via Pt-Nafion sensor.

5.3 Results and Discussion

5.3.1 RSNO and Nitrite Detection

Rapid release of NO from GSNO upon additional of a GSNO standard solution to the sample cell (containing $CuCl_2$) was observed using amperometric Pt-Nafion sensors (see Figure 5.3). A calibration curve was established by integrating the peak areas (in units of μA s) and plotting vs. the concentration of the injected GSNO standard (insert in Figure 5.3). The limit of detection was determined to be 17±10 nM. The baseline is stable and all NO appears to be liberated within 4 min of the injection. Similar performance is observed in the determination of nitrite with a limit of detection of 26±5 nM and complete conversion to NO within 1 minute of injection (Figure 5.4).

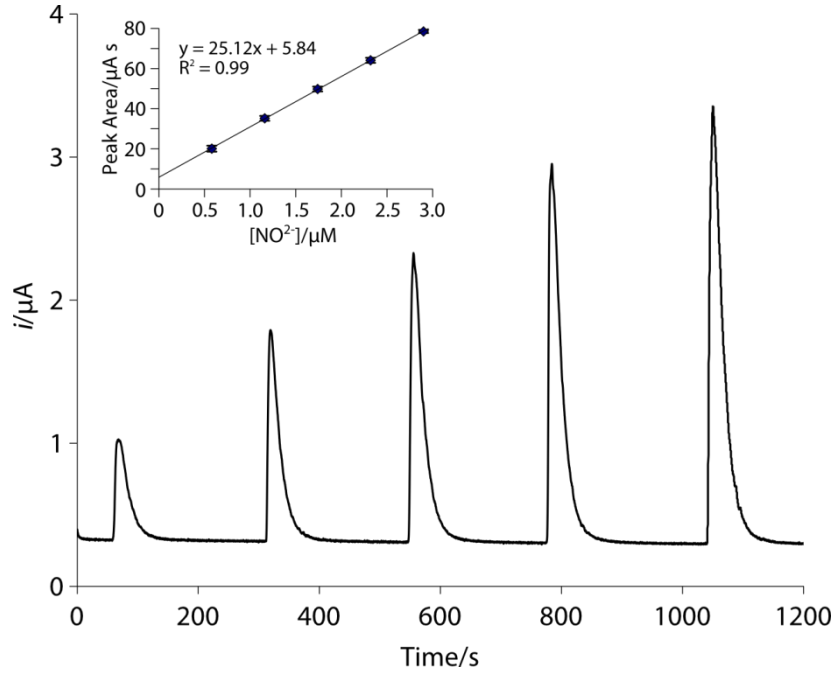

Figure 5.3. Amperometric response of Pt-Nafion NO sensors to injections of varying concentrations of $NaNO_2$ into solution containing 0.25 M H_2SO_4 in 0.6 M KI. Peaks were integrated and used to establish the calibration curve shown in the inset (n = 3).

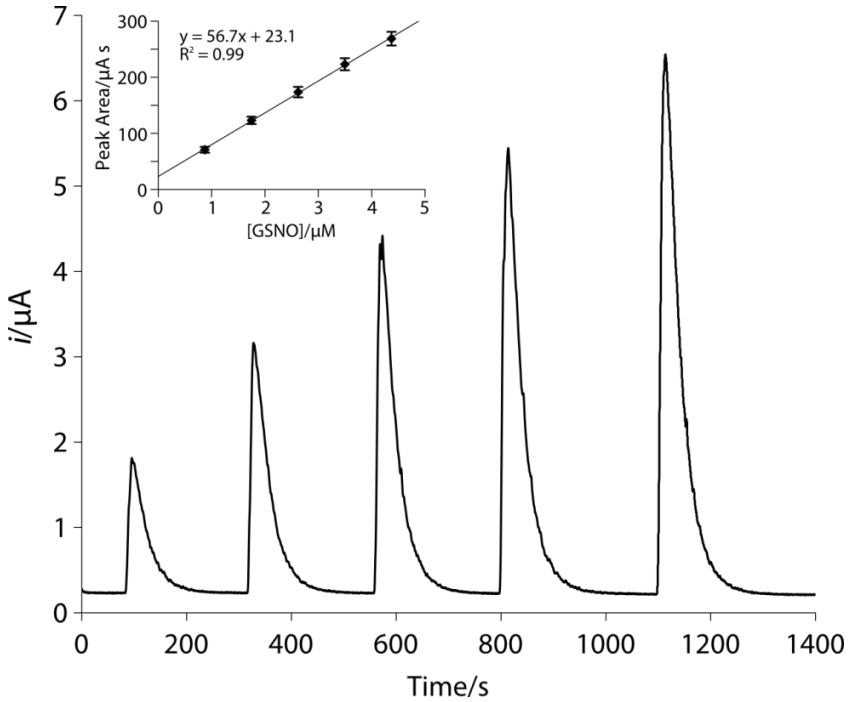

Figure 5.4. Amperometric response of Pt-Nafion NO sensors to injections of GSNO at varying concentrations into 30 μM $CuCl_2$ in 10 mM pH 7.4 PBS with 2 ng of cysteine as a reducing agent. Peaks were integrated and used to establish the calibration curve shown in the inset (n = 3).

Both methods have stable baselines and reproducible 5-point calibrations that can be performed in under 30 min without the use of expensive and cumbersome compressed NO gas standards in cylinders or chemiluminescence instrumentation.

Water samples from a University of Michigan laboratory tap were analyzed for nitrite as proof of principle (Figure 5.5). Using an amperometric Pt-Nafion sensor, it was determined that 5.2±1.1 μM nitrite (n = 3) is present in the tap water samples. This analysis was also performed using chemiluminescence as a reference method, which detected 6.0±0.3 μM nitrite (n = 3). Distilled water was analyzed for nitrite as a control and no discernible amount of NO was released from DIW. This is a surprising result as typical nitrite concentrations in municipal water supplies should be about an order of magnitude lower (0.1 mg L^{-1} or ~1 μM based on EPA drinking water standards).[14] However, there are a plethora of possible points where nitrite contamination might have occurs throughout the transport of the water from the municipal water supply to a research laboratory's tap. Analyzing samples directly from the source or from other taps might shed further light on this finding.

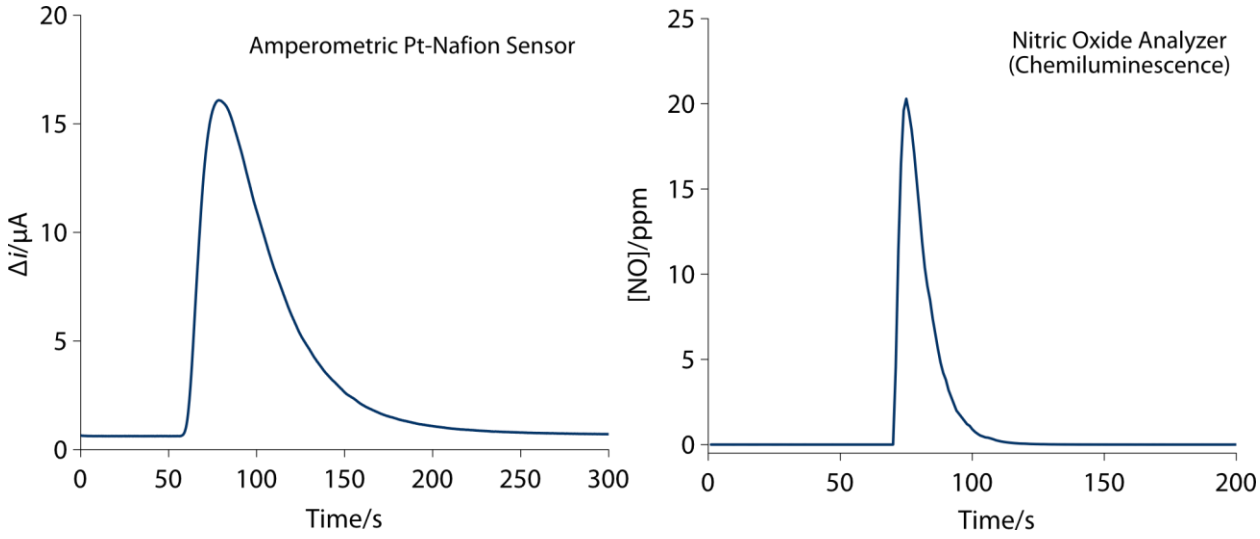

Figure 5.5. Analytical peaks from NO detected on Pt-Nafion sensor (left) and a Nitric Oxide Analyzer (right) after injection of municipal water samples.

Some of the potential challenges associated with using Pt-Nafion sensors for biological analysis of RSNO's include foaming (due to the large amounts of proteins in many biological samples), scavenging of NO by hemoglobin (in blood/plasma) and potential interfering species (free dissolved gases or gases released when reacted with $CuCl_2$). However, the latter problem can be handled by pre-purging the sample for a fixed time to remove any volatile electroactive species, before adding the reagents required to generate the NO gas from RSNOs or nitrite. Further, for the measurement of nitrite in environmental samples (water samples, etc.), it is unlikely that any of these challenges will exist.

5.3.2 NO Monitoring of an Inhaled Nitric Oxide System

Nitric oxide generated from an INO cell mixed with oxygen was monitored using a calibrated amperometric Pt-Nafion NO sensor. In one experiment, O_2 concentration was held at 20% of the final flow rate while constant current (0-5 mA) was applied across two Pt mesh

electrodes in the INO cell. The NO concentration delivered was proportional to the applied current and in this system, 9.60 ppm NO is delivered per mA of applied current (with 2.12 ppm ambient NO delivered) (Figure 5.6). This finding suggests a high degree of control can be achieved over the production of NO using a galvanostatic approach and that reproducible/reversible amperometric measurement of the NO produced is also possible.

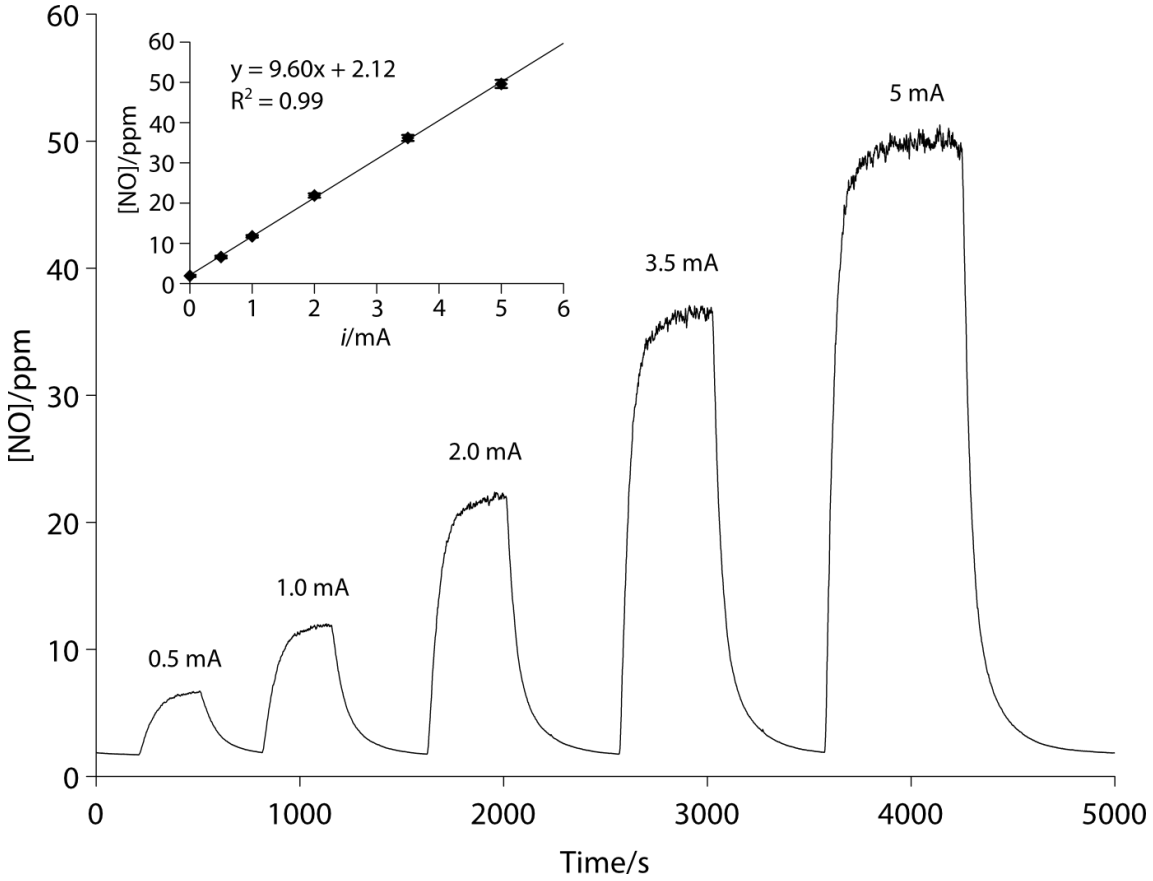

Figure 5.6. Amperometric Pt-Nafion sensor monitoring NO/O_2 mix from NO generated by INO system (7 mM $CuMe_3TACN$ in 0.5 M pH 7.9 HEPES and 1 M $NaNO_2$) at varying applied currents (0.5 mA – 5 mA) and constant O_2 (20%). Flow rate to sensor: 50 mL min^{-1}.

In a separate experiment, 2 mA was applied to the INO cell while O_2 concentrations were varied by altering the flow rate of pure O_2 into the mix (the N_2 purging flow rate through the INO cell remains 2 L min^{-1}) (Figure 5.7). The NO produced scales with the degree of O_2 dilution

and is readily detected by the Pt-Nafion sensor with a rapid response (~10 s), shows reproducible measurement ($R^2 = 0.99$), and demonstrates continuous monitoring of NO through changes in NO/O_2 concentrations. These finding also suggest that the amount of O_2 does not adversely affect the NO concentration beyond the dilution effects. A potential concern of mixing NO and O_2 is the production NO_2, which is considered toxic. If significant amounts of NO_2 are produced, the relationship between O_2 percentages and NO detected would not be linear.

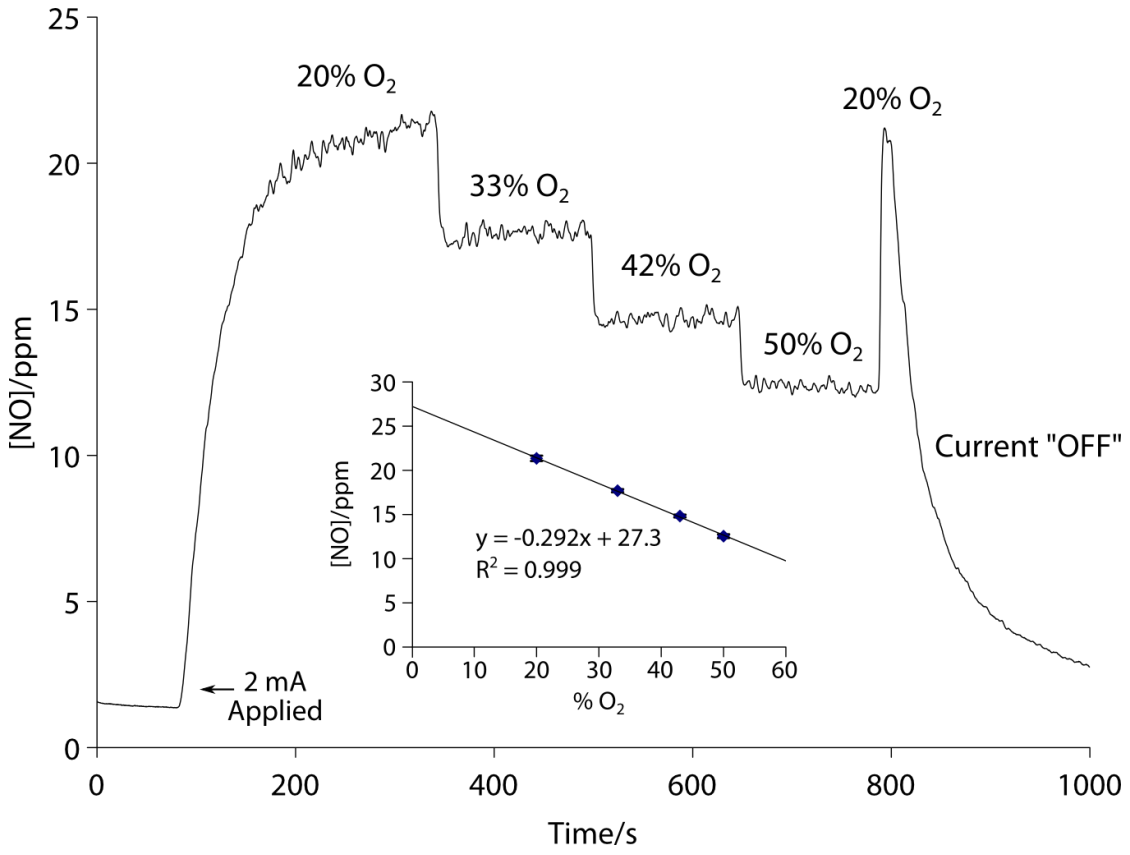

Figure 5.7. Amperometric Pt-Nafion sensor monitoring NO/O_2 mix from NO generated by INO system (7 mM $CuMe_3TACN$ in 0.5 M pH 7.9 HEPES and 1 M $NaNO_2$) at 2 mA applied current with INO sweep flow rate of 2 L min^{-1} and varying percentages of O_2. Flow rate to sensor: 50 mL min^{-1}.

While there is little evidence to support the notion that production of dangerous levels of NO_2, it would still be prudent to have a monitoring system in place for NO_2 as a safeguard. Amperometric Pt-Nafion sensors can also detect NO_2 cathodically[15] (Figure 5.8) with high sensitivity (-0.70 µA/ppm; LOD

of 2.4±0.1 ppb) and selectivity vs. NO ($\log K_{NO2,NO}$ = -3.85) when operated at a lower applied potential (0.740 V).

We also hypothesized that one of the products of NO_2 reduction would be NO, which was confirmed by passing 20 ppm NO_2 across a Pt-Nafion sensor at 200 mL min^{-1} with varying applied potentials (0.700 - 0.900 V) and analyzing the outlet stream using chemiluminescence (Figure 5.9). This finding suggests that NO is one of the products (if not the primary product) of NO_2 reduction on Pt.

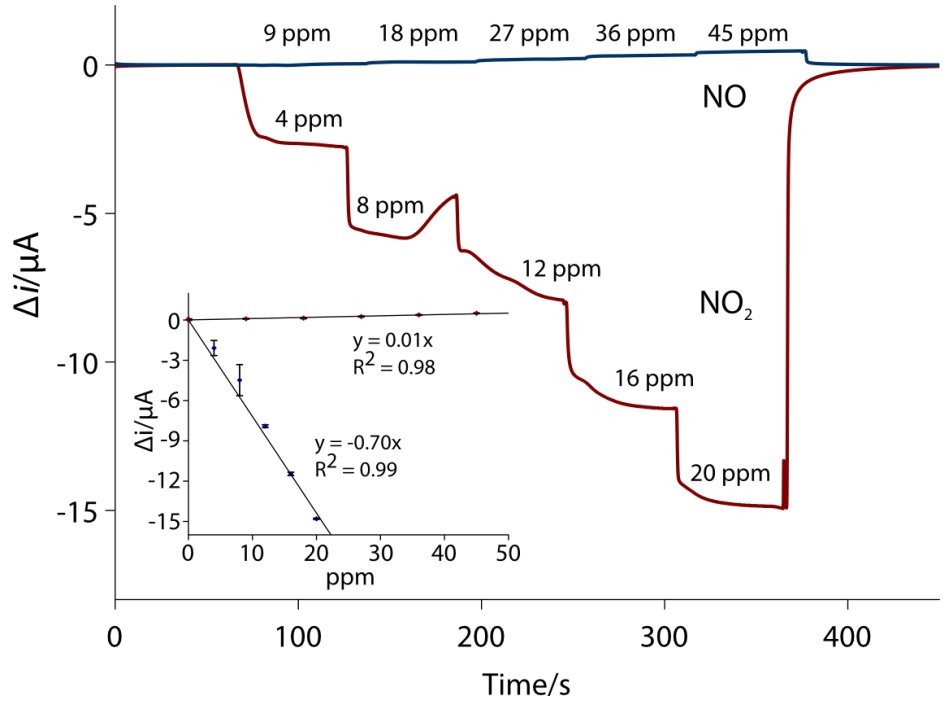

Figure 5.8. Amperometric response of Pt-Nafion sensor poised at 0.74 V at increasing concentrations of NO and NO_2 standard gases in N_2 balance. Selectivity coefficient $\log K_{NO2,NO}$ = -3.85.

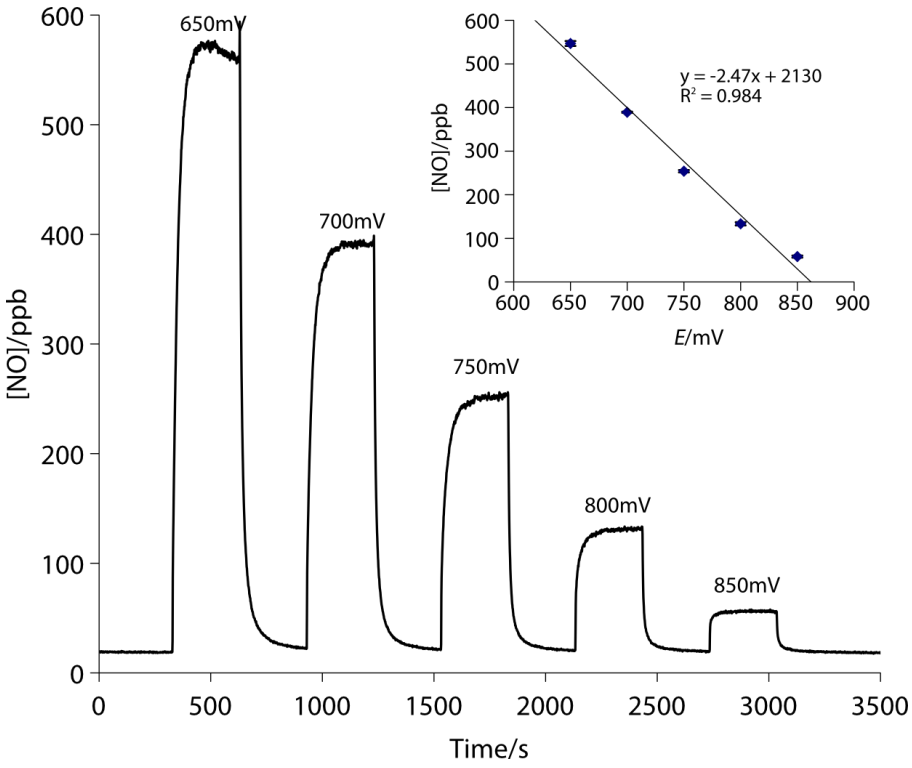

Figure 5.9. Chemiluminescence determination of NO generated from NO_2 reduction at a Pt-Nafion sensor working electrode poised at varying potentials.

In the event that significant amounts of NO_2 are produced (>0.5 ppm) or that regulations demand complete NO_2 removal from the INO system, NaOH or other hydroxides can be used to scrub the NO/O_2 gas mix of NO_2 prior to delivery to the patient. In a preliminary experiment, NO and NO_2 calibrations were performed at their respective potentials (1 V and 0.740 V) with and without scrubbing in 8 M NaOH (Figure 5.10). While the response time to NO is slightly slowed by the hydroxide scrubbing, there is little effect on the concentration of the NO. The effect of scrubbing on NO_2, however, is dramatic and we see significant removal of NO_2 through a simple scrubbing operation (>98% NO_2 removal for concentrations <12 ppm, 89% removal at 16 ppm and 78% removal at 20 ppm).

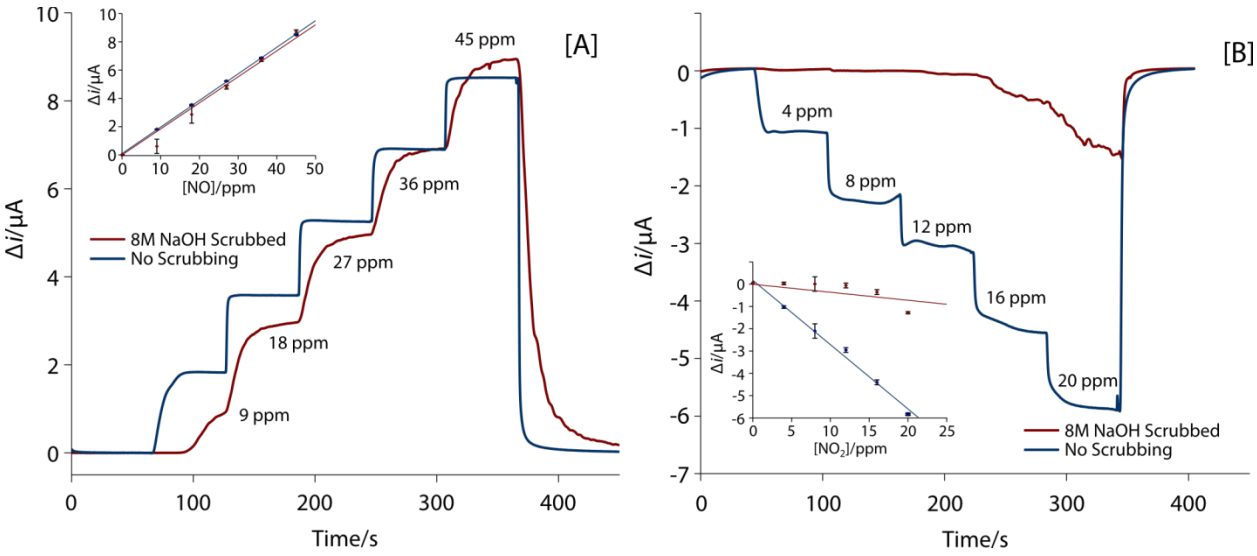

Figure 5.10. [A] NO and [B] NO_2 calibrations on an amperometric Pt-Nafion sensor with (red) and without (blue) gas sample scrubbing through 8 M NaOH.

5.4 Conclusions

In this Chapter, the high sensitivity and fast response of the amperometric Pt-Nafion NO (and NO_2) sensors were leveraged in demonstrating additional novel applications including aqueous nitrite detection and S-nitrosothiols (without the need for gas standards) and monitoring of NO in a cost effective INO therapy system.

Calibrations for determining GSNO and nitrite can be performed in less than 30 min (5 points) with excellent reproducibility and linearity in the low μM range. Due to the proven linearity, it is conceivable that a single point calibration would be sufficient in certain applications. This detection scheme also does not require a gas standard, which currently represents a major inconvenience and source of cost for gas phase sensors. Water from a municipal supply was analyzed for nitrite (12.4±0.1 μM) and the results were comparable with results (16.9±1.0 μM) from a similar experiment performed using chemiluminescence.

A cost-effective INO therapy system utilizing electrochemically modulated NO generation from inexpensive nitrite salt was previously described,[13] but requires a complementary monitoring system for additional feedback, control, and safety. As an NO monitoring device, Pt-Nafion sensors demonstrated highly sensitive and reproducible measurements with fast response to NO concentration changes in the INO system (limited only by the dead volume of the system's plumbing and time for NO generation and purging to reach equilibrium).

The potential formation of NO_2 as a result of NO and O_2 mixing is a relatively minor concern due to the short standing time after mixing.[13] However, as a precaution, Pt-Nafion sensors may be used as NO_2 sensors when poised at 0.740 V, responding cathodically to increases in NO_2 concentration. This sensor is highly sensitive (-0.70 μA/ppm; LOD of 2.4±0.1 ppb) and selective vs. NO ($\log K_{NO_2,NO} = -3.85$).

Another approach to addressing potential NO_2 formation is by cleaning the INO gas stream via hydroxide scrubbing, which was shown to remove >98% of NO_2 at concentrations <12 ppm without removing NO. Additional studies using crystalline NaOH or other hydroxides such as ethanolamine might further improve the efficacy and convenience of this INO gas treatment/cleaning method.

5.5 References

(1) Lundberg, J. O.; Weitzberg, E.; Gladwin, M. T. *Nat. Rev. Drug Discov.* **2008**, *7* (2), 156.

(2) Giustarini, D.; Milzani, A.; Colombo, R.; Dalle-Donne, I.; Rossi, R. *Clin. Chim. Acta* **2003**, *330* (1-2), 85.

(3) Ignarro, L.; Buga, G. *PNAS* **1987**, *84* (December), 9265.

(4) Palmer, R. M. J.; Ashton, D. S.; Moncada, S. *Nature* **1988**, *333* (6174), 664.

(5) Rossaint, R.; Falke, K. J.; Lopez, F.; Slama, K.; Pison, U.; Zapol, W. M. *N. Engl. J. Med.* **1993**, *328*, 399.

(6) The Neonatal Inhaled Nitric Oxide Group. *N. Engl. J. Med.* **1997**, *336*, 597.

(7) Griffiths, M. J.; Evans, T. W. *N Engl J Med* **2005**, *353* (25), 2683.

(8) Cole, F. S.; Alleyne, C.; Barks, J. D. E.; Boyle, R. J.; Carroll, J. L.; Dokken, D.; Edwards, W. H.; Georgieff, M.; Gregory, K.; Johnston, M. V; Kramer, M.; Mitchell, C.; Neu, J.; Pursley, D. M.; Robinson, W. M.; Rowitch, D. H. *Pediatrics* **2011**, *127* (2), 363.

(9) Roberts, J. D.; Fineman, J. R.; Morin, F. C.; Shaul, P. W.; Rimar, S.; Schreiber, M. D.; Polin, R. A.; Zwass, M. S.; Zayek, M. M.; Gross, I.; Heymann, M. A.; Zapol, W. M. *N. Engl. J. Med.* **1997**, *336* (9), 605.

(10) Lovich, M. A.; Fine, D. H.; Denton, R. J.; Wakim, M. G.; Wei, A. E.; Maslov, M. Y.; Gamero, L. G.; Vasquez, G. B.; Johnson, B. J.; Roscigno, R. F.; Gilbert, R. J. *Nitric Oxide* **2014**, *37* (1), 66.

(11) Ren, H.; Wu, J.; Xi, C.; Lehnert, N.; Major, T.; Bartlett, R. H.; Meyerhoff, M. E. *ACS Appl. Mater. Interfaces* **2014**, *6* (6), 3779.

(12) Zheng, Z.; Ren, H.; VonWald, I.; Meyerhoff, M. E. *Anal. Chim. Acta* **2015**, *887*, 186.

(13) Ren, H. Electrochemically Modulated Generation/Delivery of Nitric Oxide (NO) from

Nitrite for Biomedical Applications, University of Michigan, 2016.

(14) US Environmental Protection Agency. *National Primary Drinking Water Regulations: Final Rule, Part II*; 1991; Vol. 56.

(15) Lin, C.Y.; Hung, W.T.; Wu, C.T.; Ho, K.C. *Sensors Actuators B Chem.* **2009**, *136* (1), 32.

CHAPTER 6

CONCLUSIONS

6.1 Summary of Results and Contributions

Amperometric methods for NO determination have been employed for numerous biomedical and research applications over the last 25 years because of their sensitivity, spatial resolution, portability, and cost-effectiveness. However, they are not without their limitations and challenges. This dissertation aimed to address and improve the analytical performance and applicability of amperometric NO sensors through novel enhancements and detection schemes. Both Clark-type aqueous-phase NO sensors and solid polymer electrolyte (Nafion) based gas-phase sensors were explored.

In Chapter 2, a novel modification to modern Shibuki-design amperometric NO sensors to improve selectivity vs. carbon monoxide (CO) was developed and characterized. The Shibuki-design sensor is based on a Clark-type sensor (two-electrode cell housed behind a gas permeable membrane). The GPM imparts selectivity vs. relevant aqueous interfering species but fails to exclude gaseous interfering species such as CO, which has long been overlooked in the sensor's development. It was shown that improvement in selectivity vs. CO was correlated with increases in internal electrolyte pH, yielding selectivity enhancements by up to 2 orders of magnitude (pH 0 vs. pH 11.7) while maintaining a low limit of detection (<5 nM). By elevating

the internal electrolyte pH, the formation of Pt-oxides was promoted during the polarization of the sensor; this phenomenon was confirmed by pre-forming the oxide on the working electrode under different pH environments and stripping the oxide layer. The oxide layer was clearly shown to be more extensive on the Pt electrode polarized in higher pH solutions. CO adsorption and stripping voltammetry on electrodes polarized in solutions of varying pH in suggested that CO adsorption on electrodes with more extensive oxide layers (formed in higher pH environments) was inhibited to a greater extent. It was also shown using an ammonia gas sensing probe (glass pH electrode housed behind a GPM of the type used in our amperometric sensors) that titration of the thin electrolyte layer between the GPM and working electrode surface occurs rapidly in the presence of high concentrations of CO_2 (pH 11.7 drops to pH 6.6 in the presence of 10% CO_2), raising concerns about the stability of the oxide layer (and consequently the imparted selectivity vs. CO). However, it was also shown that the oxide layer formed at high pH remains largely stable when the pH drops to a neutral value. This was confirmed by pre-forming the oxide layer in high pH environments and then operating the sensor at neutral pH, showing no significant loss of selectivity.

In Chapter 3, a highly sensitive amperometric NO gas-phase sensor based on Pt electrodes deposited on a solid-polymer electrolyte (Nafion) was described, characterized, and applied to the detection of NO released from a NO-donor doped polymer and a novel electrochemical NO-generating system (inorganic Cu(II) complex-catalyzed electrochemical reduction of nitrite to NO). Amperometric Pt-Nafion sensors are very sensitive and exhibit gas phase limits of detection in the low ppb range making them suitable for analysis of therapeutic concentrations of NO and potentially suitable for exhaled NO determination. The electrode was fabricated by impregnating a solid-polymer electrolyte such as Nafion with metal ions (Pt salts in

this case) and chemically reducing the surface to form a highly porous Pt electrode that is in intimate contact with ionically conductive polymer. The sensor had a rapid response time (<5 s), a low limit of detection (4.3 ± 1.1 ppb), and was applied to the detection of gas-phase NO released from Carbosil2080A polymer films doped with *S*-nitroso-*N*-acetylpenicillamine (SNAP) and electrochemically modulated NO-release from nitrite. All measurements were repeated on a chemiluminescence analyzer and strong agreement was found between NO release/emission measurements made using Pt-Nafion sensors and chemiluminescence. Looking toward the potential application of the Pt-Nafion sensors for the determination of exhaled NO, the selectivity of the sensor over CO was also examined. It was found that initial selectivity vs. CO was poor, but improves considerably after conditioning the sensor in a high concentration of CO for up to 2 h.

In Chapter 4, strategies for enhancing the selectivity of Pt-Nafion sensors were explored with particular emphasis on CO and NH_3, both of which are relevant interfering species present in substantive concentrations in exhaled breath. A fundamental approach to enhancing amperometric sensor selectivity is to perform sensitivity studies of the target analyte (NO) and interfering species (CO, NH_3) and try to identify an applied potential where the sensor is most selective for the target analyte. While some potentials yielded slightly better selectivity vs. CO and/or NH_3, the improvement was minimal due to heavy overlap in redox potentials between NO, CO, and NH_3. Another avenue for addressing the presence of interfering species is filtration/scrubbing of the gas sample itself. While gas "cleaning" has been used extensively in industry for production and environmental safety, NO has generally been considered a pollutant and thus few if any strategies have been explored for cleaning gas streams while preserving NO. A previous report suggested that a proprietary activated carbon fiber (ACF) filter was able to

remove significant amounts of CO and NH_3 without adversely impacting NO concentrations and this finding was confirmed. Due to the promising performance of the ACF filter, activated charcoal and carbon cloth were also examined for possible gas filtration. Unfortunately, both activated charcoal and carbon cloth were too aggressive and removed all electroactive species tested (NO, CO, and NH_3). A long-standing industrial process for removing NH_3 from gas streams is sulfuric acid scrubbing, which was adapted for the Pt-Nafion sensor system and proved to be highly effective. Other similar acidic materials were tested including crystalline citric acid filtration and filtration through acidified Nafion polymer beads. Additional study of gas cleaning may further our understanding of how these materials can bring us closer to the selectivity needed for exhaled nasal NO determination.

Despite the limited selectivity of Pt-Nafion sensors in the context of NO detection in exhaled breath, there are other relevant applications of Pt-Nafion sensors that leverage its strengths without being limited by its lack of ideal selectivity. In Chapter 5, additional analytical applications of amperometric Pt-Nafion NO sensors were demonstrated including the detection nitrite and RSNOs in solution (without need of a gas standard). Reproducible and sensitive measurements of nitrite and GSNO were obtained by injecting nitrite and GSNO standards into a sample cell containing H_2SO_4/KI and $CuCl_2$/cysteine, respectively, to drive conversion to NO. The peaks were then integrated and used to establish calibration curves. This was all accomplished without the need for a compressed gas cylinder as a source for gas standards.

Also in Chapter 5, monitoring of NO delivered by a cost-effective inhaled nitric oxide therapy device was described. As an alternative to premixed/diluted compressed gas cylinders, electrochemical nitrite reduction mediated by inorganic Cu(II) complexes represents a more cost-effective and portable source of therapeutic NO for inhaled nitric oxide (INO) therapy. A

constant current was passed through a large cell containing a solution of copper(II)-1,4,7-trimethyl-1,4,7-triazacyclononane ($CuMe_3TACN$), HEPES buffer, and nitrite using two Pt mesh electrodes to electrochemically reduce nitrite to NO. The NO generated was purged from the solution with N_2(g) and mixed with a relevant concentration of O_2 before being delivered to the "patient". A small fraction of the delivered NO/O_2 mix is peeled off to a Pt-Nafion sensor for monitoring gas phase NO concentrations. It was shown that Pt-Nafion sensors show a rapid and reproducible response to changes in NO concentration delivered by the INO system. The applied current was proportional to the amount of NO produced by the system (9.6 ppm per mA of applied current under given conditions). It was also found that changing O_2 concentrations do not adversely affect the detection of NO beyond dilution effects. Concerns over the potential formation of NO_2 were also addressed. Due to the high flow rates and the proximity of NO and O_2 mixing relative to the outlet (patient), the standing time (and consequently the NO_2 produced) is minimal. However, as a safety measure, NO_2 detection using a Pt-Nafion sensor poised at 0.74V vs. Ag/AgCl with selectivity vs. NO ($\log K_{NO2,NO} = -3.85$) was demonstrated as a potential toxicity monitor for this system. NO_2 can also be selectively removed from the NO/O_2 mix by scrubbing using sodium hydroxide. It was demonstrated that for NO_2 concentrations <12 ppm, an 8 M NaOH solution can remove >98% of the NO_2 with no discernible NO loss.

6.2 Future Directions

6.2.1 Study of Gas Sample Filtration/Scrubbing Techniques

Initial experiments exploring gas sample filtration and scrubbing (see Chapter 4) suggest that certain materials might be suitable for removing interfering species such as NH_3 and CO

without adversely impacting the NO present in the gas stream. Of these materials, acidic NH_3 traps and activated carbon fiber (ACF) filters showed the most promise. The performance of acid traps might be optimized with further studies of the effect of particle size, column length, and flow rate on the removal of NH_3 (and behavior towards NO).

6.2.2 Thin Permselective Membrane Casting via Airbrush/Nebulizer

As discussed briefly in Chapter 4, there are a number of technical challenges that have prevented the use of traditional coating methods for casting thin permselective membranes over SPE sensor electrode surfaces. A potential route for casting thin layers of polymers on a large planar surface is airbrushing, which aerosolizes polymer solutions for very thin and uniform coatings with fast drying times. Spray-coating techniques have been explored recently in the solar cell research community and have proven to be effective at depositing thin (<1 μm) and uniform polymer layers.[1,2] Fluoropolymers have also been applied in this manner in hydrophobic coating research.[3,4] Some of these spray coating techniques require expensive instrumentation but airbrushing is relatively inexpensive and requires only an air compressor, spray nozzle, "paint" reservoir, and an air hose. This might be a way to avoid or at least minimize the solvent effects on Pt-Nafion electrode integrity when applying a thin permselective membrane using a polymeric material dissolved in organic solvent.

6.2.3 Alternative Electrode Materials for SPE-based Sensors

The difficulty of modifying the electrode surface of an electrode deposited within the surface of SPEs stems from solvent interactions between the permselective membrane casting

solutions and the Nafion itself (discussed briefly in Chapter 4). In order to circumvent this obstacle, highly porous electrode materials such as conductive foams (e.g., reticulated vitriolic carbon, RVC), colloidally-templated electrode structures (e.g., polystyrene inverse-opal templated electrodeposition of Pt) and Pt-coated porous structures (e.g., macroporous Si, anodized aluminum oxide, etc.) may be surface modified prior to coating with Nafion. Surface modifications might include Pt-oxide formation, inorganic complex deposition, or porphyrin[5,6] electropolymerization[7–9] layers. Some of these conductive materials may also have better native selectivity vs. relevant interfering species in exhaled breath.

RVC is a highly porous carbon foam that can be used as a high-surface-area electrode.[10] It can be coated and adhered to Nafion films with a Nafion solution to form an SPE-based electrode for amperometric gas sensing.[11] It is a relatively under-explored electrode material for SPE-based gas sensor development, but has been shown to be selective vs CO and is unaffected by changes in humidity.[11] RVC is commercially available through a number of specialty materials suppliers (e.g. KR Reynolds, Orinda CA). Other conductive foams also exist, such as copper foam, which can also be used a substrate for the deposition of more useful electrode metals prior to coating in an SPE for gas sensing.

Colloidally templated electrode structures are fabricated by allowing small particles (such as micron-scale polystyrene spheres) in a colloidal suspension to self-assemble into closed-pack arrangements on a flat conductive substrate (such as ITO or chromium sputtered on glass). It is then possible to electrochemically deposit an electrode (e.g., Pt, Au) through the template and then dissolving the template using an organic solvent, leaving a highly uniform porous electrode (Figure 6.1) that can be modified and then coated with Nafion.[12–15] There are currently no reports of such an amperometric gas sensor using polystyrene-inverse opal (PS-IO) templated

electrodes coated in Nafion so this would represent a novel and unprecedented application of PS-IO templated porous electrodes for amperometric gas sensing.

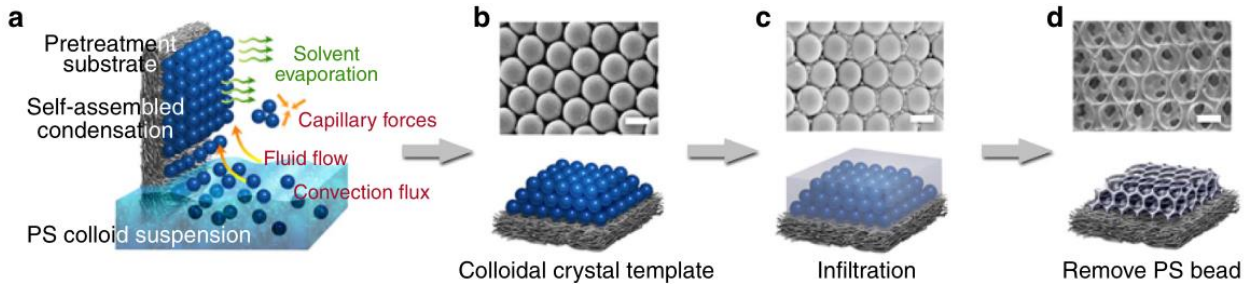

Figure 6.1. Schematic of PS-IO templated electrode fabrication.[14] Reprinted with permission from Macmillan Publishers Ltd: Nature Communications. Kim, O.H.; Cho, Y.-H.; Kang, S. H.; Park, H.-Y.; Kim, M.; Lim, J. W.; Chung, D. Y.; Lee, M. J.; Choe, H.; Sung, Y.-E. Nat. Commun. 2013, 4, 2473.Copyright 2013

In a recent pair of reports,[16,17] Pt-Nafion sensors fabricated from electrochemically micromachined Si have demonstrated analytical performance that rivals impregnation-reduction Pt-Nafion sensors with greater reproducibility and selectivity vs. NH_3 (although the mechanism of selectivity remains unclear). The electrode material is fabricated by patterning and etching small pores through Si wafers using photolithography and deep reactive ion (DRI) etching, respectively (Figure 6.2). The resulting porous Si structure is then coated in Pt via atomic layer deposition (ALD), a type of layer-by-layer chemical vapor deposition (CVD) that results in a conformal layer of Pt on the porous Si.[18] This fabrication process is incredibly expensive and laborious, however, requiring expensive clean room procedures at almost every step of the fabrication.

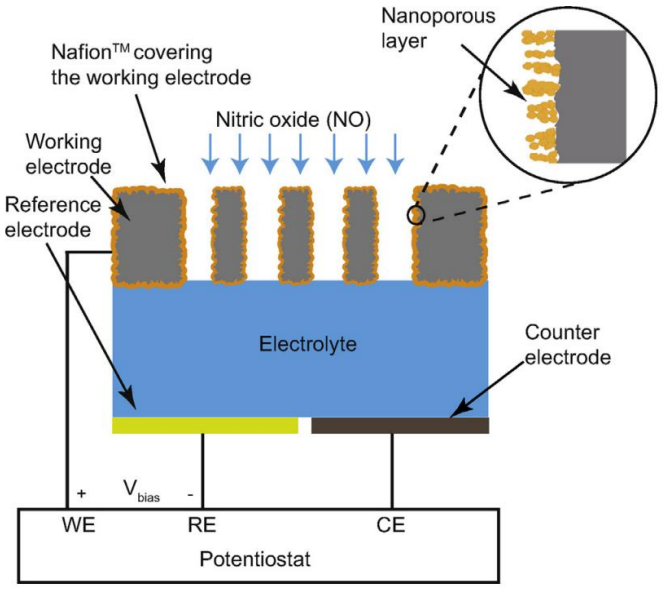

Figure 6.2. Schematic of the micromachined electrochemical sensor showing the nanoporous structure of the Nafion layer covering the working electrode.[16] Reprinted with permission from Sensors and Actuators B: Chemical, 209, Hithesh K. Gatty, Simon Leijonmarck, Mikael Antelius, Göran Stemme, Niclas Roxhed, 639-644, Copyright 2016, Elsevier

A potential alternative fabrication route that would cut down on cost and complexity, at least in the formation of the porous structure, is anodic etching of the Si wafer using hydrofluoric acid. Porous Si materials[19] have been studied extensively for decades and many have been used in spectroscopic sensing applications;[20] however, this type of material has never been applied for creating amperometric gas sensors. Si etching is anisotropic along the <100> crystal plane and results in the formation of parallel, uniform pores. The initial nucleation of these pores is random if the surface is un-patterned. Si surfaces with pre-patterned pits (using photolithography) will etch only in the pits defined by photolithography.

As an exploratory experiment, a wafer of p-type Si<100> (R:10-20 Ω cm) was secured between a stainless steel backplate and a Teflon etchant reservoir containing a 1:9 solution of 49%HF:DMF. A small area in the reservoir exposes the Si wafer to the etchant solution. The steel backplate (in ohmic contact with the Si wafer via an In/Ga eutectic) was attached to a power supply as the anode while a large Pt electrode was placed in the etchant solution as the

cathode. A constant current was applied (current density, J, of 10 mA cm^2) for several hours. The goal was to etch completely through the wafer, resulting in a high aspect ratio structure (Figure 6.3); however, once a pore depth of ~ 150 μm is reached, the cell enters an electro-polishing regime where etching is no longer anisotropic along the pore bottoms and etches outwards, widening the pores, thinning the walls and degrading the integrity of the porous structure. It turns out that, in order to achieve higher aspect ratios (and etch through wafers thicker than 150 μm), pre-patterning via photolithography is required.[21–23] This is a future direction that may be explored further.

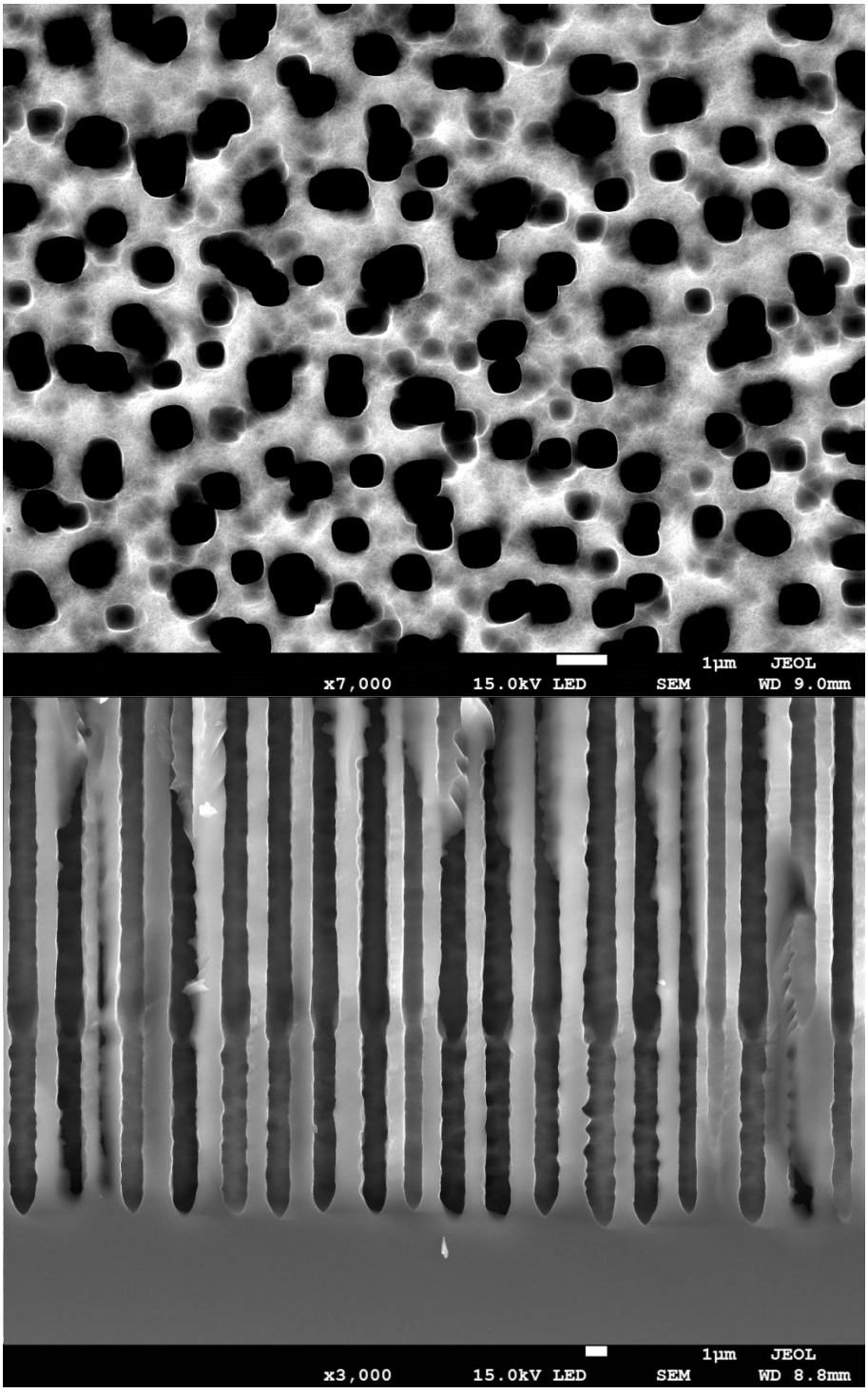

Figure 6.3. Scanning electron micrograph of p-type Si<100> (R:10-20 Ω cm) etched in 1:9 solution of 49%HF:DMF for 2 h. Top view (top) and cross section of pore bottoms (bottom).

Finally, once a porous Si "membrane" is obtained there are a number of possible routes for coating the surface in a conductor such as Pt. Benchtop electrodeposition would be the most convenient and cost-effective method, but Pt nucleates in large clusters during electrodeposition, which may clog pores and result in a non-uniform coating. ALD[18] of Pt is expensive and laborious but offers the best coating uniformity and coverage. Further exploration of coating options would be required.

It is my hope that some of these alternate approaches will be explored by a graduate student or post-doc who may continue pursuing SPE-based gas phase NO sensor development in the near future. There numerous potential biomedical applications of an NO sensor with improved gas phase selectivity, especially in monitoring patients with various chronic upper respiratory diseases. Hopefully, the research described in this dissertation will provide a strong foundation for such future research endeavors, and ultimately yield an improved NO sensor that is robust, simple to use, and inexpensive, and therefore meet the needs for use in a point-of-care setting.

6.3 References

(1) Girotto, C.; Rand, B. P.; Genoe, J.; Heremans, P. *Sol. Energy Mater. Sol. Cells* **2009**, *93* (4), 454.

(2) Susanna, G.; Salamandra, L.; Brown, T. M.; Di Carlo, A.; Brunetti, F.; Reale, A. *Sol. Energy Mater. Sol. Cells* **2011**, *95* (7), 1775.

(3) Yang, S.; Xia, Q.; Zhu, L.; Xue, J.; Wang, Q.; Chen, Q. M. *Appl. Surf. Sci.* **2011**, *257* (11), 4956.

(4) Schutzius, T. M.; Bayer, I. S.; Tiwari, M. K.; Megaridis, C. M. *Ind. Eng. Chem. Res.* **2011**, *50* (19), 11117.

(5) Bedioui, F.; Devynck, J.; Bied-Charreton, C. *Acc. Chem. Res.* **1995**, *28* (1), 30.

(6) Younathan, J. N.; Wood, K. S.; Meyer, T. J. *Inorg. Chem.* **1992**, *31* (15), 3280.

(7) Malinski, T.; Taha, Z. *Nature* **1992**, *358*.

(8) Hrbác, J.; Gregor, C.; Machová, M.; Králová, J.; Bystron, T.; Cíz, M.; Lojek, A. *Bioelectrochemistry* **2007**, *71* (1), 46.

(9) Allen, B. W.; Piantadosi, C. a; Coury, L. a. *Nitric Oxide Biol. Chem.* **2000**, *4* (1), 75.

(10) Friedrich, J. M.; Ponce-de-León, C.; Reade, G. W.; Walsh, F. C. *J. Electroanal. Chem.* **2004**, *561*, 203.

(11) Sun, J.; Hauser, P.; Zhelyaskov, V. *Electroanalysis* **2004**, *16* (20), 1723.

(12) Bartlett, P. N.; Birkin, P. R.; Ghanem, M. A. *Chem. Commun.* **2000**, No. 17, 1671.

(13) Bartlett, P. N.; Baumberg, J. J.; Birkin, P. R.; Ghanem, M. A.; Netti, M. C. *Chem. Mater.* **2002**, *14* (5), 2199.

(14) Kim, O.H.; Cho, Y.H.; Kang, S. H.; Park, H.Y.; Kim, M.; Lim, J. W.; Chung, D. Y.; Lee, M. J.; Choe, H.; Sung, Y.E. *Nat. Commun.* **2013**, *4*, 2473.

(15) Sapoletova, N.; Makarevich, T.; Napolskii, K.; Mishina, E.; Eliseev, A.; van Etteger, A.; Rasing, T.; Tsirlina, G. *Phys. Chem. Chem. Phys.* **2010**, *12* (47), 15414.

(16) Gatty, H. K.; Leijonmarck, S.; Antelius, M.; Stemme, G.; Roxhed, N. *Sensors Actuators B Chem.* **2015**, *209*, 639.

(17) Gatty, H. K.; Stemme, G.; Roxhed, N. *J. Micromechanics Microengineering* **2015**, *25* (10), 105013.

(18) Pardon, G.; Gatty, H. K.; Stemme, G.; van der Wijngaart, W.; Roxhed, N. *Nanotechnology* **2013**, *24* (1), 015602.

(19) Estevez, J. O.; Agarwal, V. *Handbook of Porous Silicon*; Canham, L., Ed.; Springer International Publishing: Cham, 2014.

(20) de la Mora, M. B. ; Ocampo, M.; Doti, R.; E., J.; Faubert, J. In *State of the Art in Biosensors - General Aspects*; InTech, 2013; pp 141–161.

(21) Zheng, J.; Christophersen, M.; Bergstrom, P. L. *Phys. Status Solidi Appl. Mater. Sci.* **2005**, *202* (8), 1402.

(22) Chao, K.; Kao, S.; Yang, C. *… Solid-State Lett.* **2000**, *3* (10), 489.

(23) Pagonis, D. N.; Nassiopoulou, A. G. *Microelectron. Eng.* **2006**, *83* (4-9 SPEC. ISS.), 1421.